NUMERICAL AND EXPERIMENTAL STUDIES OF NON REACTIVE AND REACTIVE MIXING

SHAD WAHEED SIDDIQUI

CHEMICAL ENGINEERING

June, 2004

KING FAHD UNIVERSITY OF PETROLEUM & MINERALS

DHAHRAN 31261, SAUDI ARABIA

DEANSHIP OF GRADUATE STUDIES

This thesis, written by **SHAD WAHEED SIDDIQUI** under the direction of his thesis advisor and approved by his thesis committee, has been presented to and accepted by the Dean of Graduate Studies, in partial fulfillment of the requirements for the degree of **MASTER OF SCIENCE IN CHEMICAL ENGINEERING.**

Thesis Committee

_____
Dr. Habib D. Zughbi
(Thesis Advisor)

_____
Dr. Ashrafhusein I. Fatehi
(Thesis Co-Advisor)

_____
Prof. Mazen A. Shalabi
(Member)

_____
Prof. Mohamed B. Amin
(Department Chairman)

_____
Prof. Tomoyuki Inui
(Member)

_____
Prof. Osama A. Jannadi
(Dean of Graduate Studies)

_____
Dr. Habib H. Al-Ali
(Member)

_____
Date

To

my nani

&

the FLUENT Inc.

Acknowledgements

Many thanks are due to *Dr. Habib D. Zughbi,* thesis advisor, for his invaluable guidance and encouragement throughout this works period. I owe him more than I can put in black and white.

I am indebted to *Dr. Ashrafhusein Fatehi*, thesis co-advisor and thesis committee members, *Prof. Tomoyuki Inui*, *Prof. Mazen A. Shalabi* and *Dr. Habib H. Al-Ali*, for their fruitful comments and sincerest help that I derived from their immense research experience. I am sure without their guidance, this work would not have had taken this final shape.

I am all the more thankful to Prof. M. B. Amin, Chairman, Chemical Engineering Department, King Fahd University of Petroleum & Minerals, for providing the facilities. I am indebted to all faculty members who made my stay here fruitful and enriched with all academic experience. All help from Riasat Khan sb., Department Secretary and office members, Jerico, Abdullah and Tahir, is truly acknowledged. They helped me in whatever capacity they could have had.

My sincerest thanks are due to Mahdi, Romeo, Mariano, Ibrahim, Syed Kamal sb., Inam and Bashir sb., from the Chemical Engineering Workshop and Laboratory, who helped me out with my work in least possible time. I remember long hours Mahdi and Romeo have spent in fabricating the experimental setup, and ever-willingness of Mariano and Syed Kamal sb., to supply me the common laboratory chemicals and apparatus, during my experimentation.

I acknowledge my family's support and belief in me. I always knew that they would be there whenever I needed them.

Lastly but certainly not the least, I truly acknowledge King Fahd University of Petroleum & Minerals for providing me such a wonderful learning experience, both academically and personally, here in this beautiful campus at Dhahran.

June 25, 2004 SWS

Table of Contents

List of Figures

List of Tables

Thesis Abstract

NAME: SHAD WAHEED SIDDIQUI

TITLE: EXPERIMENTAL AND NUMERICAL STUDIES OF NON REACTIVE AND REACTIVE MIXING

MAJOR FIELD: CHEMICAL ENGINEERING

DATE: JUNE 2004

Mixing plays an important role in chemical industries. It is a means of achieving a desired degree of homogeneity and may be used to promote chemical reactions, heat and mass transfer. It may be achieved in various ways including mechanical means and fluid jets. Fluid jet mixing include jet agitated tanks and pipelines with tees. Until recently very little was known about the fluid flow, velocity field and mixing characterization that are generally involved in mixing systems.

Jet mixers usually serve an economical way of mixing different phases. They require least hardware and maintenance over long periods of usage. These jet mixers are suitable for both jet agitated tanks or pipeline assemblies.

Extensive studies have been carried out in both of the above systems for both reactive and non-reactive liquid phased compounds. The sole objective in the previous studies was to optimize the mixing time. In this study the effects of various tank bottom shapes, on mixing time in fluid agitated cylindrical tanks, for non reactive systems and the effect of velocity ratio (jet velocity to main pipe velocity), in case of reactive systems are investigated. This study comprises an experimental and numerical investigations of

mixing in a fluid jet agitated tank and effects of mixing on fast chemical reactions in a pipe with side tees.

Results show that the 95% mixing time (t_{95}) in a cylindrical tank with a hemispherical bottom is about 18% to 25% shorter than t_{95} for a flat base tank. Cylindrical tanks with a conical base also gave shorter mixing times.

The ratio of t_{99}/t_{95} was also investigated. It was found that this ratio varies from one tank arrangement to another, the ratio found in this study ranges from 1.25 to 2.5. This compares favorably to the published data.

The present study also investigated the effects of mixing on instantaneous chemical reaction in a pipeline with side tees. These instantaneous reactions are diffusion controlled. It was found that mixing helps in breaking the segregation and improves the contact between the reactants.

Thesis Abstract in Arabic

ملخص الرسالة

الإســـم : شاد وحيد صديقي

عنوان الرسالة : دراسات مخبرية ورياضية للخلط التفاعلي واللاتفاعلي.

الدرجـــة : الماجستير

التخصـص : هندسة كيميائية

التاريـــخ : يونيو 2004م

عملية الخلط تلعب دوراً مهماً في الصناعات الكيميائية. وتعتبر إحدى الطرق التي يمكن بواسطتها الحصول على درجة عالية من التجانس وتستخدم أيضاً في زيادة التفاعلات الكيميائية والإنتقال الحراري وانتقال الكتلة. يمكن إجراء عملية الخلط بطرق متعددة ومنها الطرق الميكانيكية ونفاثات الموائع. الخلط بواسطة نفاثات الموائع يشمل خزانات الخلط النفاث والأنابيب ثلاثية الرأس. حتى الآن عرف القليل فقط عن إنسياب الموائع وحقل السرعة وصفات الخلط والتي تستخدم في أنظمة الخلط.

الخلاطات النفاثة تستخدم كطرق اقتصادية لخلط المواد ذات الحالات المختلفة. حيث لايستدعي استخدام هذه الخلاطات الكثير من الأجهزة ولاتحتاج إلى صيانة على مدى فترات طويلة من الإستخدام. وتعتبر هذه الخلاطات طريقة ملائمة للخلط في خزانات الخلط النفاثة والأجزاء الأنبوبية المختلفة.

تم إجراء العديد من الدراسات للخلط في هذين النوعين من الأنظمة وذلك للسوائل في الحالات التفاعلية واللاتفاعلية. في الدراسات السابقة كان الغرض الأساسي هو دراسة زمن الخلط الأمثل.أما في هذه الدراسة فقد تم بحث تأثير شكل قاع الخزان على زمن الخلط وذلك في خزانات الموائع الإسطوانية وذلك في حالة عدم وجود تفاعل كيميائي. وكذلك تأثير نسبة السرعة النفاثة إلى السرعة الرئيسية في الإنبوب في حالة الأنظمة المتفاعلة. اشتمل هذا البحث على دراسة مخبرية وعددية للخلط داخل خزان نفاث وأيضاً تأثير الخلط على التفاعلات الكيميائية السريعة في الأشكال الأنبوبية الثلاثية.

أظهرت النتائج أن زمن الخلط لـ درجة 95% (t_{95}) في الخزانات الإسطوانية ذات القاع النصف كروي أقل بحوالي 20% من زمن الخلط في الخزانات ذات القاع المسطح. والخزانات الإسطوانية ذات القاع المخروطي أعطت زمن خلط أقل أيضاً.

تم بحث أيضاً القيمة $\left(\frac{t_{99}}{t_{95}}\right)$ ووجد أن هذه القيمة تختلف من خزان لآخر تبعاً لأشكالها. ووجد أن هذه القيمة تمتد من 1ر25 إلى 2ر5. وكانت هذه النتائج مطابقة لما وجد في الدراسات السابقة.

في هذه الدراسة تم أيضاً بحث تأثير الخلط على التفاعلات اللحظية. لقد وجد أن الخلط يساعد على تكسير التكتلات الجزيئية ويحفز تلاصق المواد المتفاعلة.

Chapter 1

Introduction

1.1 Introduction

Mixing is an important operation in many chemical engineering applications. The term "mixing" is applied to processes used to reduce the degree of non-uniformity, or gradient of a property in a system such as concentration, viscosity or temperature. It is a means of achieving a desired degree of homogeneity. The mechanisms by which mixing occur can be summarized as diffusion and convection.

If two miscible liquids are placed together in a tank, they will gradually intermix due to the diffusion of the molecules. Due to the slow diffusion process, this mixing may be very slow. To speed up the phenomena, some forced convection source such as a mechanical mixer or a fluid jet is used. This introduces bulk or convective flow so that there are no low velocity zones. Both of these sources are energy consuming and ultimately the mechanical energy is dissipated as heat. The proportion of heat attributable to each varies from one application to another. Natural convection may also play a role in enhancing mixing.

The viscosities of liquids to be mixed play an important role in the convection process. For good mixing, a liquid should be convected to all parts of a mixing tank. For highly viscous fluids the convection in a tank may become low. This is because the viscous forces dampen down the inertial forces so that the liquid is convected only a short distance away from a jet or a stirrer. Consequently, this does not lead to a very efficient

mixing. So for efficient mixing, the inertial forces should be large enough to overcome the viscous forces. Heating may be used as a means of reducing viscosity.

The flow in mixing vessels may be laminar or turbulent, with a substantial transitional zone in between the two. Frequently, both types of flow occur simultaneously in different parts of the vessel. Continuous mixing of two fluid streams can be achieved using a number of mixer geometries. However using baffles and complex internal geometries may lead to excessive pressure drop and significantly increase the cost of the mixing device.

The turbulent mixing of two miscible fluids to promote chemical reactions is a common process in the chemical industries. Effective use of turbulence can increase reactants contact and yield, which can significantly reduce the cost of producing many chemicals. It also promotes heat transfer, eliminates corrosion, scale formation and thermal shocks.

Mixing also contributes to the selectivity of parallel reactions. Consequently, there is a need to design the mixing device in such a way as to include the rapid mixing so as to avoid the formation of the undesired product.

There are well defined criteria for the degree of mix. The basis for such criteria is achieving 95% or 99% mixing. These are calculated according to standard procedures using the concentration of an inert tracer, temperature or conductivity as the measured variable.

Mixing may be achieved by using mechanically driven impellers, jet agitation, and pipelines with tees or static mixers. This study concentrates on non-reactive mixing in fluid jet agitated tanks and reactive mixing in pipeline with side tees.

Traditionally jet mixers were designed individually for each specific process and optimization of such systems was largely done by trial and error.

Recently, non-reactive mixing in a jet agitated tank was numerically and experimentally investigated by Rakib (2000), Zughbi and Rakib (2000, 2002 and 2004), Ahmad (2003), Ahmad and Zughbi (2003), Zughbi and Ahmad (2003) and Zughbi et al. (2003). It was found that the convective mixing time is a function of the flow patterns and the angle the jet makes with a plane parallel to the tank bottom. It was also found that the mixing time does depend on the jet asymmetry.

In this study, the effects of the shape of the tank bottom and the irregular shape of the tank on mixing time in a jet agitated tank is investigated. The scale up of jet mixers is also addressed.

Mixing in pipeline with side tees has been well researched and most of the applications include the use of right angle side tees.

Numerical and experimental investigations of mixing in pipelines with side tees for achieving thermal homogeneity in case of non-reactive system, were recently carried out by Khokhar (2002), Khokhar et al. (2002, 2003) and Zughbi et al. (2002, 2003). It was found that the length of the pipe required to achieve 95% mixing is a function of the angle at which the jet is injected into the pipe.

Pipeline with side tees can also be suitably used as a reactor while transporting the fluid. For reactor application, homogeneity need be achieved in short times and reactor length, if the reaction times are small.

In this study, experimental investigations of reactive mixing in pipelines with side tees are carried out.

Previous studies have been carried out to study the limiting case of an instantaneous (diffusion controlled) reaction. Segregation of reactants retards the reaction. Therefore, there is a need to break these segregations to a size below which it may be assumed that complete micromixing has occurred or that the reactants are mixed at microscales. This scale is referred to as the Kolmogoroff scale of mixing.

As this study focuses on non-reactive mixing in jet agitated tanks and reactive mixing in pipelines with tees, the next few sections will briefly discuss the mechanisms of mixing, mixing in fluid jet agitated tanks, optimum design of tee mixers and reactive mixing.

1.2 Mechanisms of Mixing

Mixing is often carried out to enhance the rate of heat transfer, chemical reactions, disperse immiscible materials and distribute one material into another to achieve uniform properties.

Mixing occurs under laminar and turbulent regimes. The basic mechanisms in the laminar regime are: (i) laminar shear and (ii) elongation or extensional flow, distributive mixing, molecular diffusion and stresses in laminar flow. Turbulent flow brings with it quick and rapid mixing and the mechanisms may be described as: (i) distributive mixing, where large eddies exchange positions and convect material so that uniformity is achieved on a scale larger than the eddy size. (ii) Dispersive mixing, where a finer grained mixture is formed due to the decay of the large eddies and (iii) Diffusive mixing,

where diffusion within the finely dispersed structure (eddies) results in mixing at the molecular scale. Convective mixing refers to (i) and (ii) while (iii) is defined as diffusive mixing.

These three stages occur consecutively where distributive mixing takes place first, then dispersive mixing and finely diffusive mixing. These three also occur to some extent simultaneously. Diffusive mixing however is less important than convective mixing in certain applications such as blending of chemicals. However, it is always important in chemical reactions. It is the only mechanism that takes place on a molecular scale and enables contact between individual molecules and therefore it is the precursor to chemical reactions.

Turbulent eddy diffusion leads to a more rapid mixing than that associated with the mechanism of laminar flow. However for homogenization to occur at the molecular level, molecular diffusion must occur.

According to Kolmogoroff (Nienow et al., 1997), the smaller eddies are isotropic and independent of the bulk motion. For scales larger than the Kolmogroff scale (L), eddies will be in the inertial sub-range. Those corresponding to scales smaller than Kolmogoroff scale belong to the viscous range. The Kolmogoroff length scale is the size where inertial forces balance the viscous forces. It may be mathematically expressed as reference:

$$L = (\upsilon^3/\epsilon)^{1/4} \qquad (1.1)$$

Where, υ is the kinematic viscosity and ϵ is the power input per unit mass of turbulent fluid also known as the energy dissipation rate.

Micromixing is one of the processes that is dependent on turbulent eddies and their associated forces and thereby it is well correlated by the energy dissipation rate and the Kolmogoroff's theory (Nienow et al., 1997). The scale of mixing must be molecular in order to influence a chemical reaction which is clearly defined by the Kolmogoroff scale of mixing.

1.3 Mixing in a Fluid Jet Agitated Tank

In jet mixing, a fast moving (jet) stream of a liquid or gas is injected into a slow moving or stationary (bulk) liquid or gas. At the boundary of the jet some of the bulk fluid is entrained leading to what is known as a mixing layer. This layer grows in the direction of the jet flow.

The time required to achieve a certain degree of mixing is a function of the jet Reynolds number, Re_j. This Reynolds number is defined as $Re_j = \rho_L V_j d_j / \mu_L$, where ρ_L and μ_L are the density and viscosity of the fluid and V_j and d_j are the velocity and diameter of the jet respectively. According to Revill (1997), the jet is not an effective mixing tool for $Re_j < 100$. The mixing time is a very strong function of Re_j for $100 < Re_j < 2{,}000$ but only a weak function for $Re_j > 2{,}000$. This proposed study focuses on cases where $Re_j > 5{,}000$ i.e. in the fully turbulent regime.

An important observation in jet flows is that it expands laterally due to entrainment as it penetrates the main fluid. The velocity and turbulence of the jet flow decrease because the jet expands steadily at a angle ranging between 15 and 25 degrees (Lane, 1981).

Jet mixers have recently been optimized by Ahmed (2003). This study investigates further optimization of jet mixers.

1.4 Optimum Design of Tee Mixers

Tee mixers have been investigated by many researchers. Forney and Gray (1990) suggested guidelines for optimum design of a tee mixer for fast reactions. They assumed fully developed turbulent flow in both the main pipe and the tee inlet pipe such that Reynolds number of either flow has no effect on the quality of mixing. These conditions are met if $Re_m > 10{,}000$ and $Re_j > 6{,}000$ according to O'Leary and Forney (1985), where Re_m is the main pipe Reynolds number and Re_j is the jet Reynolds number. Forney and Lee (1982) identified conditions for optimum mixing at a junction. Yao et al. (1998) presented a theoretical tool for the optimum design of a mixer based on the distribution of local mixing efficiency. Maruyama et al. (1983) determined optimum velocity ratio and optimum injection angle for a number of single and dual jet injections.

Forney et al. (1996) studied the optimum jet mixing in a tubular reactor. He stated that the configuration of a turbulent jet in a cross flow or a tee-mixer is the most efficient passive design for rapid mixing. The numerical simulations of jets in a tubular reactor suggested that large jet-to-tube momentum ratios with no back mixing are superior.

Khokhar (2002) recommended an optimum tee angle for efficient mixing. This study investigates reactive mixing in pipeline with side-tees.

1.5 Reactive Mixing

In chemical and pharmaceutical industries, many times two or more chemically reacting liquid compounds need to be mixed. This mixing, if not properly undertaken, could lead

to the formation of certain undesired products/compounds. The irony is that the reactions are bound to happen and so the least that can be done is to minimize those undesirable byproduct formations by suitable mixing means. A good example is an instantaneous reaction. For a chemical reaction to occur, mixing need be carried out at the smaller possible level in the reaction zone, i.e. at micro levels. Therefore, chemical reactions depend directly on the molecular scale mixing of the reagents, a process that in turn is influenced by convective (coarser) mixing.

For single chemical reactions, the rate of very fast reactions is greatly influenced by mixing. This is due to the fact that reagents have to come together in order to react. The volumes which have to be provided to achieve a required reaction rate are an order of magnitude greater than those calculated from chemical kinetics. This applies for both single and multiphase reactions. For multiple reactions, the rates of very fast multiple reactions are also influenced by mixing rates.

Chemical reactions can be divided into two limiting cases and one intermediate case. The two limiting cases occur when either hydrodynamics or kinetics completely dominate a combined mixing-reaction system. In the first limiting case, the kinetics of the reaction are so rapid that the reaction is complete when mixing is complete. Reactions of this type are commonly called diffusion-controlled reactions, since the molecular diffusivity is the only reaction-limiting factor in the fine structure of the flow field. The second limiting case is the situation in which the kinetics is so slow that the reactants are completely and thoroughly mixed before any appreciable reaction has taken place. There have been many studies carried in a chemical reactor as to see how conversion in a

chemical reactor is affected by the rate at which the reactants mix (Bourne, 1992, McKelvey et al., 1975).

Previous studies were carried out to mathematically solve the limiting case of an instantaneous or diffusion controlled reaction**.** The fact that the diffusion-controlled chemical reaction and mixing system are mathematically equivalent when flow hydrodynamics are identical was extensively studied by Keeler et al. (1965).

This study concentrates on studying fast reactions in tee-mixers.

Chapter 2

Literature Review

2.1 Mixing in a Fluid Jet Agitated Tank

A through revision of mixing in a fluid jet agitated tank was given by Rakib (2000) and Ahmed (2003). Accordingly this literature review is selective, rather brief and concentrates on the specific topics that are of direct interest to this study. There have been many experimental investigations of mixing in a fluid agitated tank. Fossett and Pooser (1949) carried out the first study which was aimed at blending tetra-methyl lead in gasoline tanks. They recommended an expression to calculate the time required for 95% mixing to be achieved. The expression is:

$$T = 9.0 * D^2/(V*d) \quad (2.1)$$

where, D is the diameter of the tank, d is the jet diameter and V is the jet velocity. Fossett and Prosser experimented for Reynolds number varying from 4,500 to 80,000 and in large tanks i.e. volume of about 3000 ft^3. Fossett and Prosser's expression for the mixing time was independent of Reynolds number. Van de Vusse (1959) carried out experiments in inclined side entry jet mixing. His expression for mixing time was similar to that of Fossett and Prosser, i.e. independent of Reynolds number. Okita and Oyama (1963) recommended an expression for mixing time similar to the previous one and independent of jet Reynolds number. Coldrey (1978) also proposed an expression for mass transfer that was independent of the jet Reynolds number. Fox and Gex (1956) investigated fluid jet mixing in the laminar and turbulent regime and suggested expressions for the mixing time which was a function of Reynolds number.

For the laminar regime:

$$T = C_1 * h^{0.5} * D/(R_{ej}^{1.33} * V_d^{0.67} * g^{0.167}) \quad (2.2)$$

For the turbulent regime:

$$T = C_2 * h^{0.5} * D/(R_{ej}^{0.17} * V_d^{0.67} * g^{0.167}) \quad (2.3)$$

where, C_1 and C_2 are constants, T is the mixing time, h is the height of the liquid in the tank, D is the tank diameter, Re_j is the jet Reynolds number and g is acceleration due to gravity.

Lane (1981) and Lane and Rice (1981,1982) proposed an expression for mass transfer for an inclined side entry jet in a flat based cylindrical tank and recorded an expression for 95% mixing dependent on the jet Reynolds number. This is referred to as side-pump-around as shown in Figure 2.1a. Maruyama (1986) supported the findings that mixing time, for horizontal, inclined and vertical jets, is a function of the jet Reynolds number. Grenville and Tilton (1996) recommended an expression of mixing time for turbulent jet mixed vessels. Their expression is:

$$t_{99} = 3*(X/d_j)^2*(d_j/V_j) \quad (2.4)$$

where, X is the free jet path, V_j is the jet velocity, d_j is the jet diameter, t_{99} is the 99% mixing time.

Recently, a number of Computational Fluid Dynamics (CFD) investigations of mixing in fluid jet agitated tanks were carried out. These include Zughbi and Rakib (2000), Jayanti (2001) and Patwardhan (2002).

Rakib (2000) and Zughbi et al. (2002, 2004) used the *k*–ε model to simulate mixing in a fluid agitated tank and in pipelines with tees respectively. They obtained good overall agreement between numerical and experimental results. However, to obtain good agreement

in the vicinity of the jet, the RSM model proved to be superior to the k–ε model. In this study the standard k–ε model was used.

The optimum design of a jet mixer has been the subject of a number of criteria. One of the criteria is that jets should be injected along the diameter of tanks as the longest jets give the shortest mixing time (Coldrey (1978), Rakib (2000), Zughbi and Rakib (2004) found that this need not be the case. They found that the mixing time is a strong function of the jet angle of injection. An angle of 30^o rather than 45^o was found to be the optimum jet angle of injection. According to Zughbi and Rakib (2004), mixing time depend on the flow patterns inside the tank, aspect ratio, jet velocity, and the angle of injection. Ahmad (2003) investigated mixing in a bottom-pump-around as shown in Figure 2.1b.

Other factors that affect mixing time include:

(i) the selective position of the jet inlet and the recycle off take

(ii) respective sizes of the tank and the jet

(iii) jet protrusion and

(iv) the shape of the tank base.

Lane and Rice (1982) reported shorter mixing time in a cylindrical tank with a hemispherical base compared to a flat based tank. Jayanti (2001) carried out numerical investigations of the effects of the tank bottom. He found that the conical base with a half cone angle of 31^o gave the shortest mixing time. He examined a hemispherical base, an ellipsoidal base, two conical bases with a half cone angle of 31^o and 58^o respectively.

From the above discussion it is obvious that the tank base is one of the factors which influence mixing time in tanks. The effect of the tank base on a bottom-pump-around has not been studied.

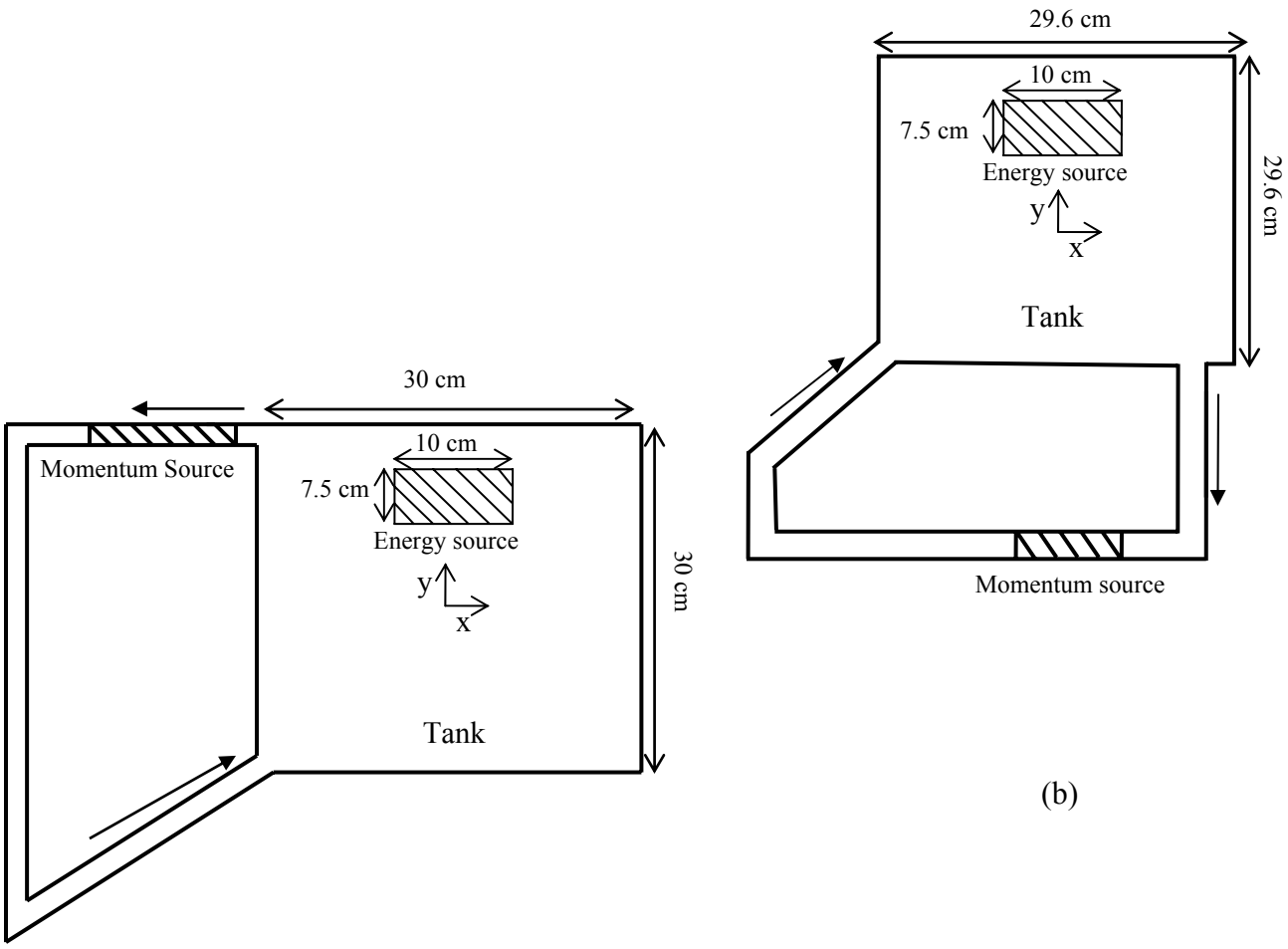

Figure 2.1: A two-dimensional view of (a) the side pump around tank geometry used by Raqib (2000) and by Lane and Rice (1982) and (b) the tank geometry for the bottom pump around used by Ahmad (2003).

Ahmad (2003) found that an asymmetric jet reduces the mixing time for a bottom-pump-around. The effects of breaking the flow symmetry, this time by using an irregular shape of the tank have been investigated.

2.2 Mixing in Pipelines with Side-Tees

A review of various flow arrangements is presented by Gray (1986). A general review of turbulent mixing in a chemically reactive flow was provided by McKelvey et al. (1975). Khokhar (2002) presented a thorough review of the experimental and numerical work done on mixing in pipelines with side, opposed and multiple-tees. In this study a brief review of the convective mixing in pipelines with side-tees is presented. A review of reactive mixing is also presented in a later section.

A pipe tee is a simple device for mixing two fluid streams. It is formed by two pipe sections joined traditionally at a right angle to each other. One stream passes straight through the tee while the other enters perpendicularly at one side as shown in Figure 2.2. This flow arrangement is known as a side-tee.

Applications where pipeline mixing with tees is used include low viscosity mixing such as the dilution of concentrated acids or bases, waste water treatment and blending of some oils (injection of additives) and petrochemical products. Other applications include blending of fuel gas, mixing of feed streams for catalytic reactors and mixing of hot flue gases with ambient air. A number of local companies use many of the abovementioned processes.

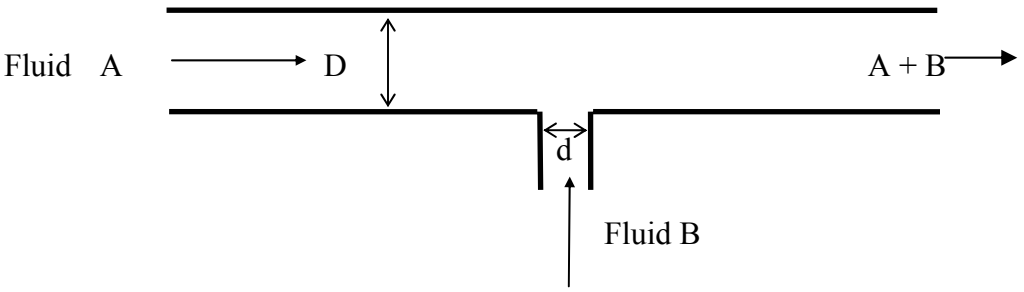

Figure 2.2: A schematic diagram of a pipeline with a side-tee

2.2.1 Experimental Studies of Mixing in Pipeline with Side-Tees

The first systematic study of pipeline mixing by side injection was conducted by Chilton and Genereaux (1930), who used smoke visualization technique to determine optimum mixing conditions at a glass tee. Chilton and Genereaux found that when the ratio of the velocity of side-to-main flow was in the range of 2 to 3, satisfactory mixing was obtained in 2 to 3 pipeline diameters.

Deflected turbulent jet in an ambient cross flow gets diluted more rapidly than jets without cross flows, are not axisymmetric or uniformly self similar. Forney et al. (1979, 1982), and Marauyama et al. (1982 and 1983) studied the jet injection of fluid into a pipeline over the first twelve pipe diameters from the injection point. Typically, the standard deviation or second moment of the tracer concentration was observed to decrease with increasing jet momentum at a fixed measurement point downstream. However, it was difficult to establish a distinct minimum in the second moment of the tracer concentration distribution with increasing jet momentum, particularly within the first twenty pipe diameters from the injection point

The mixing criteria in many of the experiments assumed that optimum mixing in a pipeline was achieved if the side jet was centered along the pipeline axis after entering the main flow. The above assumption of a geometrically centered jet appeared to be useful if the measurement point was at distances far from the injection point or $15 < x/D < 120$ (Forney et al. 1982).

Some of the data of Maruyama et al. (1983) and Gosman and Simitovic (1986) indicated that mixing of an inert tracer could be improved by the impingement of secondary/side tee fluid against the opposite wall of the pipe near the tee inlet.

Hansen et al. (2000) studied the effects of inlet condition on downstream mixing in turbulent pipe flow with the use of photo-activable fluorescence techniques. The different inlet conditions included both geometry changes and changes in the manner in which the constituents were introduced into the flow. Results indicated that small changes in inlet geometry could affect the downstream mixing more than the manner in which constituents were introduced into the flow. They also did experiments using static mixers.

Zughbi et al. (2003) studied mixing in a pipeline with side-tees and found that adjusting the angle of the tee is an efficient factor in shortening the pipe length required to achieve good mixing.

2.2.2 Numerical Simulation of Mixing in Pipeline with Side-Tees

Cozewith et al. (1991) simulated tee mixing characteristics both in the absence and presence of a reaction for a tee with d/D = 0.188 (where, d is the side tee diameter and D is the main pipe diameter) over a range of side stream/main stream velocity ratios from 1.2 to 6.5. A three-dimensional model was constructed and the k-ε model was used to model turbulence. Monclova and Forney (1994) simulated pipeline side-tee mixing quality with the commercially available fluid flow package PHOENICS. The $k-\varepsilon$ model was used to model turbulence. They compared numerical results with the experimental results of Sroka and Forney (1989) and obtained reasonable agreement.

Yuan et al. (1999) reported a series of large-eddy simulations of a round jet issuing normally into a cross flow. Simulations were performed at two jet-to-cross flow velocity ratios, 2.0 and 3.3, and two Reynolds numbers, 1050 and 2100, based on cross

flow velocity and jet diameter. The mean and turbulent statistics computed from the simulations matched experimental measurements reasonably well. Zughbi et al. (2003) simulated mixing in pipelines with side-tees. The effects of the angle of the side-jet, the side- to main-velocity ratio, ratio of pipe diameters and scale up were investigated.

Cozewith et al. (1991) also simulated the case of reactive flows. A copolymerization reaction was used to investigate the effects of mixing on the reaction rate. It was found that the copolymer composition distribution is considerably broader than for the instantaneous mixing case due to inhomogeneity in concentration. Baldyga et al. (2001) carried out an experimental study and CFD modeling, precipitation of barium sulphate in a pipe. A closure previously proposed by Baldyga et al. (1997) employed the presumed beta PDF of the inert type composition variables formed with the local values of Ba^{2+} and SO_4^{2-} concentrations and the turbulent mixer model. They computed the flow fields using the k-ε model.

Cozewith (1991) carried out numerical calculations using a k-ϵ turbulence model. He supported the idea that the jet impingement was necessary to minimize the second moment (standard deviation, spread) of a tracer concentration for a fixed tee mixer geometry near the tee inlet, $x/D < 3$. It may be desirable, however to promote rapid mixing of two fluids with a tee mixer in a short distance downstream from the injection point at $x/D < 3$.

In particular, the suitability of a pipeline mixing tee for reactor applications, where the reaction times are small, depend on achieving homogeneities of the reactant concentration in short times.

2.3 Reactive Mixing in Pipeline with Side-Tees

Reactive mixing in pipelines with side tees, tubular reactors and stirred tanks has been studied by many researchers over the past thirty years. The findings for various geometries are similar and can be summarized by the fact that mixing is the limiting step in processes with instantaneous reactions. In the next subsections, reactive mixing in various geometries is reviewed.

Cozewith and Busko (1989) measured the distance downstream from the tee inlet required for neutralization of a base indicator. They found a minimum distance to mix for certain tee mixer geometries. They demonstrated that it was necessary to increase the momentum of the side tee such that the secondary fluid impinges the opposite wall of the pipe near the tee inlet. This requirement may not be necessary as explained by Zughbi et al. (2003). Tosun (1987) studied the product yield of tee mixers with competitive consecutive reactions. The experimental data demonstrated a distinct minimum in the undesirable product yield for certain tee mixer geometries**.** He studied micromixing by means of the consecutive competitive azo coupling reactions first proposed by Bourne and co-workers (1981). Conversion and selectivity were measured in experiments where linear velocities, velocity ratio, and the viscosity of the larger stream were varied, the non-viscous smaller stream being always in turbulent flow. The velocity ratio which resulted in the best micromixing was determined for the side tees with opposed tees seemed to suggest that the same relationship may also hold for the opposed tees. An overall mixing index had to be defined for quantifying the intensity of mixing. For both types of tees, it was found that mixing index increased to a Reynolds number of 10^4 and remained constant beyond this value with selectivity leveling off at about 0.12. It meant

that a maximum level of micromixing was attained only at full turbulence and that increasing the velocities beyond Re_m of 10^4 did not result in further improvement. Because of the high level of turbulence required, achieving good micromixing in side and opposed tees could be difficult at viscosities higher than about 50 cp, due to excessively high pressure drops.

Baldyga et al. (1995) investigated jet reactor scale-up for mixing controlled reaction. Product distribution of fast reactions were measured at small scale in turbulent viscous and aqueous solutions as well as using two larger nozzles (0.012 m and 0.25 m) and two larger semibatch reactors (0.10 m^3 and 0.25m^3). Baldyga et al. (1994) stated that the product distribution of a multistep reaction depends not only upon the chemical kinetics, but also upon how the reagents are mixed when the chemical half-life is of the order of the half life for mixing. Although several aspects of turbulent free jets had already been studied, multi-step mixing controlled reactions in liquid jets were not widely investigated.

Bourne (1983) stated that large scale fluid dynamics was influenced primarily by convection and not directly related to mixing on molecular scale. He discussed how the intensity of segregation at the molecular scale could be related to the observable rate of a second order reaction taking place between two reactants, which were initially present in separate streams. Thus, in the limit, no reaction could occur when segregation was complete and the rate attained its maximum value when the mixture is chemically uniform. Any segregation present must therefore retard the reaction. Bourne showed how to use diffusion controlled reaction (e.g. neutralization) to determine the intensity of segregation. He also stated that inhomogeneity at the molecular scale developed if the

half-life time which would be required by a chemical reaction in a homogeneous solution was of the same order as or less than the half-time for micro-mixing in the absence of reaction. The use of the diffusion-reaction equations to describe the course of a reaction during micro-mixing lead to the second Damkoehler number, which is proportional to the ratio of the diffusion time to the reaction time i.e. its value indicated whether the reaction regime was slow (controlled by kinetics), fast (kinetic and diffusion both important) or instantaneous (fully diffusion controlled). Evidence of the large effect of viscosity on micromixing existed whereas macromixing in the turbulent regime was scarcely dependent upon viscosity.

Mao and Toor (1971) studied very rapid second order chemical reactions in a turbulent tubular reactor with reactants fed separately through many small tubes. The reaction chosen for the study was an acid-base neutralization reaction. It was noted that very rapid reactions were diffusion controlled. The reactions were followed by measuring the small temperature rise along the axis of the tube, which was related to the conversion in the same manner as by Vassilatos and Toor (1965). Temperature measurements were made at each position and the average of these measurements were reported. The maximum temperature rise over the reactor was $0.38^{o}C$.

Li and Toor (1986) carried out the yield study of a non premixed series parallel reaction at complete conversion in a turbulent, tubular-flow reactor with single and multiple jet feeds. It was observed that the yield of the intermediate decreased as mixing was slowed relative to the chemical kinetics, either by decreasing the Reynolds number, or by using a less efficient mixing device, or by increasing the feed concentration.

Singh et al. (1993) noted that if the total reactant diffusivities were equal, the time average concentration fields which resulted from turbulently mixing reactants could be measured thermally provided the temperature difference between the feed streams was suitably chosen. Each reactant profile was obtained from measurements of the temperature profile in an experiment in which the inlet temperature of that reactant was less than that of the other reactant by an amount equal to the adiabatic reaction temperature change of the measured reactant. The reactants were HCl and NaOH. The studies were carried out in a tubular reactor.

Keeler et al. (1965) studied mixing and a rapid, second-order irreversible chemical reaction in a turbulent chemical flow reactor, with a point conductivity probe used to detect changes in concentration. They suggested that the fast reaction was diffusion controlled and that such a reaction could be treated in mathematical equivalence to the mixing systems. The reactants used were acetic acid and ammonium hydroxide. An electrolyte was used as a tracer. The experimental approach was based on the fact that at low electrolyte concentrations, the conductivity of an aqueous solution was directly proportional to the concentration of the electrolyte.

Hayes et al. (1998) stated that in a turbulent flow, the rate of reaction was controlled by the micromixing, which in turn depends on the turbulent kinetic energy. In laminar mixing, the degree of micromixing was controlled predominantly by the convection motion, and the final intimate mixing at the molecular level by molecular diffusion. They studied the cases of very fast (instantaneous), intermediate and slow reactions

So far several techniques have been used to evaluate the performance of mixing vessels. The simple methods include the thermal method, the use of colored tracers and fast chemical reactions. More complex methods involve the use of magnetic tracers and radioisotopes.

2.4 Reactive Mixing in Stirred Tank Reactor/CSTR

Extensive studies of reactive mixing in stirred tank reactors were carried in the last two decades. It is a well known fact that in order for the chemicals to react, they need to be mixed homogenously. This has been extensively studied in case of tanks fitted with stirrers. Inhomogeneity of concentration (or temperature) at the molecular scale leads to segregation in a reacting system if the characteristic time for mass (or heat) transfer is of the same order as or greater than the characteristic reaction time. Mass transfer promoting homogenization (mixing), and reaction no longer proceed consecutively (e.g. slow reactions), but simultaneously. Reaction occurs in inhomogenous zones, where steep concentration gradients are developed to sustain the mass fluxes required by the reaction.

Belevi et al. (1981) discussed several possible representations of inhomogeneity in mixtures and their influence on chemical reactions. A diffusion-reaction formulation was developed to model the mixing dependent product distributions leaving a CSTR. McKelvey et al. (1975) used the information on mixing to predict the course of reaction where both the turbulent mixing and kinetics were the contributing factors. They also investigated rapid reactions, where the chemical rate was unimportant, and the conversion was controlled by the turbulent mixing.

Bourne et al. (1977) stated that if the reaction mechanism of a chemical reaction was known then it could indicate quantitatively how partial segregation and feed configurations influenced the rates of formation of the desired and undesired products and hence the selectivity. This method was previously applied to a second order reaction. He considered both incompletely mixed continuous tank reactors (CSTR) and turbulent reactors.

Verchuren et al. (2001) stated that before a chemical reaction could occur, the reactants had to be mixed on a molecular scale. When a reaction is slow in comparison to the mixing process, the solution would be homogenously mixed before reaction takes place and the product distribution would only depend on the chemical kinetics. However, when a reaction is fast relative to the mixing rate, the mixing rate would also determine the yield and selectivity of the process. Examples of mixing sensitive reactions are monoacylation of symmetrical di-amines, precipitation reactions and fermentation processes. The reactor type used in this study was a cylindrical vessel equipped with a Rushton turbine stirrer and four baffles. The hydrodynamic parameters for this reactor types were determined extensively by laser Doppler velocimetry experiments.

Angst et al. (1982) studied a competitive, consecutive reaction type $A + B \rightarrow R$ and $R + B \rightarrow S$. The reactor initially containins only the reagent B into which the reagent A diffuses. Depending upon whether B was immobile or could diffuse within the reaction zone, different distributions of the products R and S were obtained. The reaction studied was the coupling of 1-naphthol (A) and diazotized sulphanilic acid (B) The product distribution was measured spectrophotometrically. Bourne et al. (1992) presented some experimental results of acid-base neutralization and alkaline hydrolysis of ethyl chloro-

acetate. Qualitative conclusions about the rate of micro-mixing for two parallel reactions were drawn and discussed. Bourne suggested that when mixing was perfect, no molecular segregation existed. When the segregation was intense, the product distribution became independent of the kinetics. When segregation was partial, the product distribution varied with the mixing intensity, and the micromixing model was needed to relate these quantities. All studies were carried out in baffled tanks with a Rushton turbine.

Ou et al. (1983) applied a stretching model to complex reactions as well as simple reactions. For complex reactions, different product distributions resulted from different mixing rates. For competitive reactions, better mixing generally favor products of reactions with higher reaction rate constants until reactions reached the reaction control limit, when the so-called perfect mixing prevailed. These effects were demonstrated in case of competitive parallel reactions.

Verschuren (2001) stressed that mixing affect, the yield and selectivity of fast competitive parallel and consecutive reactions, because slow mixing would retard desired reactions and promote undesired ones. An example of a mixing sensitive competitive parallel reaction was the addition of an acid or base to a solution of an organic substrate that degraded in the presence of a low or high pH. It was observed that slow mixing limited the neutralization reaction, which allowed the organic substrate to react with the acid or the base, thus forming unwanted byproducts.

The reaction between NaOH and HCl is much faster than the reaction between NaOH and ECA. NaOH will only reacted significantly with ECA when the reaction between NaOH and HCl is limited by mixing. Therefore, the amount of ethanol produced increased when the mixing rate decreased. The amount of ethanol and ECA present at the

end of an experiment in the reactor and the solution leaving the reactor were determined chromatographically. The mixtures were immediately analyzed to avoid the acid catalyzed hydrolysis of ethyl chloroacetate.

Manthanwar (2001) stated that the residence time distribution was a characteristic of the mixing occurring in a reactor. Thus, knowing the effluent concentration as a function of time, one can determine the residence time distribution (RTD) function. All the reactions are elementary. Moreover tracer streak lines functions in FLUENT had been used to generate an RTD function for a given reaction mixture in a given geometry.

2.5 Summary

Mixing could largely be classified as that in reactive and non reactive systems. In case of non reactive systems it is largely physical mixing, whereas in case of reactive mixing, convective mixing plays a very important role in the product distribution of complex parallel reactions. Studies were carried out in a chemical reactor as to see how the conversion in a chemical reactor is affected by the rate at which the reactants mix. A few studies were been carried out to study the limiting case of an instantaneous or diffusion controlled reactions in case of CSTR while a considerable gap existed in case of mixing in pipelines. It was found that for a reaction to occur, mixing needs be carried out at micro scales. As the reaction proceeds, segregation occurs throughout the reactant body. This segregation retards the reaction and the desired product. The need is to break these segregations to a size below which it may be assumed that complete micro-mixing had occurred or that the reactants are mixed at micro-scales.

Residence time distribution (RTD) could be used as a means to measure the degree of mixing. The temperature may also be used as a measured variable for highly exothermic reactants as in the case of neutralization reactions.

It was however noticed that the effect of few parameters like tank bottom-shape, irregular geometry and free liquid surface on mixing times in fluid agitated tanks have not been fully studied. This also applies to the effect of velocity ratio (jet velocity to main pipe) and the impinging jet angle with main pipe, on complex chemical reactions.

Chapter 3

Formulation of the Problem and Approach to the Solution

3.1 Preliminary Model Equations

The governing equations for a general mixing problem are the mass, momentum and energy equations. These govern the flow and heat transfer in pipelines with side tees or in a tank agitated by a fluid jet. The initial and boundary conditions for each case are different. These equations are written below in cylindrical coordinates. A general purpose three dimensional commercial Computational Fluid Dynamics (CFD) package, FLUENT, is used to solve these equations.

The equation of continuity in three-dimensional cylindrical coordinates is:

$$\frac{\partial \rho}{\partial t} + \frac{1}{r}\frac{\partial}{\partial r}\left(\rho r u_r\right) + \frac{1}{r}\frac{\partial}{\partial \theta}\left(\rho u_\theta\right) + \frac{\partial}{\partial z}\left(\rho u_z\right) = 0 \qquad (3.1)$$

The density is considered constant because the flow considered in this study is considered to be incompressible.

The r - component,

$$\left[\frac{\partial u_r}{\partial t} + u_r\frac{\partial u_r}{\partial r} + \frac{u_\theta}{r}\frac{\partial u_r}{\partial \theta} - \frac{u_\theta^2}{r} - u_z\frac{\partial u_r}{\partial z}\right] =$$

$$-\frac{1}{\rho}\frac{\partial p}{\partial r} + \nu\left[\frac{\partial}{\partial r}\left(\frac{1}{r}\frac{\partial}{\partial r}\left(r u_r\right)\right) + \frac{1}{r^2}\frac{\partial^2 u_r}{\partial \theta^2} - \frac{2}{r^2}\frac{\partial u_\theta}{\partial \theta} + \frac{\partial^2 u_r}{\partial z^2}\right] + g_r \qquad (3.2)$$

The $\theta-$component,

$$\left[\frac{\partial u_\theta}{\partial t}+u_r\frac{\partial u_\theta}{\partial r}+\frac{u_\theta}{r}\frac{\partial u_\theta}{\partial \theta}-\frac{u_r u_\theta}{r}-u_z\frac{\partial u_\theta}{\partial z}\right]=$$

$$-\frac{1}{r}\frac{1}{\rho}\frac{\partial p}{\partial \theta}+\nu\left[\frac{\partial}{\partial r}\left(\frac{1}{r}\frac{\partial}{\partial r}\left(ru_\theta\right)\right)+\frac{1}{r^2}\frac{\partial^2 u_\theta}{\partial \theta^2}-\frac{2}{r^2}\frac{\partial u_r}{\partial \theta}+\frac{\partial^2 u_\theta}{\partial z^2}\right]+g_\theta \qquad (3.3)$$

and the $z-$component,

$$\left[\frac{\partial u_z}{\partial t}+u_r\frac{\partial u_z}{\partial r}+\frac{u_\theta}{r}\frac{\partial u_z}{\partial \theta}+u_z\frac{\partial u_z}{\partial z}\right]=$$

$$-\frac{1}{\rho}\frac{\partial p}{\partial z}+\nu\left[\frac{\partial}{\partial r}\left(r\frac{\partial u_z}{\partial r}\right)+\frac{1}{r^2}\frac{\partial^2 u_z}{\partial \theta^2}+\frac{\partial^2 u_z}{\partial z^2}\right]+g_z \qquad (3.4)$$

The temperature field of the fluid flowing in pipes can be resolved by solving the energy equation.

$$\rho\hat{C}p\left(\frac{\partial T}{\partial t}+u_r\frac{\partial T}{\partial r}+\frac{u_\theta}{r}\frac{\partial T}{\partial \theta}+u_z\frac{\partial T}{\partial z}\right)=$$

$$k\left[\frac{1}{r}\frac{\partial}{\partial r}\left(r\frac{\partial T}{\partial r}\right)+\frac{1}{r^2}\frac{\partial^2 T}{\partial \theta^2}+\frac{\partial^2 T}{\partial z^2}\right]+2\mu\left\{\left(\frac{\partial u_r}{\partial r}\right)^2+\left[\frac{1}{r}\left(\frac{\partial u_\theta}{\partial \theta}+u_r\right)\right]^2+\left(\frac{\partial u_z}{\partial r}\right)\right\}$$

$$+\mu\left\{\left(\frac{\partial u_\theta}{\partial z}+\frac{1}{r}\frac{\partial u_z}{\partial \theta}\right)^2+\left(\frac{\partial u_z}{\partial r}+\frac{\partial u_r}{\partial z}\right)^2+\left[\frac{1}{r}\frac{\partial u_r}{\partial \theta}+r\frac{\partial}{\partial r}\left(\frac{u_\theta}{r}\right)\right]^2\right\} \qquad (3.5)$$

These differential equations representing the conservation equations (mass, momentum and energy) may be written in a general form as*:*

$$\frac{\delta\left(R_i\rho_i\phi_i\right)}{\delta t}+div\left(R_i\rho_i U_i\phi_i-R_i\Gamma_{\phi_i}grad\,\phi_i\right)=R_i S_i \qquad (3.6)$$

$$\begin{bmatrix}\text{Transient}\\ \text{Term}\end{bmatrix}\quad\begin{bmatrix}\text{Convection}\\ \text{Term}\end{bmatrix}\quad\begin{bmatrix}\text{Diffusion}\\ \text{Term}\end{bmatrix}\quad\begin{bmatrix}\text{Source}\\ \text{Term}\end{bmatrix}$$

where,

Γ_{ϕ_i} Exchange coefficient of ϕ in phase *i*

R_i Volume fraction of phase *i*

$S_{\phi i}$ Source rate of ϕ_i per unit volume

ϕ_i Any conserved property of phase *i*

U_i Velocity vector of phase *i*

Thus, the continuity equation for phase *i* become:

$$div\left(R_i \rho_i U_i\right) + \frac{\partial(R_i \rho_i)}{\partial t} = m_i \tag{3.7}$$

where,

m_i Mass per unit volume entering phase i from all sources

ρ_i Density of phase *i*

and the conservation of momentum for variable ϕ_i becomes:

$$div\left(R_i \rho_i U_i \phi_i - R_i \mu_{eff} \, grad \, \phi_i\right) = R_i S_{\phi_i} \tag{3.8}$$

where,

μ_{eff} Effective viscosity

$S_{\phi i}$ Source of ϕ_i per unit volume

3.2 Boundary and Initial Conditions

3.2.1 For Fluid Jet Agitated Tanks

The assumptions are as follows:

(i) At all walls, velocity is zero i.e. no slip condition exists.

(ii) Values of velocities are specified at the entrance of the jet.

(iii) Initial temperatures are specified for the tank fluid and the tracer.

(iv) Temperature = f(space coordinates , time)

(v) Un steady state operation.

Initial conditions used are:

(i) Temperature of the bulk water = $27^{o}C$

(ii) Temperature of the tracer water = $80^{o}C$

(iii) Bulk velocity = 0 m/s

(iv) Tracer velocity = 0 m/s

The boundary conditions used for mixing in a fluid jet agitated tank are:

(i) Heat flux at walls = 0 $Watt/m^2$

(ii) No slip condition at walls

(iii) Value of momentum source: this emulates the function of a pump and different momentum values. Momentum values (N/m^3) are specified for a given volume in the negative x direction to create different jet velocities.

3.3 Solution Algorithm

To solve the Navier-Stokes Equations, a linkage between velocity and pressure is required. The difficulty in calculating the velocity field lies in the unknown pressure field. The pressure gradient forms a part of the source term for a momentum equation. Yet there is no obvious equation for obtaining pressure. It is true that for a given pressure field, there is no particular difficulty in solving the momentum equations. But the way to determine the pressure field seems rather obscure. The choice of algorithms is a critical issue for solving the system of transport equations involving several dependent variables.

3.3.1 Discretization of the Domain: Grid Generation

To break the domain into a set of discrete sub-domains or computational cells or control volumes, a grid is used. Also called a mesh, the grid contains elements of many shapes and sizes, namely tetrahedral, quadrilateral or trigonal. In general, the density of cells in a computational grid needs to be fine enough to capture the flow details, but not so fine that the overall number of cells in the domain are excessively large, since problems described by large numbers of cells require more time to solve. Non uniform grids of any topology can be used to focus the grid density in regions where it is needed and allowed for expansion in other regions. For 3D simulations, when the grid is structured, a single grid plane can be displayed. In addition to showing the distortion in the grid, this type of display can also show fine and coarse grid regions. For unstructured grids, single grid planes do not exist. It is to be taken care of that the details smaller than the cell size cannot be resolved. Often, small flow features in one region need to be resolved in great detail in order to accurately predict large flow features in other regions. For example, a jet penetrating into a vessel will appear to diffuse more rapidly than in actual fact if a

course grid is used in the jet region. Satisfying grid needs such as this may lead to a finer grid containing far more cells than was initially estimated.

3.3.2 Discretization of the Equations

In order to solve the flow dynamics and heat transfer, the continuity equation, momentum conservation equations and the conservation of energy equation need be solved. In order to solve them they need to be discretized. These equations can be suitably descretized by the finite volume method. The basic idea is to integrate the equations over an arbitrary control volume in a grid. The resulting equations contain fluxes at the boundaries of the control volume, which can typically be discretized by the finite difference method.

3.3.3 The Solution Method

The result of the discretization process is a finite set of coupled algebraic equations that need to be solved simultaneously in every cell in the solution domain. Because of the non-linearity of the equations that govern the fluid flow, an iterative solution procedure is used for the purpose. These are, segregated and coupled solution approaches. A segregated solution approach is one where one variable at a time is solved throughout the entire domain. A coupled solution approach is one where all variables, are solved simultaneously in a single cell before the solver moves to the next cell, where the process is repeated. Typically, the solution of a single equation in the segregated solver is carried out on a subset of cells, using a Guass-Seidal linear equation solver.

Pressure velocity coupling is achieved by discretization of the continuity equation to derive an equation for pressure from the discrete continuity equation. Pressure velocity coupling is required only for the segregated solver (FLUENT/UNS). FLUENT provides

the option to choose among three pressure-velocity coupling algorithms: SIMPLE, SIMPLEC, and PISO. The semi-implicit method for pressure-linked equations (SIMPLE) algorithm is described very precisely by Patankar (1980). The essence of the algorithm is that a guessed pressure field is used in the solution of the momentum equations (for all but the first iteration, the guessed pressure field is simply the last updated one). The new velocities are computed, but these will not in general, satisfy the continuity equation. Some corrections to the velocities are determined. Based on the velocity corrections, a pressure correction is computed which, when added to the original guessed pressure, results in an updated pressure. Following the solution of the remaining problem variables, the iteration is complete and the entire process repeated. Fluent manuals (1998) provide good explanation of the abovementioned algorithms.

3.3.4 Pressure-Implicit with Splitting of Operators Algorithm

The Pressure-Implicit with Splitting of Operators (PISO) pressure-velocity coupling scheme, part of the SIMPLE family of algorithms, is based on the higher degree of the approximate relation between the corrections for pressure and velocity. One of the limitations of the SIMPLE and SIMPLEC algorithms is that the new velocities and corresponding fluxes do not satisfy the momentum balance after the pressure-correction equation is solved. As a result, the calculation must be repeated until the balance is satisfied. To improve the efficiency of this calculation, the PISO algorithm performs two additional corrections: a neighbor correction and a skewness correction.

The main idea of the PISO algorithm is to move the repeated calculations required by SIMPLE and SIMPLEC inside the solution stage of the pressure-correction equation. After one or more additional PISO loops, the corrected velocities satisfy the continuity

and momentum equations more closely. This iterative process is called a momentum correction or "neighbor correction". The PISO algorithm takes a little more CPU time per solver iteration, but it can dramatically decrease the number of iterations required for convergence, especially for transient problems.

For meshes with some degree of skewness, the approximate relationship between the correction of mass flux at the cell face and the difference of the pressure corrections at the adjacent cells is very rough. Since the components of the pressure-correction gradient along the cell faces are not known in advance, an iterative process similar to the PISO neighbor correction described above is desirable. After the initial solution of the pressure-correction equation, the pressure-correction gradient is recalculated and used to update the mass flux corrections. This process, which is referred to as "skewness correction", significantly reduces convergence difficulties associated with highly distorted meshes. The PISO skewness correction allows FLUENT to obtain a solution on a highly skewed mesh in approximately the same number of iterations as required for a more orthogonal mesh.

The PISO algorithm with neighbor correction is highly recommended for all transient flow calculations. It allows the use of a larger time step, as well as an under-relaxation factor of 1.0 for both momentum and pressure. For steady-state problems, PISO with neighbor correction does not provide any noticeable advantage over SIMPLE or SIMPLEC with optimal under-relaxation factors. PISO is recommended for transient calculations, while SIMPLE and SIMPLEC are generally used for steady-state calculations

3.4 Turbulence Models

Turbulence is a phenomenon of great complexity. A turbulence model is a computational procedure to close the system of mean flow equations so that a more or less wide variety of flow problems can be calculated. For most engineering purposes it is unnecessary to resolve the details of the turbulent fluctuations. Only the effects of the turbulence on the mean flow are usually sought. For a turbulence model to be useful in a general purpose CFD code, it must have a wide applicability, be accurate, simple and economical to run. The most common turbulence models are:

Classical Models

These are based on (time-averaged) Reynolds equations and include

1. The Standard k – ε Model
2. The RNG k-ϵ Model
3. The Realizable k-ϵ Model
4. The Reynolds Stress Equation Model

Among the classical models, the k – ε model is the most widely used and validated model so far. This is based on the presumption that there exits an analogy between the action of viscous stresses and Reynolds stresses on the mean flow.

A full discussion of each of these and other models of turbulence is available in the FLUENT manuals (1998). In the following subsections a very brief discussion of each of the above models is presented.

3.4.1 The Standard k – ε Model

This is the most widely used model. It is quite robust in nature. Its main advantages are rapid, stable calculation, and reasonable results for many flows, especially those with high Reynolds number. It is not recommended for highly swirling flows, round jets, or for flows with strong flow separation.

3.4.2 The RNG k – ε Model

It is a modified version of the k – ε model. This model yields improved results for swirling flows and flow separation. It is not well suited for round jets, and is not as stable as the standard k – ε model.

3.4.3 The Realizable k-ϵ Model

Another modified version of the k-ϵ model, the realizable k-ϵ model correctly predicts the flow in round jets, and is also well suited for swirling flows and flows involving separation.

3.4.4 The Reynolds Stress Equation Model

The full Reynolds stress model provides good predictions for all types of flows, including swirl, separation, and round and planar jets. Because it solves transport equations for the Reynolds stresses directly, longer calculations times are required than for the k-ϵ Models. On average, the RSM in FLUENT requires 50-60% more CPU time per iteration compared to the *k*–ε models. For certain cases of jet mixing, the increase in CPU time when using RSM was about 300% compared to that when using the standard k–ε. Further more, 15-20% more memory is needed.

The advantages of RSM include:

- Only initial and/or boundary conditions need be supplied.
- Accurate calculation of mean flow properties and all Reynolds stresses for many simple and more complex flows

The disadvantages of RSM model include:

- Large computing time (seven extra PDE's).
- Behaves similar to $k - \varepsilon$ model in some flows owing to identical problems with the ε-equation modeling (e.g. axisymmetric jets and unconfined recirculating flows).

3.5 The Solution Methodology

(i) Fluid Agitated Tanks

The numerical model in this study were based on a flat base jet agitated tank model proposed by Ahmad (2003).

The solution approach consists of creating a tank geometry in Gambit, defining the boundary and initial conditions, meshing the geometry and exporting it to FLUENT. In FLUENT, the mesh file is read, a solver is chosen, boundary condition, material and operating conditions defined, the parameters initialized and then finally iterated. Afetr the solution converges, the results can be presented as temperature and velocity plots.

(ii) Pipeline with Side-Tees

The use of a tee mixer inevitably causes concentration gradients in the mixed streams that persist for some distance downstream of the injection point. If a tee is used to mix reactants, the effect of those gradients on reactor performance depends upon both the reaction kinetics and the rate constants. If, the fluids are very viscous or the reactions are

fast enough, the product distribution is influenced by the degree of mixedness on the molecular scale in the reaction zone, in addition to the kinetic factor. For infinitely fast reaction, the zone of reaction reduces to the dividing boundary between the A-rich and B-rich regions, where A and B are the reactants. This is because the rate of consumption of the reagents is sufficiently higher than their transport to and from the reaction zone and causes steep concentration gradients between segregated A-rich and B-rich regions and the reaction occur in the narrow zones between these regions. In practice, A-rich and B-rich regions are the eddies and the arrangements which result in the smaller segregation length facilitate micromixing.

Competitive consecutive reactions of the type:

$$A + B \rightarrow R \text{ and } R + B \rightarrow S$$

were studied in tanks and pipelines, where R is the intermediate compound formed. The objective in those studies was to depress R's formation and thus indirectly boost the formation of S (the desired product).

The following reaction is studied in the current study:

$$HCl + NaOH \rightarrow k1 \rightarrow NaCl + H_2O$$

where, k1= $1.3 * 10^8$ m^3/mol.s at 298 K;

The effect of mixing on the reaction is studied in the range $4{,}600 < Re_j < 40{,}000$.

In this work the effects of mixing on the neutralization reaction in a pipeline with side tee, is studied. The HCl enter the main pipe while NaOH is fed from the side tee. The effect of mixing is studied by comparison with non reactive system. Both the reactive and non reactive runs were carried at varying ratios of U_j/U_m.

Chapter 4

Effects of the Tank Bottom Shape on Mixing

4.1 Introduction

The major objective of the current study and the earlier ones by Rakib (2000) and Ahmad (2003) is to provide an efficient design of a jet mixer. Rakib (2000) found that the up-angle and the number of jets reduce the 95% mixing time in a side-pump-around assembly of a cylindrical tank with a flat base. Ahmad (2003) investigated mixing in a bottom-pump-around assembly and found that the jet up-angle and the side-angle (jet asymmetry) reduce the 95% mixing time. Rakib (2000) and Ahmad (2003) investigated mixing in a flat base tank. In this chapter the effects of the shape of the tank base on mixing time are investigated.

Lane and Rice (1981) investigated liquid mixing in a cylindrical tank with a jet at the center of the base. Conductivity was used as the measured variable in determining the 95% mixing time. 95% mixing time is defined as the time at which the value of the measured variable anywhere inside the tank does not vary more than ± 5% from the equilibrium value. Lane suggested the following correlations to calculate the mixing time. The mixing time is a function of the jet velocity, V_j, acceleration due to gravity, g, the liquid height in tank, h, the tank diameter, D, the jet diameter, d_j, and F, mixing time factor (read from the plot of F versus the jet Reynolds number, Re_j). For a flat base tank:

$$t_{95} = F * (h^{0.50}D)/((V_j d_j)^{0.667}\, g^{0.166}) \qquad (4.1)$$

and for a hemispherical base tank:

$$t_{95} = F * (h^{0.50}D^{0.75})/((V_j d_j)^{0.5}\, g^{0.25}) \qquad (4.2)$$

Lane and Rice (1981) suggested that the mixing time was dependent on the jet Reynolds number. The same was also suggested by Fox and Gex (1956). This dependence is shown in the calculation of the factor F in both of the above equations.

Lane and Rice (1982) investigated the flow characteristics of a submerged bounded jet in a closed system. Different designs were used for this purpose namely, an axial vertical jet with a hemispherical base cylindrical tank, an axial vertical jet in a flat base cylindrical tank and an inclined side entry jet in a flat based cylindrical tank. Lane and Rice (1982) reported that 95% mixing time for a cylindrical tank with a hemispherical base is shorter than that for a flat based cylindrical tank of the same volume.

Zughbi and Rakib (2000), Rakib (2000) and Jayanti (2001) simulated various mixing vessel configurations and showed that minimizing the low velocity or dead zones reduced the mixing time. Investigation of the hydrodynamics of the mixing process proved that circulation patterns were characteristics of a given geometry and it was the sole cause of dead or low velocity zones. Jayanti (2001) concluded that there exists a shape which optimizes the mixing time. He observed the low velocity regions at the bottom of the flat bottom vessel and that it took long time for complete mixing because of slow flow in this zone. The low velocity zones could be minimized or even eliminated by making the bottom shape more streamlined such as a hemispherical, an ellipsoidal or a conical base (with half cone angle of 31^{o} and 58^{o}). In these cases, the volume was maintained as in the flat bottom tank. It was observed that the mixing time varied with the different shaped bottoms. Of the various shapes investigated, Jayanti concluded that a half cone angle of 31^{o} gave the least mixing time, for shorter vessels. Simulations results

indicated that better mixing times were obtained for greater liquid height to tank diameter (H/D) ratio, and that optimum configurations for a given vessel characteristics (tank diameter, D and liquid height, H) were not universal and depended on flow patterns created within the vessel.

The above literature clearly indicates that the shape of the tank bottom affects the flow patterns created inside a given geometry and hence the extent of mixing. The H/D ratio is also observed to have a considerable effect on the mixing patterns (Lane 1981, Grenville and Tilton 1996, Ahmad 2003). The mixing time could, therefore, be optimized by careful consideration of the different shapes of the tank bottom.

In this study, mixing in cylindrical tanks with hemispherical and conical bottoms have been numerically investigated. 95% mixing times were compared and the geometry which optimized the mixing time identified. Before any choice of a particular geometry was made, the solution independence of the grid and time step sizes was established for different tank geometries. The optimum grid spacing and time step size were identified and used for further simulation.

4.2 The Numerical Model

Ahmad (2003) developed a model for a flat bottom tank with a symmetric jet to study the effect of the geometry on mixing in liquid jet agitated tanks. In this model, the symmetric jet passed through a central plane of the tank. The tank outlet was located at the tank bottom, 2.5 cm from the tank wall, while the liquid jet inlet was located at the edge of the tank bottom at 45^{o} to the horizontal. This model was numerically validated against experimental results. The degree of mixing was expressed in terms of a measured variable, the conductivity, and recorded at selective points. These monitoring points were

chosen at positions in the tank space where mixing time was expected to be longest, based on experience and simulation results. Numerical calculations of 95% mixing time were carried out using a mesh spacing of 10 mm and a time step size of 1 second. Simulations were carried out for a wide range of the jet Reynolds number. The velocity of the entering jet was monitored as the area weighted average at the jet inlet to the tank.

This study simulates mixing in a tank with hemispherical and conical bottoms, agitated by a symmetric jet. These models are based on a flat base jet agitated tank, numerical model developed and validated by Ahmad (2003). Tank geometries with different inlet and outlet positions for the case of hemispherical bottom, for different mesh spacings, were created and simulations carried out using various time step sizes. A known volume of a hot fluid was introduced as a tracer and the temperature was monitored at different points throughout the whole tank volume. The temperature distribution at each corresponding time step was processed and the 95% mixing time computed. Simulations were carried out using the general purpose three dimensional, CFD package FLUENT. The solution independence of the size of mesh and the time step was established by carrying out a number of parametric runs with a number of mesh sizes and time step sizes. A case with an asymmetric jet agitated flat bottomed tank and a jet Reynolds number of 15,000, was simulated. The mixing time of 55 seconds came in agreement with the result of Ahmad (2003).

4.2.1 Effect of the Mesh Size

In order to reduce the impact of numerical error in the study of mixing, the solution needs to be independent of the mesh size. To establish the grid independence of the numerical solution, the geometry for the symmetric jet agitated tank with a hemispherical bottom was meshed with various spacings and the results closely analyzed. When the results of two consecutive mesh sizes were found to be close enough, the larger of the two grids, to save computational time, was chosen. For a more stringent approach the smaller one could also be chosen. This mesh size is referred as the optimum.

The tank geometry was meshed with spacing of 9, 10, 11 and 12 mm respectively, and each case was simulated. Temperature values were plotted on two different lines namely x central line and z central line. A central x-line join (-0.15,0,0) and (0.15,0,0) horizontally whereas a z-line joins (0, 0, -0.15) to (0, 0, 0.15) also horizontally but perpendicular to the x-line. Temperature values were numerically obtained for points on these lines. When the solution does not significantly change for two mesh sizes, the larger of the two sizes was chosen. A similar approach was followed in order to choose the size of the time step.

Figure 4.1 (a) shows plots of temperature versus the position along the x and z lines. It is observed that the temperature values corresponding to the mesh spacing of 9, 10 and 11 mm show close agreement (for the corresponding x co-ordinates) and the same was observed in Figure 4.1 (b) for the position along the z line. Table 4.1 summarizes the results, namely the total number of cells and the 95% mixing time for the various mesh sizes. From Figure 4.1 and Table 4.1 it can be concluded that for a mesh size of 10mm,

the solution dependence on mesh size is minimal and therefore this mesh size is used for subsequent runs.

Table 4.1: Mesh size, number of cells and 95% mixing time corresponding to position 3 as the inlet.

Mesh Size (mm)	12	11	10	9
Number of cells	83, 392	126, 345	147, 944	209, 325
95% Mixing Time (s)	55	49	51	46

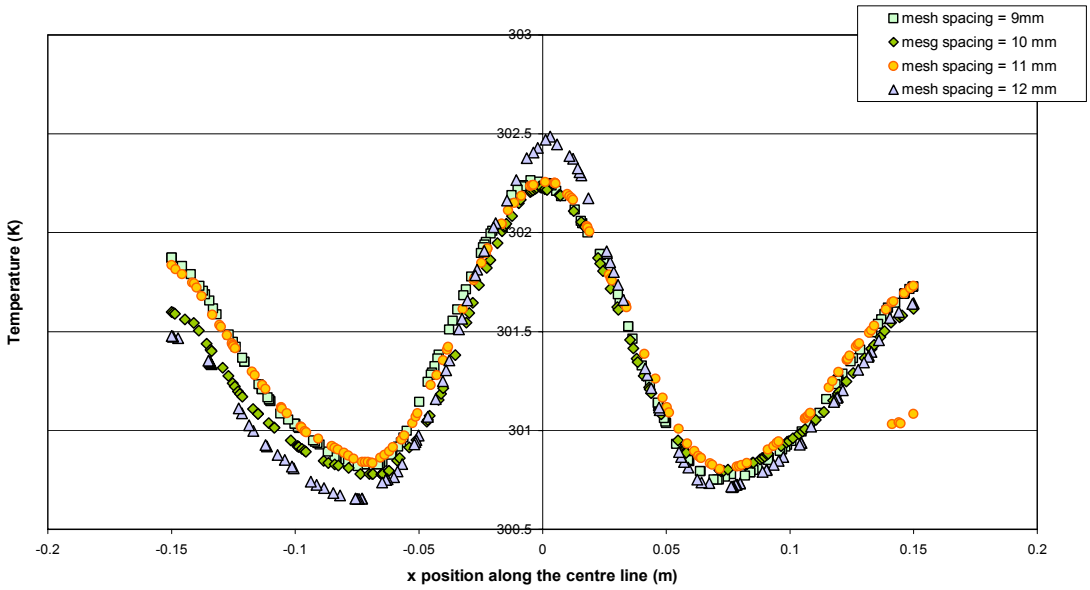

(a)

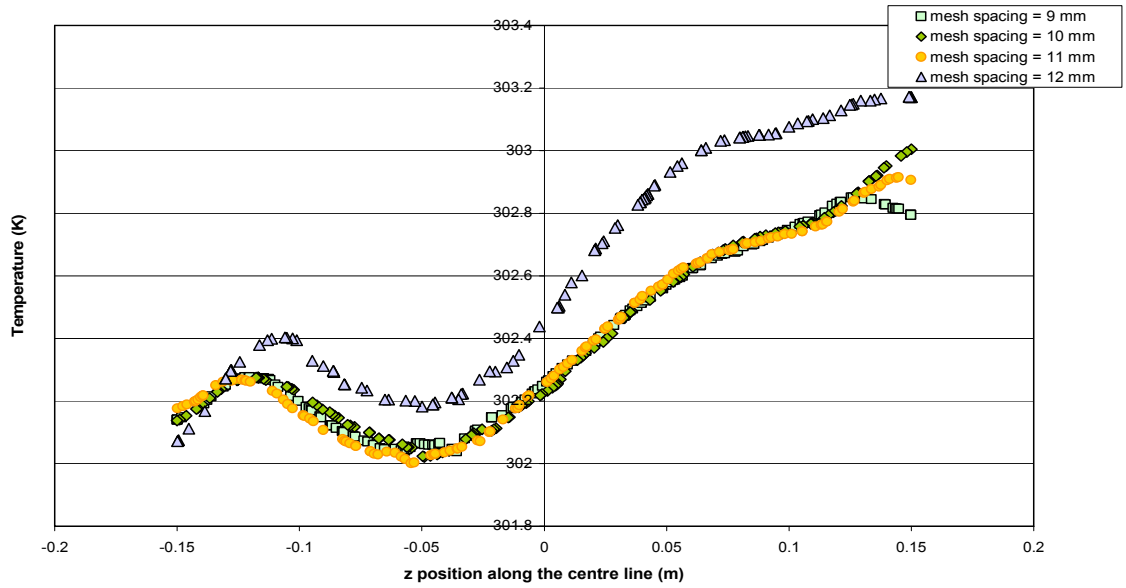

(b)

Figure 4.1: Temperature plots along the centre lines for various mesh sizes for a symmetric jet, liquid jet agitated hemispherical shaped bottom tank, for a jet inlet positioned at the edge.

4.2.2 Effect of the Time Step Size

As in the previous section, an x-centerline joining (-0.15, 0, 0) and (0.15, 0, 0) was marked in the tank geometry and temperature plotted against the x position. The temperature values were plotted for time step sizes of 0.5, 1 and 2 seconds. From Figure 4.2 it is observed that the temperature values corresponding to 0.5 and 1 second differ by 0.01 K or less. Thus the solution is assumed to be independent of the time step size, for a step size of 1 second. The temperature profiles correspond to a run time of 20 seconds, a time period found to be sufficient for the flow to become fully developed. Table 4.2 shows the total number of cells and the 95% mixing time for time step sizes of 2, 1 and 0.5 seconds. Based on these results, a time step size of 1 second is chosen as the optimum.

Table 4.2: Time Step size, number of cells and 95% mixing time corresponding to position 3 as the inlet for a mesh spacing of 10 mm

Time Step Size (s)	2	1.0	0.5
Number of cells	147, 944	147, 944	147, 944
95% Mixing Time (s)	54	51	50

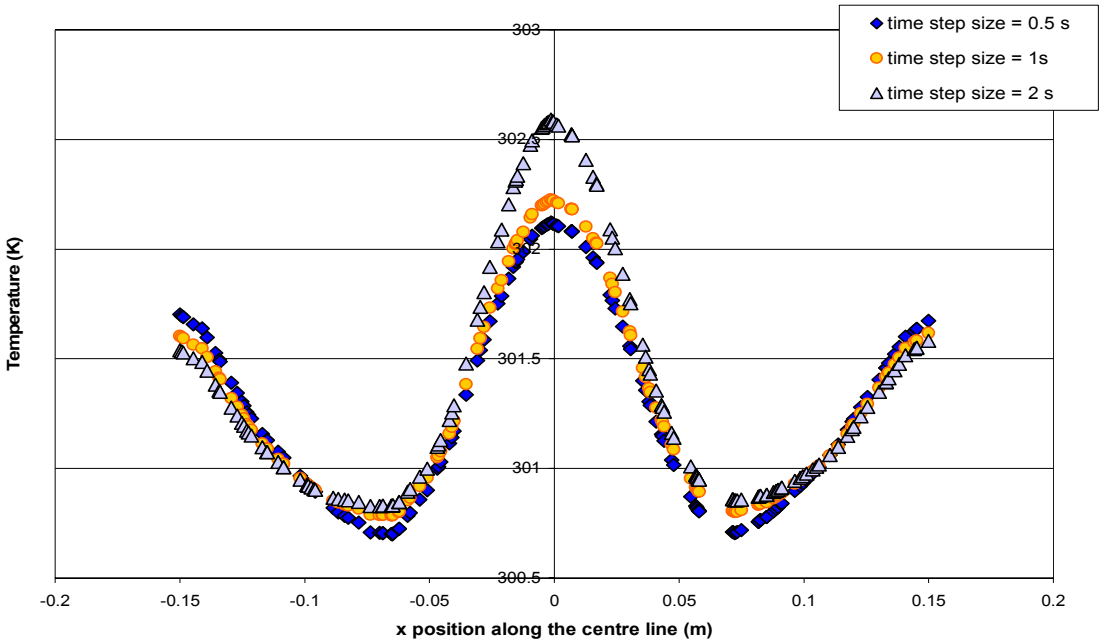

(a)

Figure 4.2: Temperature plots along the centre lines for various time step sizes for a symmetric jet, liquid jet agitated hemispherical shaped bottom tank.

4.2.3 Effects of Various Inlet and Outlet Combinations on Mixing in a Cylindrical Tank with a Hemispherical Base

The effects of various possible combinations of inlet and outlet positions on mixing in a hemispherical bottom tank, were investigated. The outlet was kept at center-bottom of the hemisphere. The inlet to the tank was moved from the edge (where the vertical cylinder and the hemispherical base meet) to a position near to the outlet, always making an angle of 45^{o} with the horizontal plane. These inlet positions were referred to positions 1, 2, 3 and 4, as shown in Figures 4.3 a, b, c and d. Other combinations where the jet outlet was moved from the center of the hemisphere to a distance of D/4 (D, tank diameter) from the right end of the vessel were also tested. These positions are shown in Figure 4.4 a, b, c and d are referred as positions 5, 6, 7 and 8. All cases were run for a jet Reynolds number of 15,000. The 95% mixing time for a tank with inlet positions 1, 2, 3 and 4 were 44, 73, 51 and 67 seconds, respectively. The outlet position in each case was located at the lowest point of the tank, corresponding to the centre of the tank bottom. The 95% mixing time corresponding to the position 1 was found to be the lowest in comparison with the with the other inlet positions. Likewise, different hemispherical bottom tank geometries for various inlet positions but for an outlet position placed at a horizontal distance of D/4 from the tank's edge, were generated and numerically simulated. The 95% mixing time corresponding to the inlet positions 5, 6, 7 and 8 was found to be 47, 83, 51 and 61 seconds, respectively.

The outlet at the centre bottom, the lowest point contributes significantly to the reduction of the low velocity zones in tank. This is because of the fluid flowing in from all directions, it being the lowest point in the whole geometry. Velocity vectors and

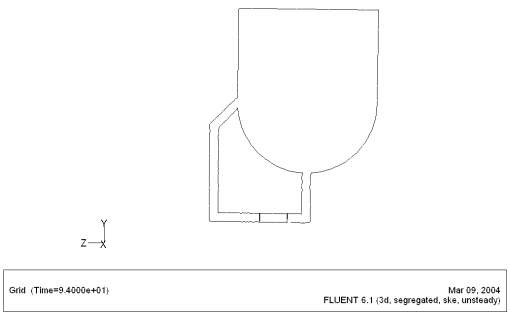

Position 1:(a)

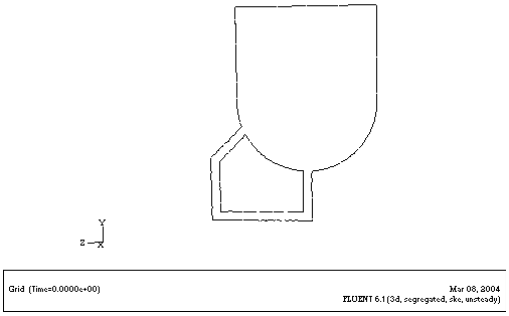

Position 2: (b)

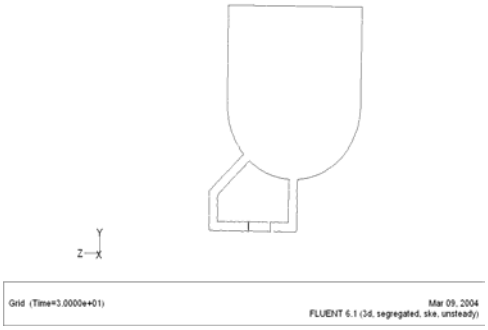

Position 3: (c)

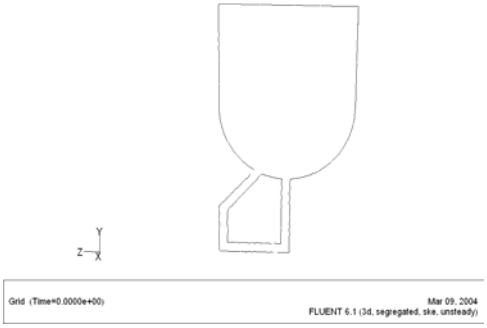

Position 4: (d)

Figure 4.3: Geometries with different inlet positions for an outlet at the centre-bottom of the hemispherical base

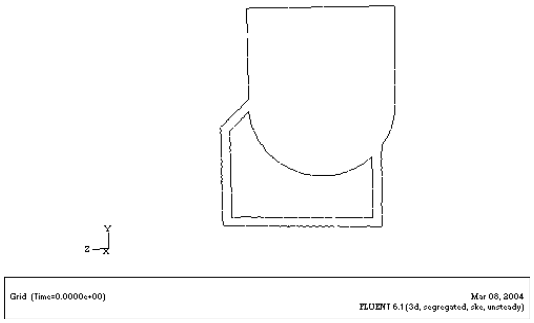

Position 5: (a)

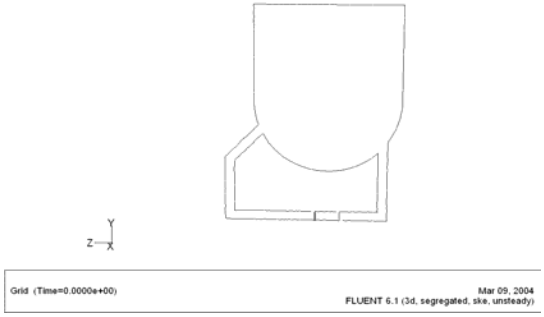

Position 6: (b)

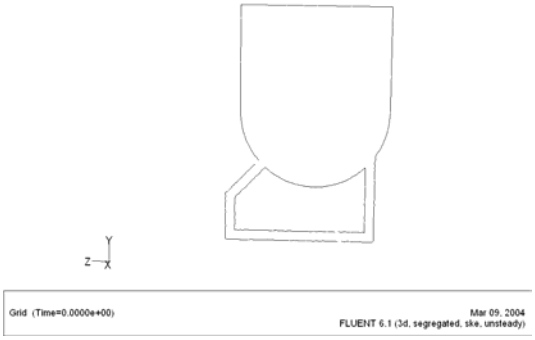

Position 7: (c)

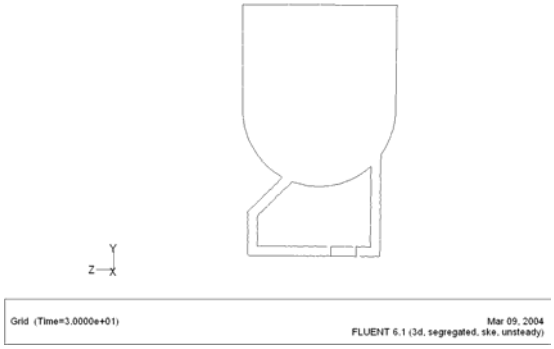

Position 8: (d)

Figure 4.4: Geometries with different inlet positions for an outlet positioned at a horizontal distance of D/4 from the right side.

contours of magnitude less than 0.3 m/s are plotted in Figures 4.5 to 4.12, though the maximum velocity encountered in the system was 1.13 m/s. This was done so as to locate any dead or low velocity zones, which took longest to mix.

Figures 4.5 to 4.12 correspond to the jet inlet located at position 1, 2, 3 and 4, respectively, for the same tank outlet position. Figures 4.5a, and 4.6a, show that the low velocity zone is located at the top centre of the part of the tank, where the velocity is in the range of 0.0025 to 0.003 m/s. Figures 4.5b and 4.6b show the positions of the low velocity zones to the upper centre, right and left halves of the tank. Whereas in Figures 4.6a and 4.7a somewhat extensive low velocity zone exists in the top right corner and extends to the bottom of the tank. Figures 4.7a and 4.8a show the occurrence of low velocity zones in the upper half (just above the jet trajectory), upper left corner and also towards the bottom of the tank.

Figures 4.7b and 4.8b show shifting of the low velocity zones toward the bottom of the tank. Low velocity zones are now no more located in either the right or left corners because the jet flushes them out after it connects to the right wall. Likewise in Figure 4.9a and 4.10a, the entering jet strikes the opposite wall, and connects to it creating a low velocity zone in the upper half of the tank. Figure 4.9b and 4.10b clearly depict how the entering jet connects to the wall in the lower half of the tank, leaving behind extensive low velocity zones. The extent of the low velocity zones in the fluid body indicates the variation of the 95% mixing time with the inlet position (from 1 to 4 positions). It is noted that in all cases, the mixing time varies with the generated flow patterns.

Figure 4.11 and 4.12 show the location of low velocity zone in the centre of the tank, which extends from the left end to the right end.

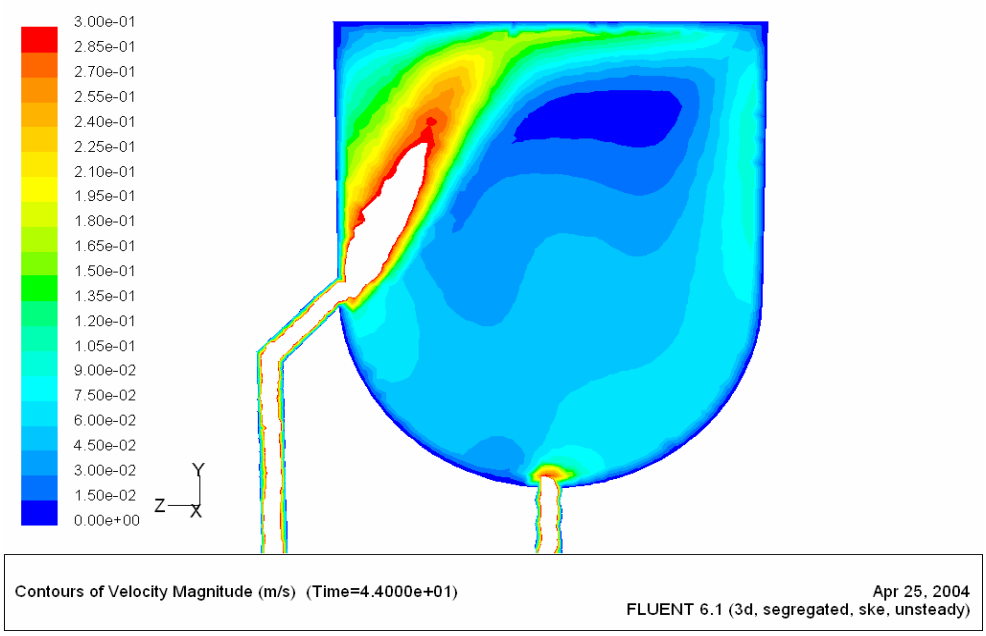

(a)

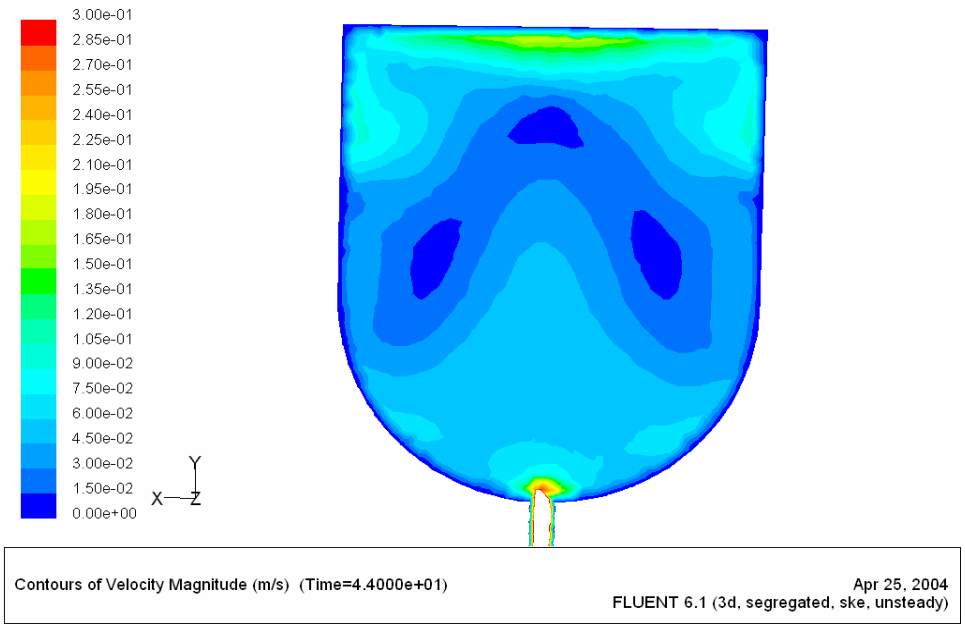

(b)

Figure 4.5: Velocity contours in a hemispherical bottom tank showing zones of low velocity for a jet position 1: (a) in a plane passing through the jet inlet and outlet and (b) in a plane normal to the plane of the jet inlet and outlet.

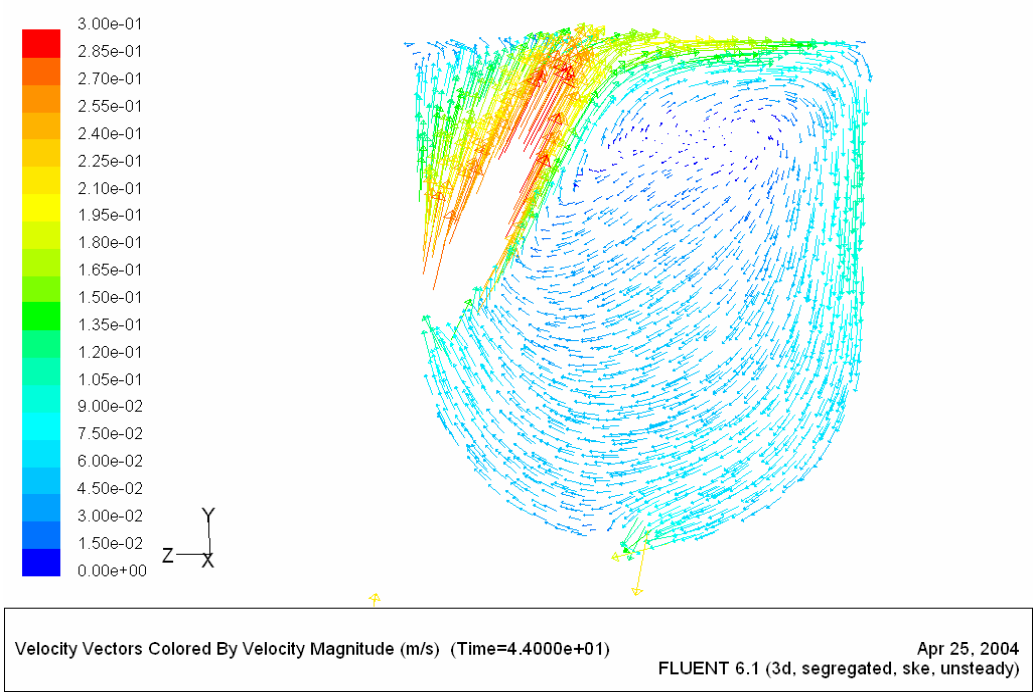

(a)

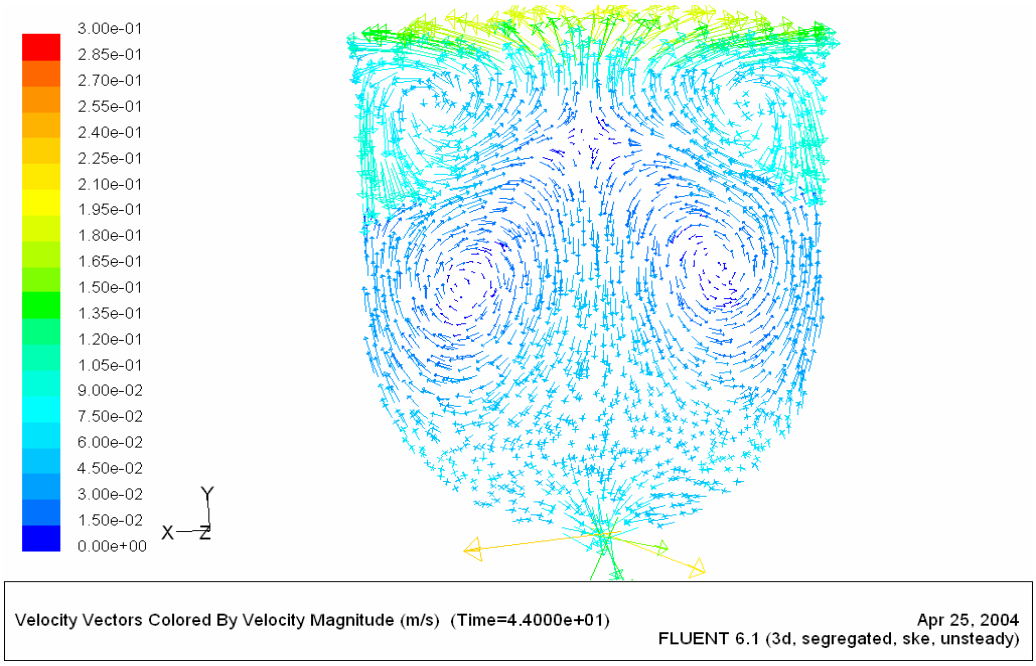

(b)

Figure 4.6: Velocity vectors in a hemispherical bottom tank showing zones of low velocity for a jet position 1: (a) in a plane passing through the jet inlet and outlet and (b) in a plane normal to the plane of the jet inlet and outlet.

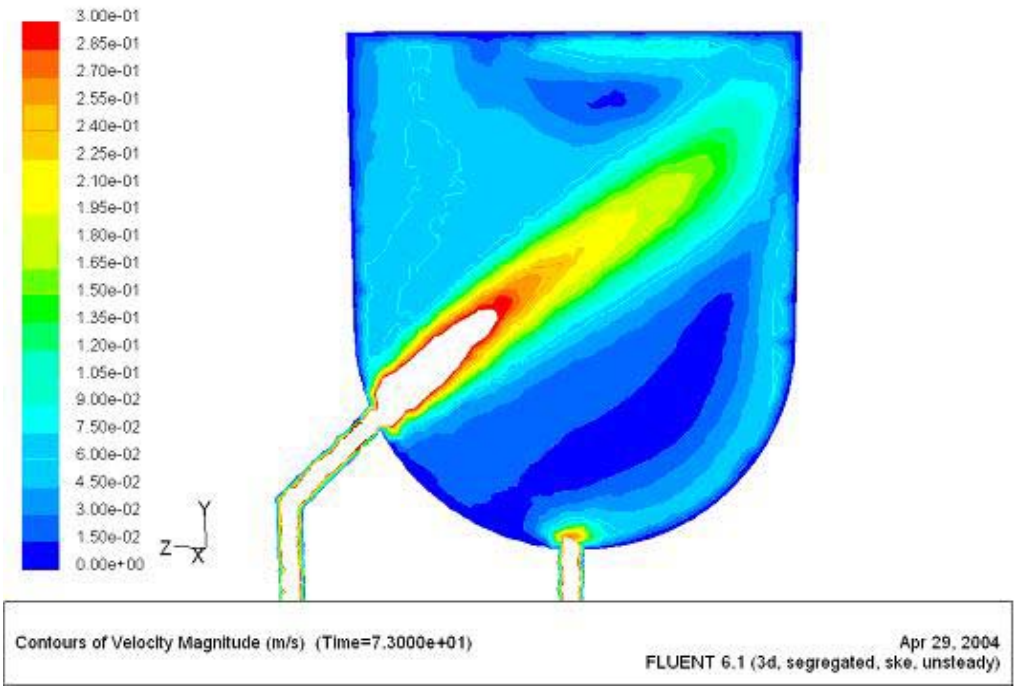

(a)

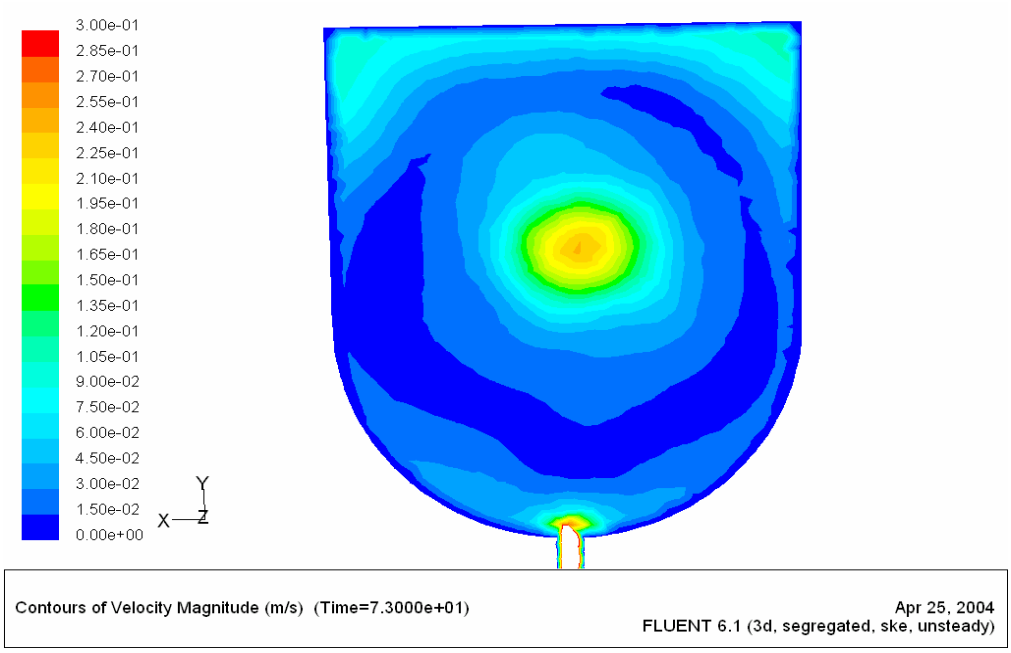

(b)

Figure 4.7: Velocity contours in a hemispherical bottom tank showing zones of low velocity for a jet position 2: (a) in a plane passing through the jet inlet and outlet and (b) in a plane normal to the plane of the jet inlet and outlet.

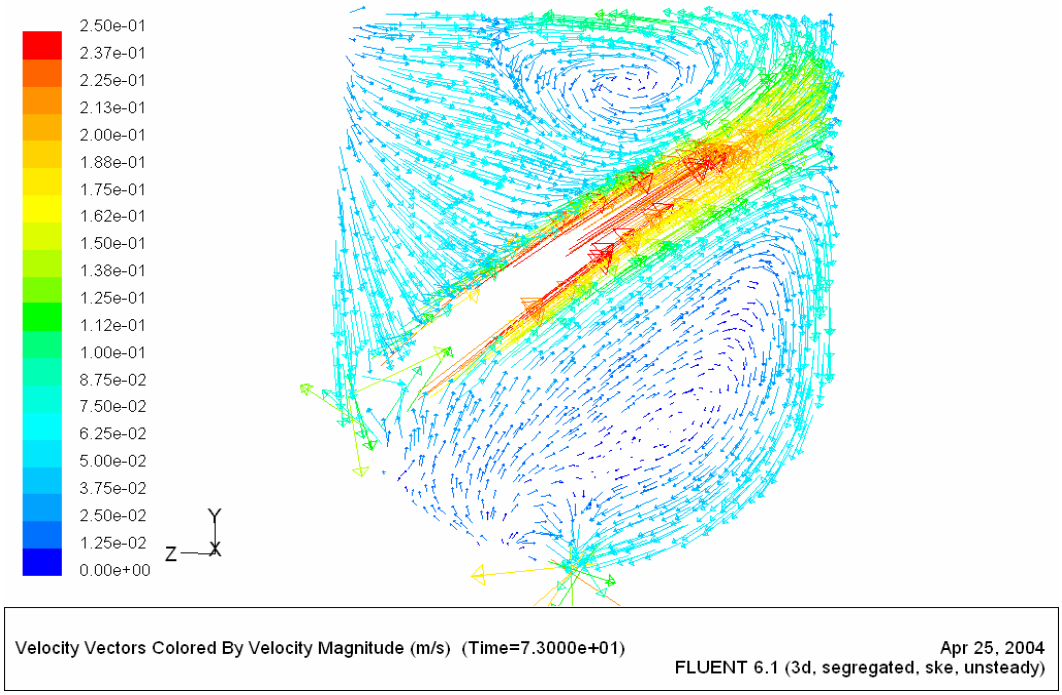

(a)

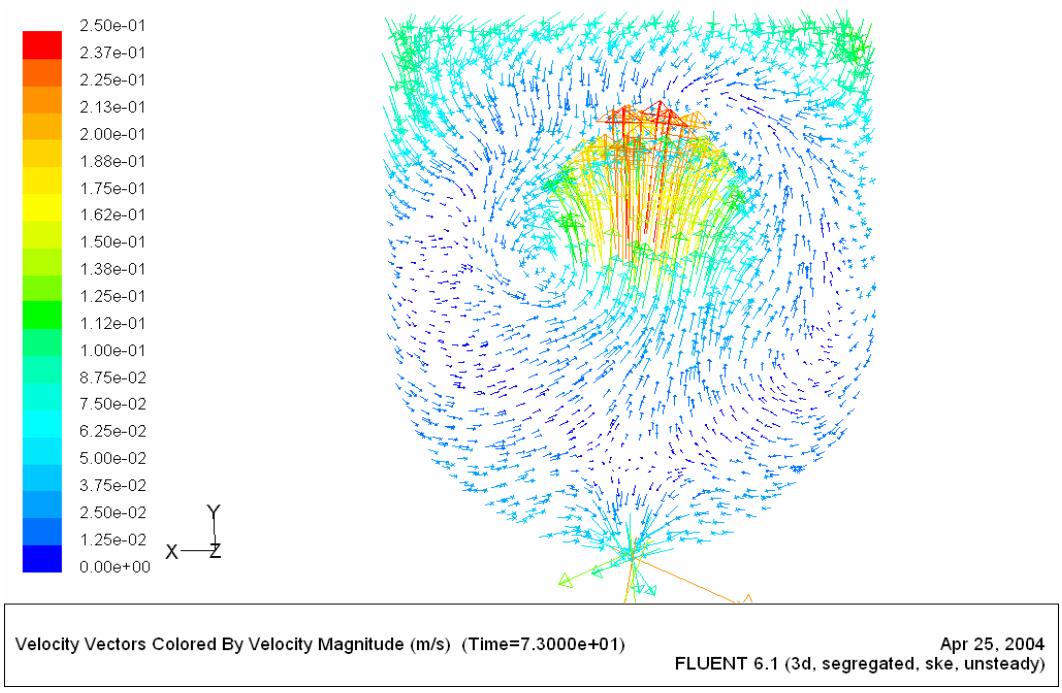

(b)

Figure 4.8: Velocity vectors in a hemispherical bottom tank showing zones of low velocity for a jet position 2: (a) in a plane passing through the jet inlet and outlet and (b) in a plane normal to the plane of the jet inlet and outlet.

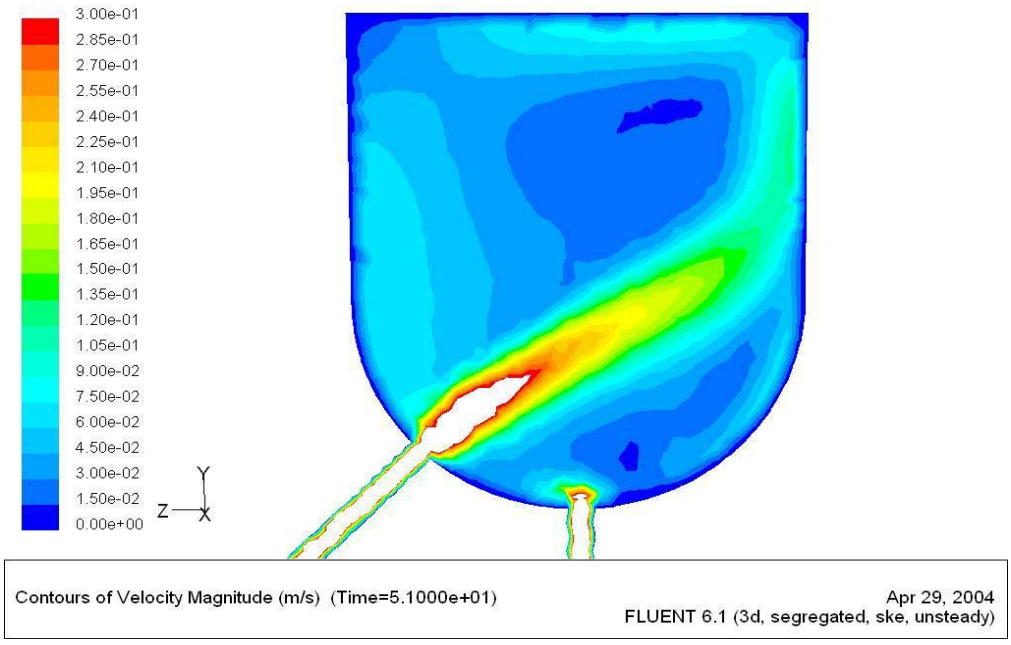

(a)

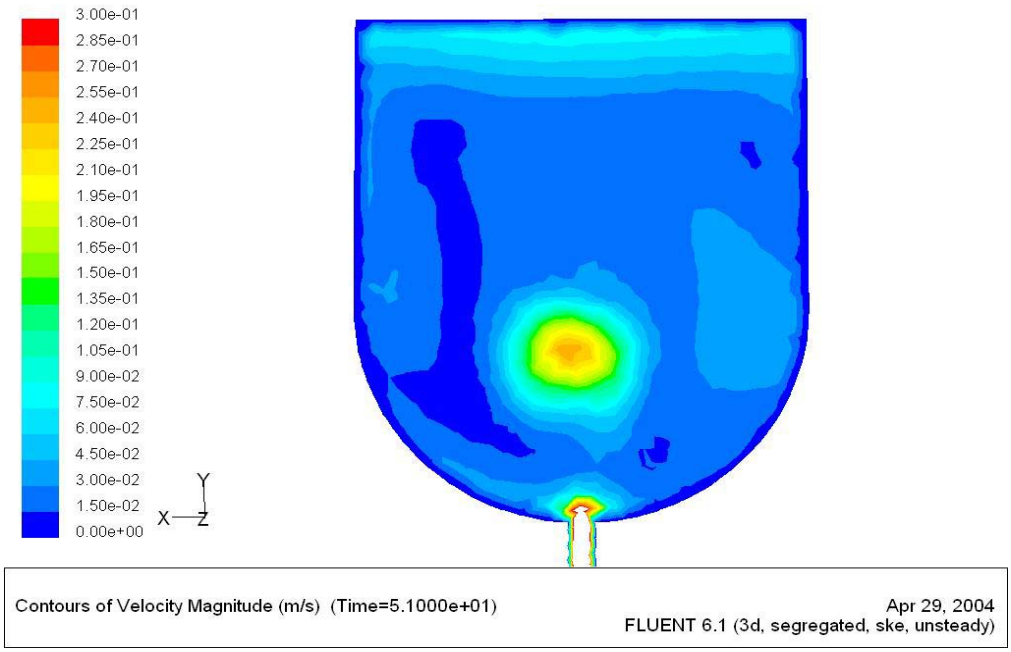

(b)

Figure 4.9: Velocity contours in a hemispherical bottom tank showing zones of low velocity for a jet position 3: (a) in a plane passing through the jet inlet and outlet and (b) in a plane normal to the plane of the jet inlet and outlet.

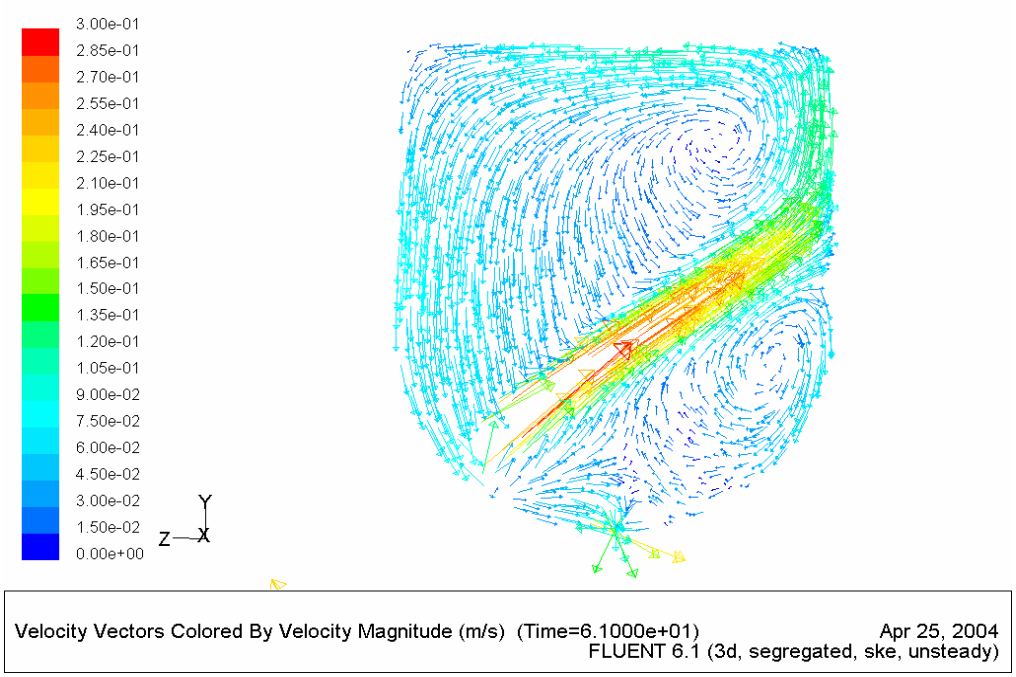

(a)

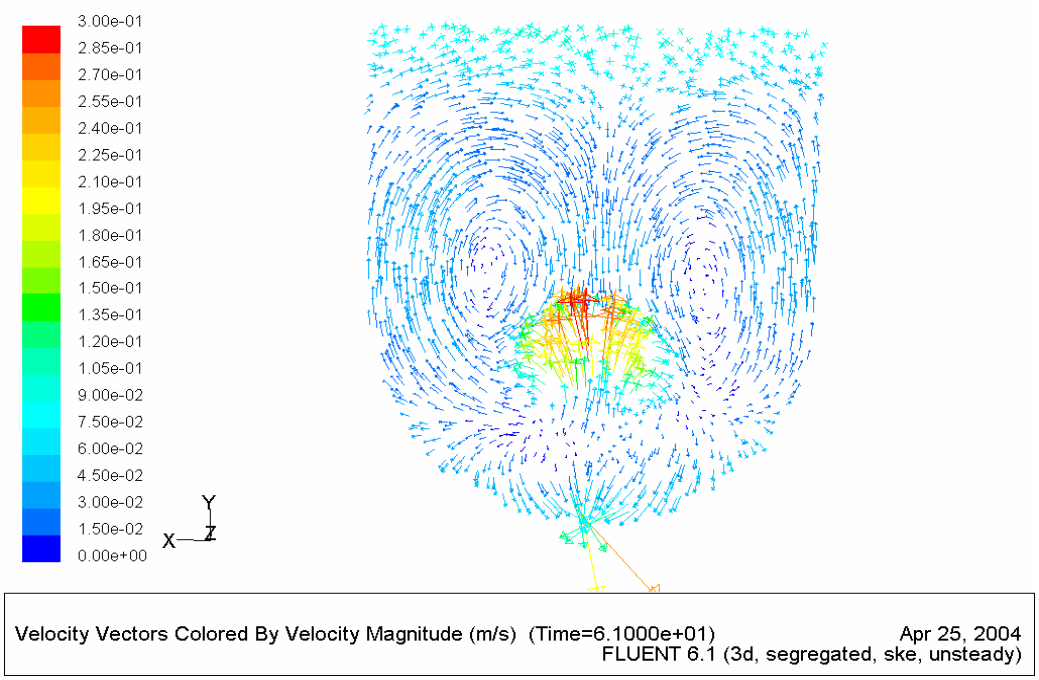

(b)

Figure 4.10: Velocity vectors in a hemispherical bottom tank showing zones of low velocity for a jet position 3: (a) in a plane passing through the jet inlet and outlet and (b) in a plane normal to the plane of the jet inlet and outlet.

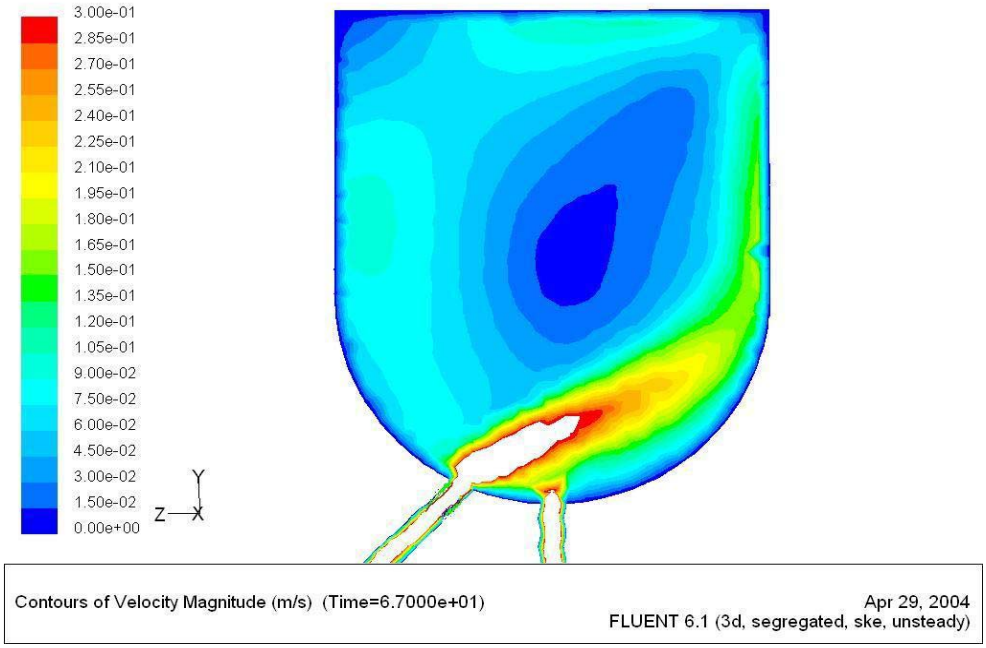

(a)

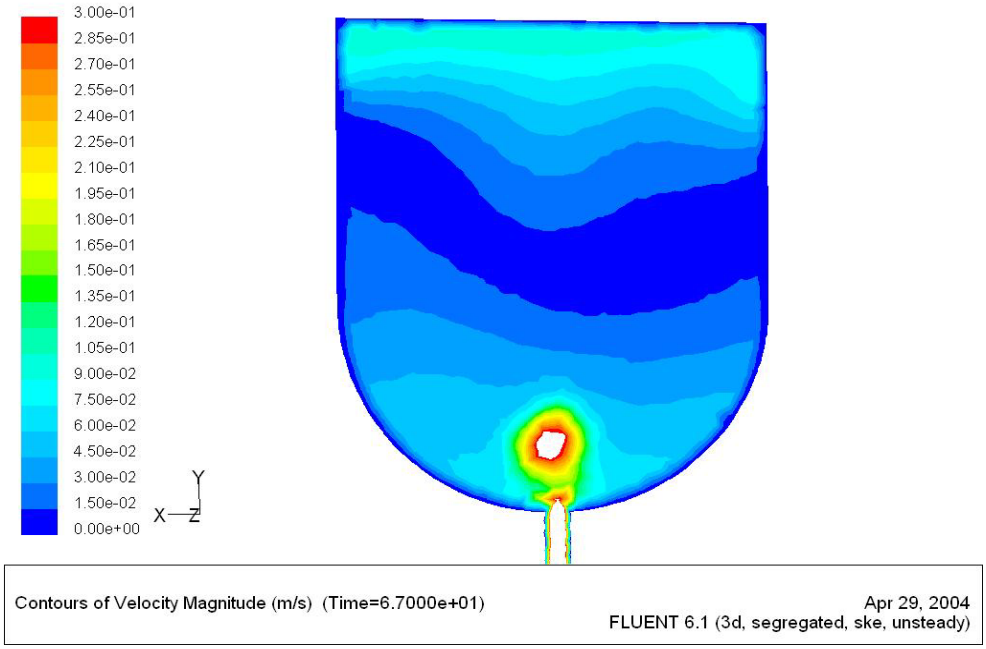

(b)

Figure 4.11: Velocity contours in a hemispherical bottom tank showing zones of low velocity for a jet position 4: (a) in a plane passing through the jet inlet and outlet and (b) in a plane normal to the plane of the jet inlet and outlet.

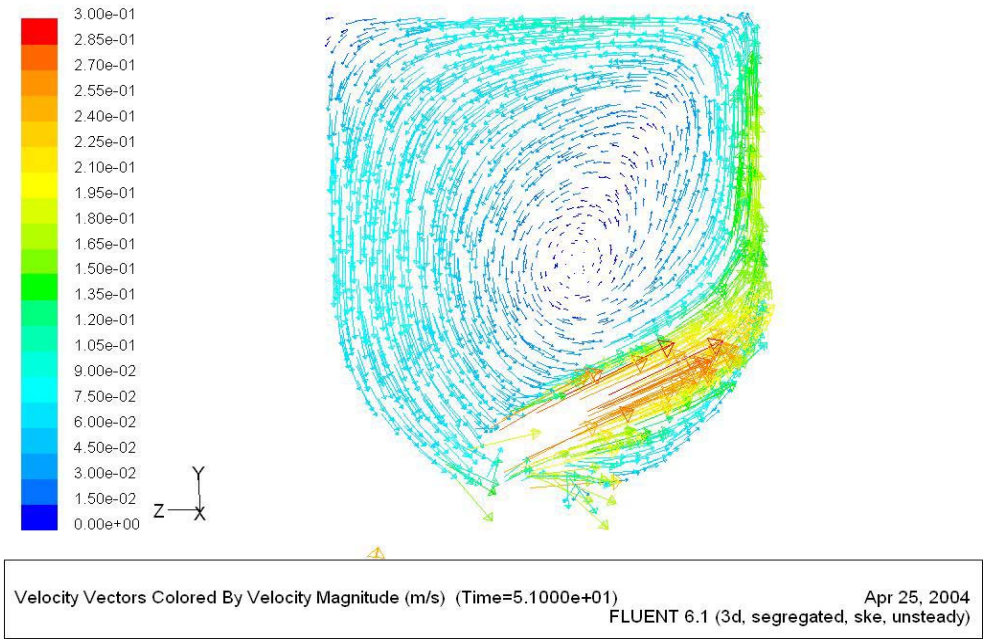

(a)

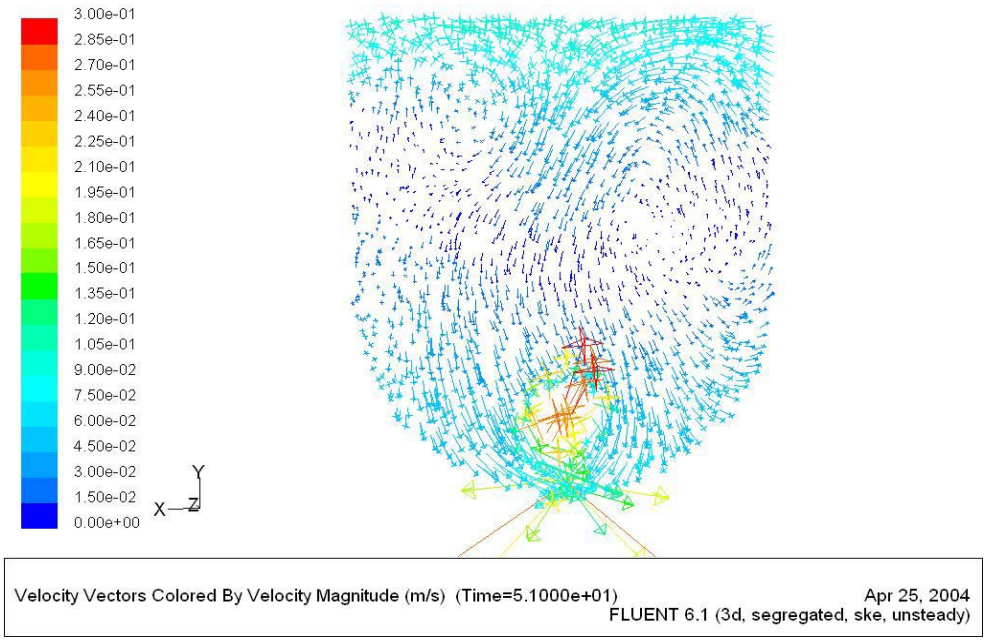

(b)

Figure 4.12: Velocity vectors in a hemispherical bottom tank showing zones of low velocity for a jet position 4: (a) in a plane passing through the jet inlet and outlet and (b) in a plane normal to the plane of the jet inlet and outlet.

All figures correspond to simulation results with a jet Reynolds number of 15,000, a mesh spacing of 10 mm and a time step size of 1 second. Since the tank contents reached 95% mixing criteria earliest, corresponding to the inlet position 1 and outlet at the centre bottom, therefore this inlet and outlet combination was chosen for all subsequent runs. Table 4.3 corresponds to the 95% mixing time for the various inlet positions and outlet located at the center of the hemispherical tank bottom. Whereas Table 4.4 summarize the mixing time values for the same inlet positions (as in Table 4.3) but with an outlet positioned at a distance of D/4 (D, tank diameter) from the tank edge.

4.3 Comparison of Flat and Hemispherical Bottoms

Figure 4.13, shows a comparison, of the 95% mixing time for a tank with a flat base (Ahmad, 2003) and one with a hemispherical bottom. The inlet jet in the proposed model made an angle of 45^{o} with the horizontal as that used by Ahmad (2003). This figure shows a 25% reduction in t_{95} for a Re_j of 9,000 and 18% for a Re_j of 40,000. However, according to Jayanti (2001), t_{95} for a hemispherical base tank is 40% less than t_{95} for a tank base. Figure 4.14 shows a comparison between the mixing times calculated using the Lane's correlation and the current simulation values of the hemispherical model. Lane's correlation under-predicts t_{95} for the whole range of Reynolds number. Lane deduced his 95% mixing time (t_{95}) mixing time by measuring conductivity at a given point while in the numerical simulation, t_{95} was calculated based on mixing in the whole tank.

Table 4.3: The 95% mixing time for various inlet positions and an outlet located at the center of the hemispherical bottom.

Time Step size (s)	1	1	1	1
Inlet position	1	2	3	4
95% Mixing Time (s)	44	73	51	67

Table 4.4: The 95% mixing time for various inlet positions and an outlet located at a distance of D/4 from the tank edge of the hemispherical bottom.

Time Step size (s)	1	1	1	1
Inlet position	1	2	3	4
95% Mixing Time (s)	47	83	51	61

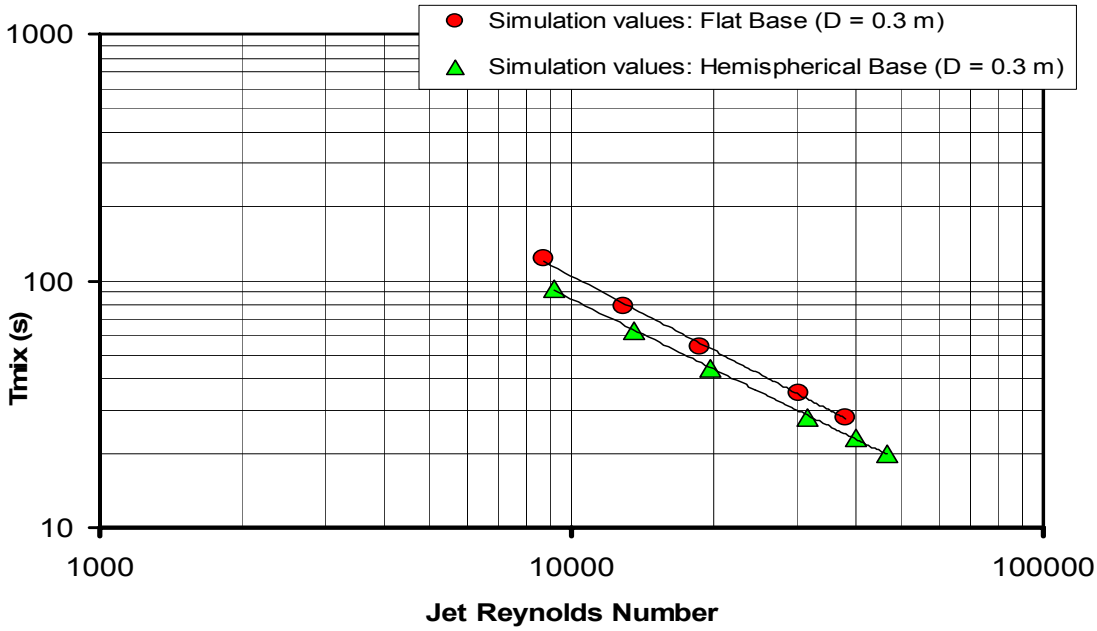

Figure 4.13: A plot of 95% mixing time (corresponding to Ahmad (2003) and the proposed symmetric jet agitated tank with a hemispherical shaped bottom) versus jet Reynolds number

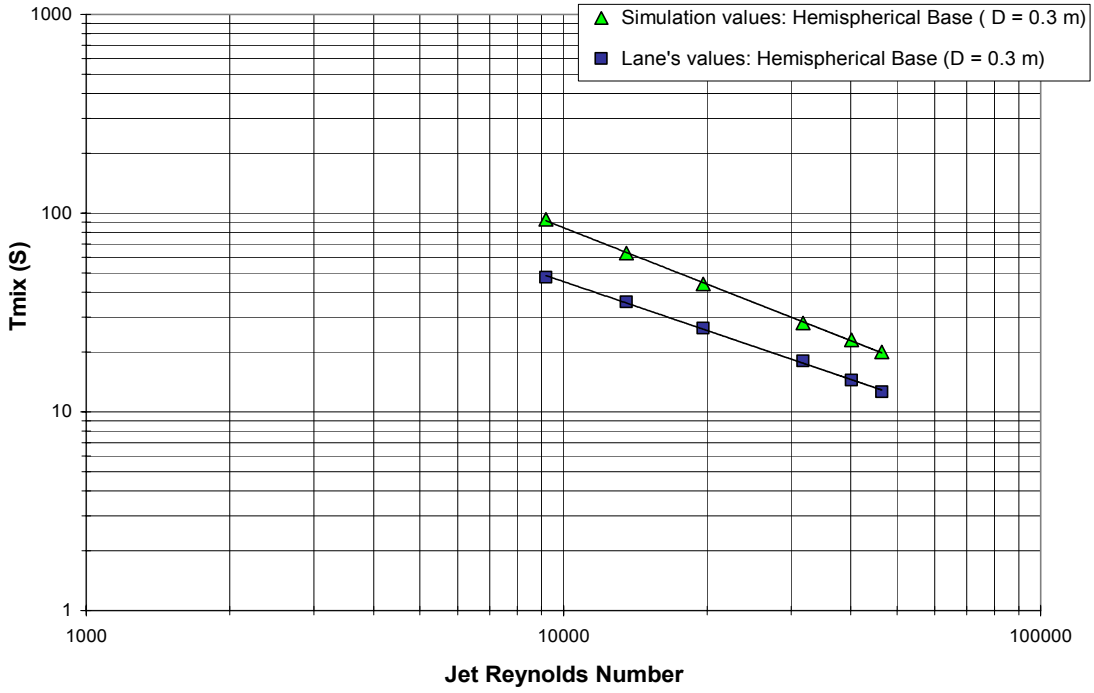

Figure 4.14: A plot for 95% mixing time (simulation values and Lane's correlation values) versus jet Reynolds number

4.4 Results for Tanks with Conical Base

Simulations for various designs as cited by Jayanti (2001) for cylindrical tanks with various cone base angles, were carried out. For this purpose, tank geometries with cone angles of 31, 58 and 116 degrees were created. Figure 4.15 gives the various designs of the mixing tank with a conical bottom. Figure 4.16 shows that the mixing time increases slightly as the cone base angle changes from 116 to 58^{o}. 95% mixing time (t_{95}) starts to decrease as the cone base angle is changed to 31. This is explained in Figure 4.17. However the effect of the cone base angle on the mixing time tends to decrease as the jet Reynolds number increases. This is because at high jet Reynolds number, higher turbulence exists inside the geometry and so any further increase in the turbulence does not affect the mixing times to the same extent as it did previously.

4.5 Comparison of Mixing Times of Hemispherical, Flat and Conical Bottomed Tank

Figure 4.18 shows the mixing time plots for the various shaped bottom tanks. It is observed that the mixing times for the hemispherical shape are substantially lower than those for a flat base (18% to 25%). For conical bases, the investigated cone angles, 31, 58 and 116 degrees, encountered lesser 95% mixing times as compared to tank with flat base. It was observed that 116 degree corresponded to the least of all the three. Conical base tank had lower mixing time by 42% (at Re_j of 9,000) to 29% (at Re_j of 40,000) than the flat base tank with the same volume.

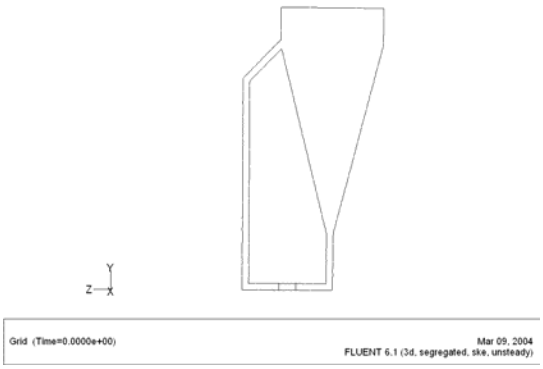

(a)

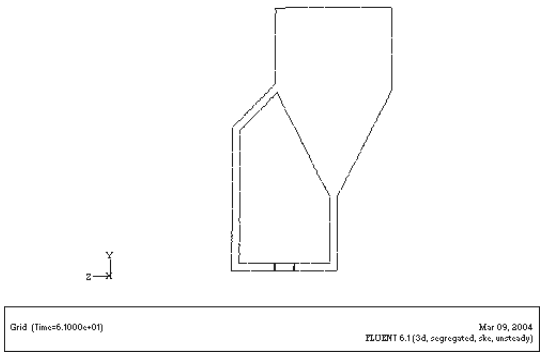

(b)

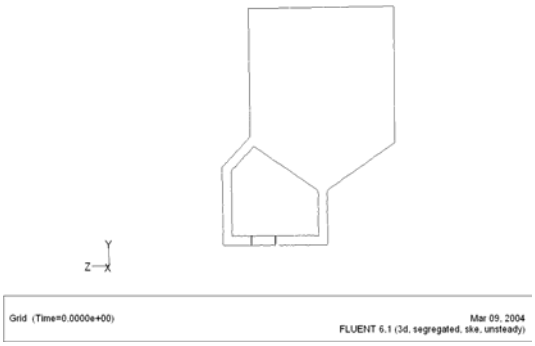

(c)

Figure 4.15: Geometries with various base angles for a conical bottom and an outlet positioned at the vertex of the cone: (a) a cone angle of 31 degrees, (b) 58 degrees and (c) 116 degrees.

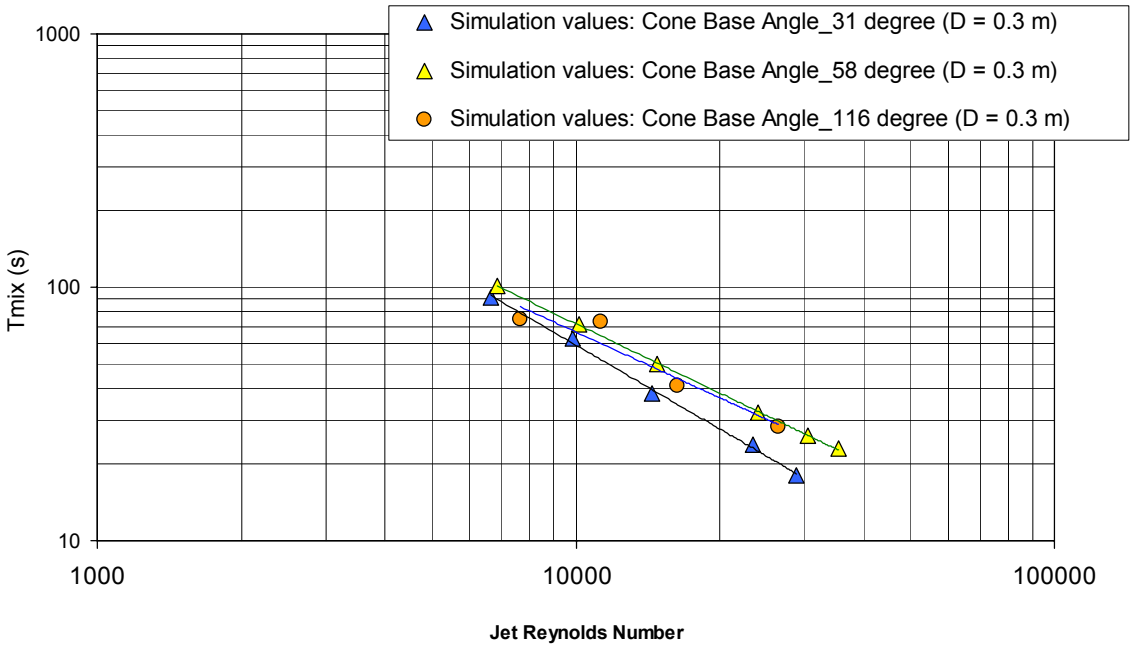

Figure 4.16: A plot of the 95% mixing time (for cone base angles of 31, 58 and 116 degrees) versus jet Reynolds number

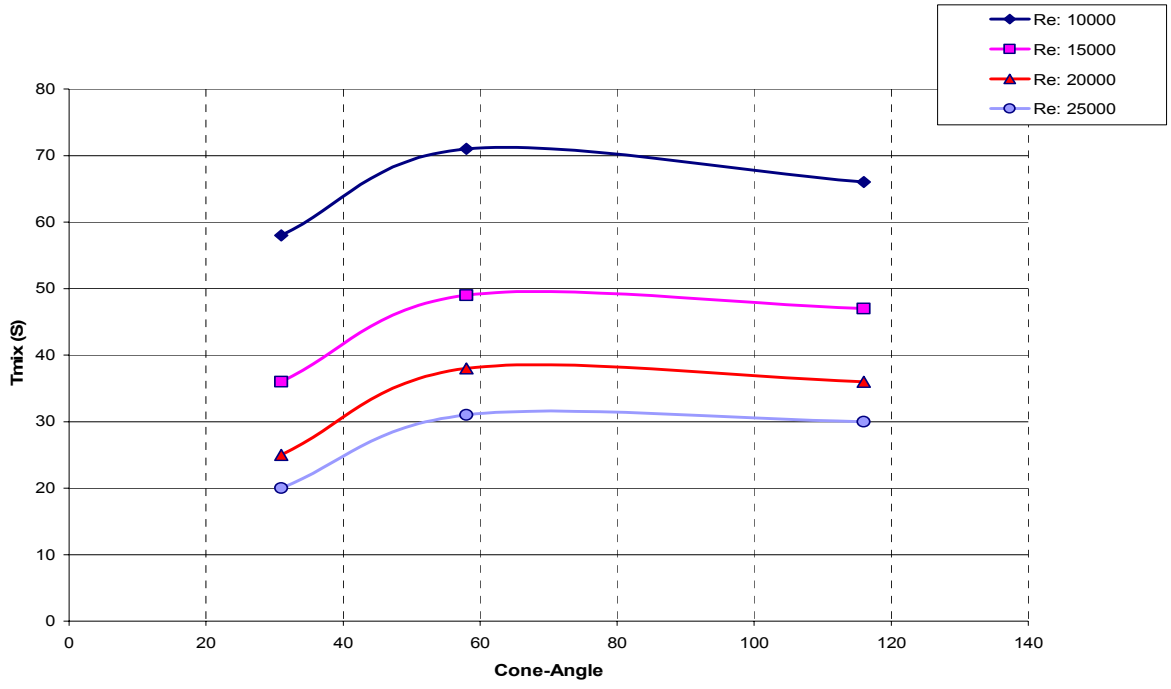

Figure 4.17: A plot of the 95% mixing time versus cone base angle for a cylindrical tank.

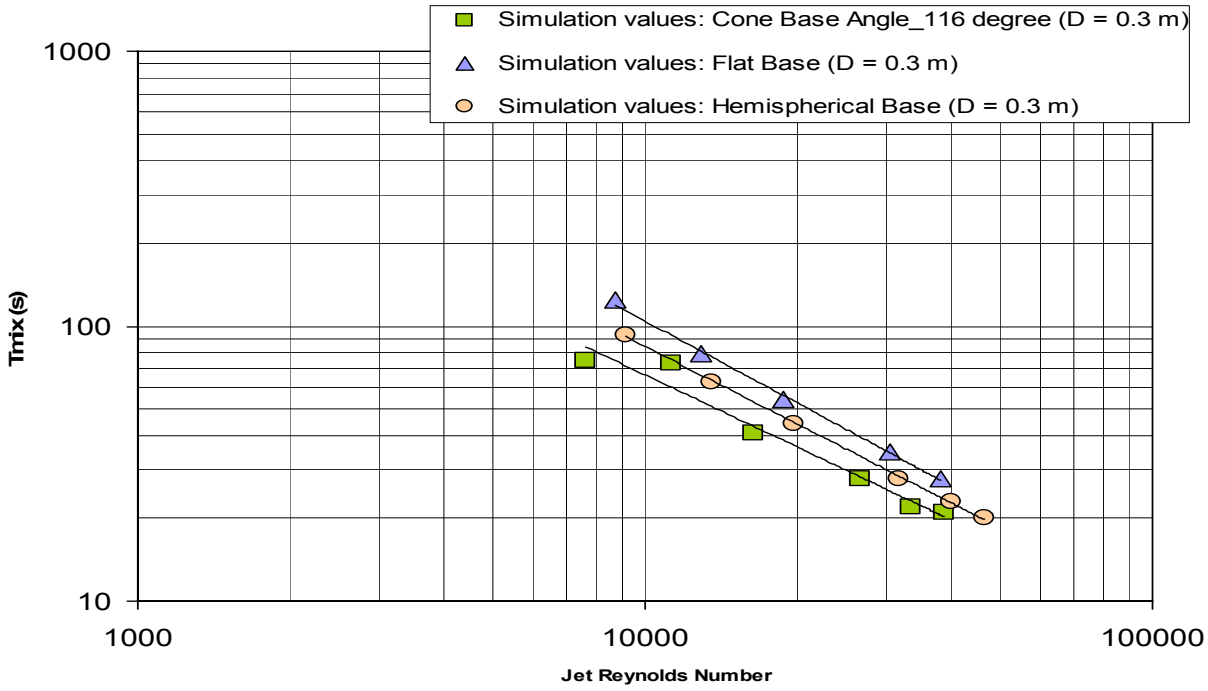

Figure 4.18: A plot of 95% mixing time (for cone base angles of 116 degrees, flat base and hemispherical base) versus jet Reynolds number

Chapter 5

Effects of Irregular Tank Shape, Aspect Ratio on Mixing Time, Correlation of t_{95} and t_{99} and Scale-Up Studies

5.1 Results for a Tank with an Irregular Geometry

It was observed that asymmetric flow in a tank with a flat base, resulted in better mixing and consequently in lower mixing times for the same Re_j. Asymmetric flows were created by injecting the jets at various side-angles (Ahmad, 2003). A side-angle is defined as the angle the jet makes with a vertical plane passing through the jet inlet and outlet. In this chapter the flow asymmetry is created in a different way. This alternative way may be easier to implement industrially as it might be quite difficult to provide a side inclination to the precise degree.

In an attempt to achieve homogenization faster, a tank with an irregular shape was constructed. This geometry was created by inserting a flat plate vertically in the cylindrical tank at a distance of 0.8R from the central axis. The jet was oriented to hit the plate at quarter length from the plate's vertical edge as shown in Figure 5.1. This plate was introduced to break the symmetrical flow pattern inside the tank.

The total volume of the tank is kept the same as that of the cylindrical tank with a flat base used by Ahmad (2003). This means that the height of tank was 36cm as compared to the previous 30cm. Numerical simulations of mixing in this tank were carried out using temperature as the measured variable.

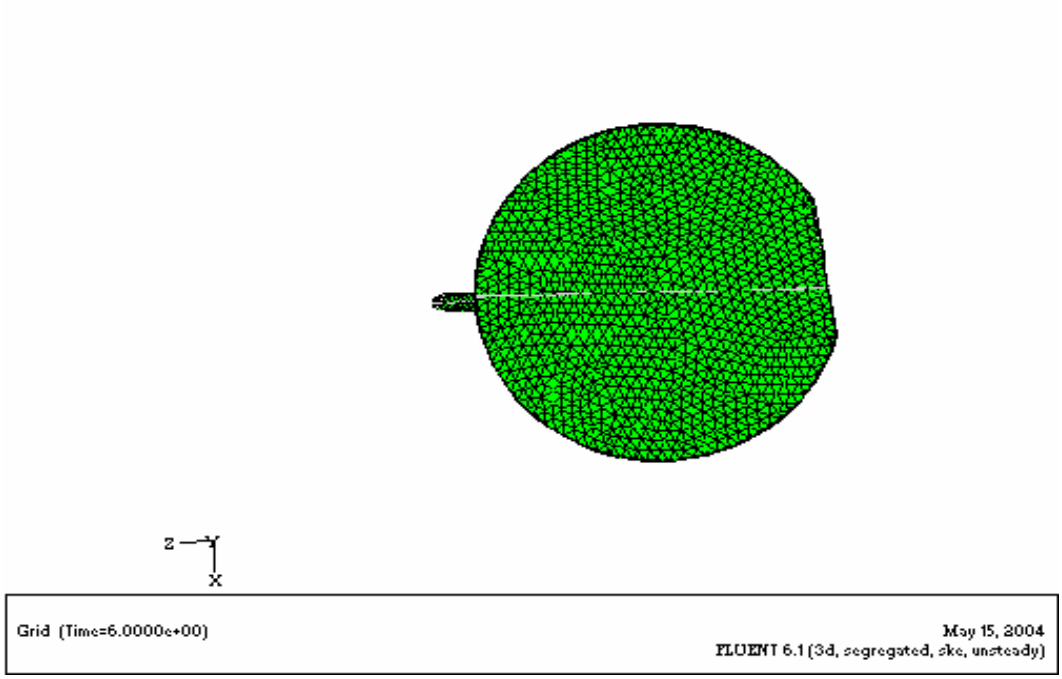

(b)

Figure 5.1: Plan of an irregular mixing tank

Figure 5.2 shows a comparison between the experimental and simulation values (95% mixing time) for the flat based tank, hemispherical base, base cone angle of 116 degrees and that with an irregular shape, for a wide range of jet Reynolds numbers. Results show that using this irregular shape of the tank does not help in reducing the 95% mixing time. It is observed that a tank with a cone angle of 116 degrees requires least time to reach 95% homogenization. The important aspect of using an irregular shape is that it is simple to construct whereas hemispherical or conical bases are difficult to construct.

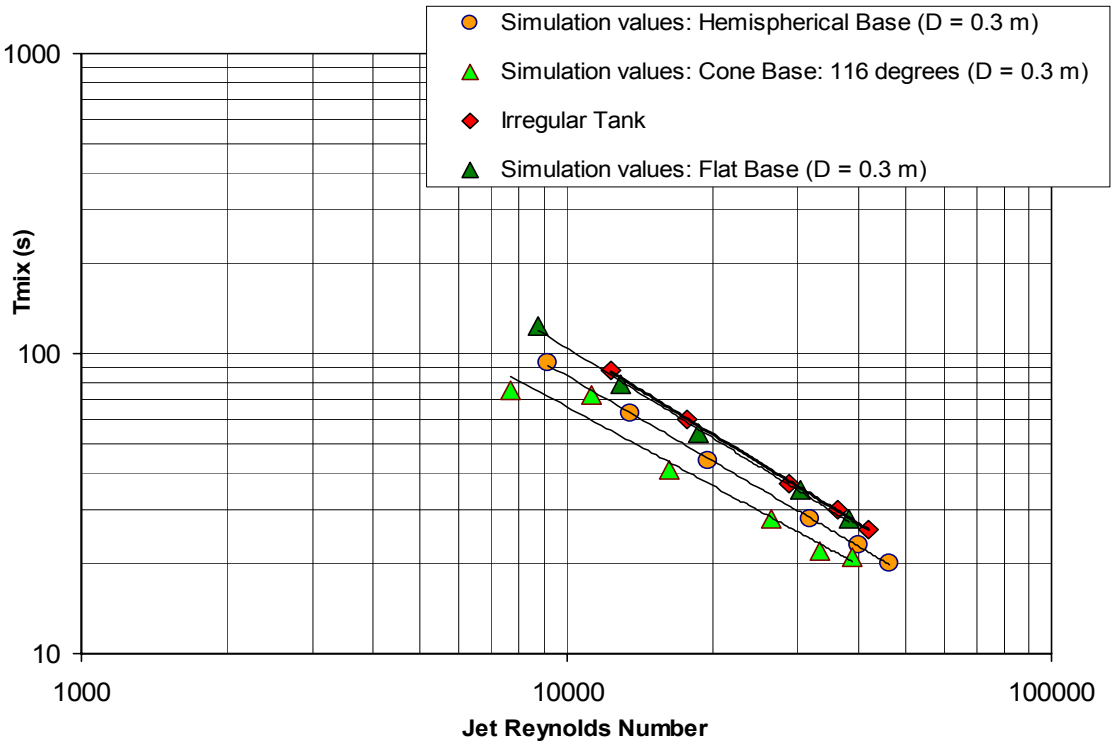

Figure 5.2: A plot of 95% mixing time versus jet Reynolds number for a cylindrical tank and irregular tank geometry.

5.2 95% versus 99% Mixing Time

The 95% mixing time is defined as the time at which the value of the measured variable anywhere inside the tank does not vary by more than ± 5% from the equilibrium value. Certain industries require more stringent criteria of mixing, especially the pharmaceutical industries. One such criteria is the 99% mixing which is defined in a way similar to the 95% mixing time except the range of variations is ± 1%.

For a hemispherical base cylinder tank with an axial upward jet various correlations were suggested:

Khang and Levenspiel (1976) suggested that $t_{99}/t_{95} = 1.44$,

whereas, Hilby and Modigell (1978) suggested that $t_{99}/t_{95} = 1.59$

and Lane and Rice (1981), proposed that $t_{99}/t_{95} = 1.48$.

In order to investigate the 99% mixing time for the cases that were discussed earlier in this chapter, plots of 99% and 95% mixing times are presented. Figure 5.3 shows a comparison of 95% and 99% mixing times for a tank with hemispherical base. The ratios are 1.29 and 1.25 for Re_j of 9,180 and 46,500, respectively.

For a cone angle of 31 degree the t_{99}/t_{95} ranges from 1.43 to 1.38, for a cone angle of 58 degree t_{99}/t_{95} ranges from 1.58 to 2.56 and for a cone angle of 116 degrees, t_{99}/t_{95} ranges from 1.79 to 1.29, for a Re_j range of 6,660 to 38,880. The plots are available as Figures 5.4, 5.5 and 5.6. Figure 5.7 draws a comparison between t_{95} and t_{99} for a tank with an irregular shape.

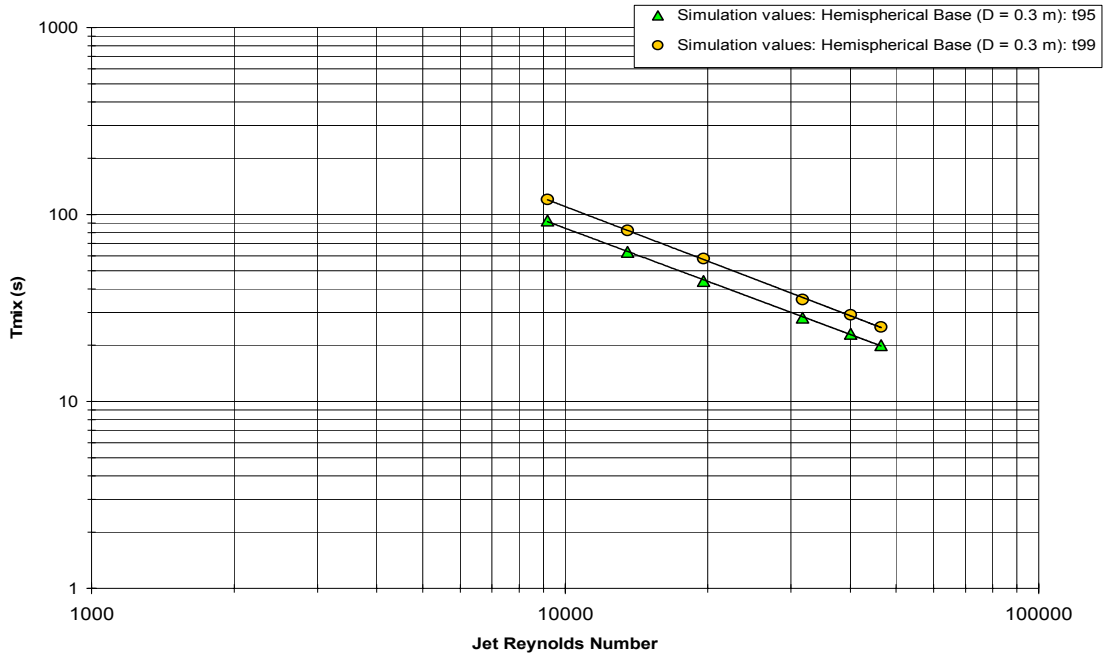

Figure 5.3: A plot of t_{95} and $t_{99,}$ for a hemispherical tank, versus a jet Reynolds number.

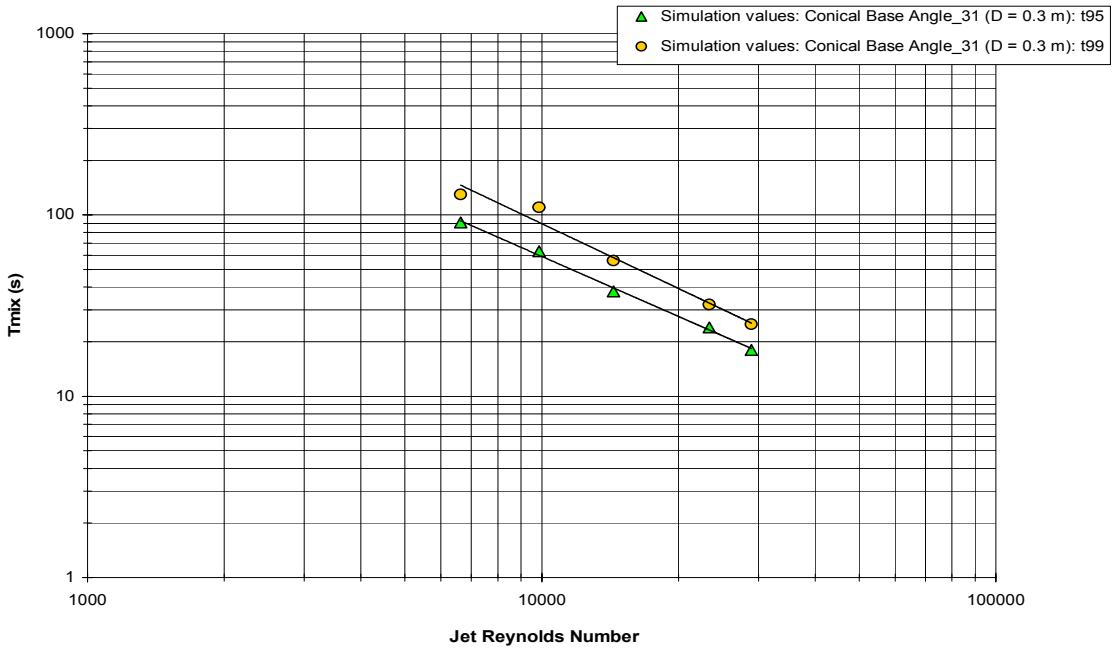

Figure 5.4: A plot of t_{95} and $t_{99,}$ for a tank with a cone angle of 31 degrees, versus a jet Reynolds number

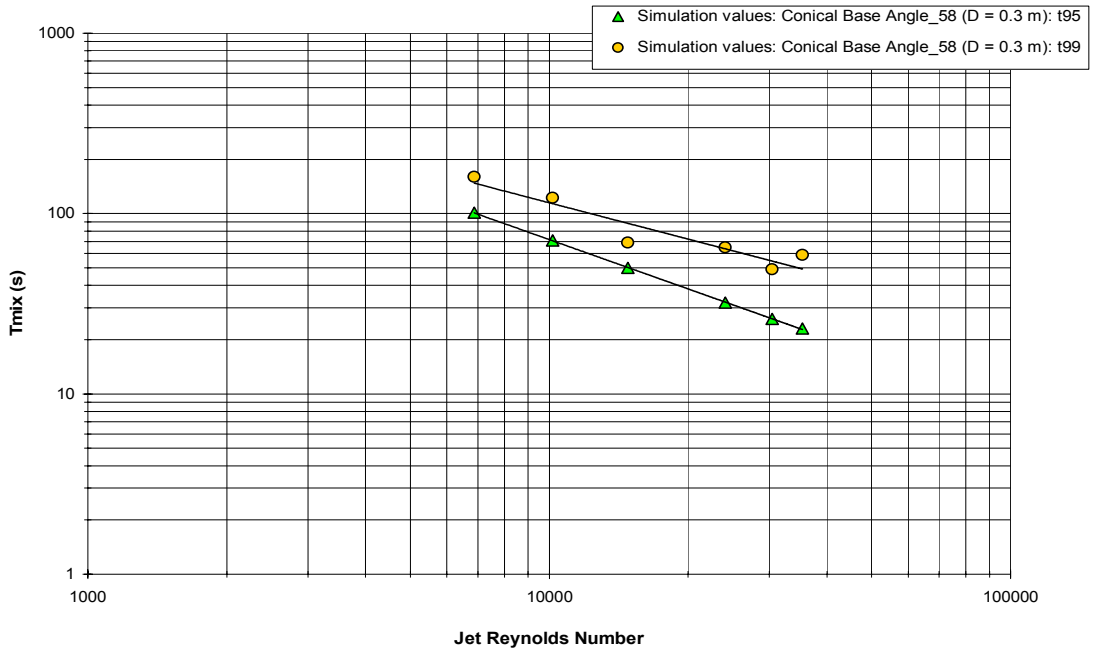

Figure 5.5: A plot of t_{95} and $t_{99,}$ for a tank with a cone angle of 58 degrees, versus a jet Reynolds number.

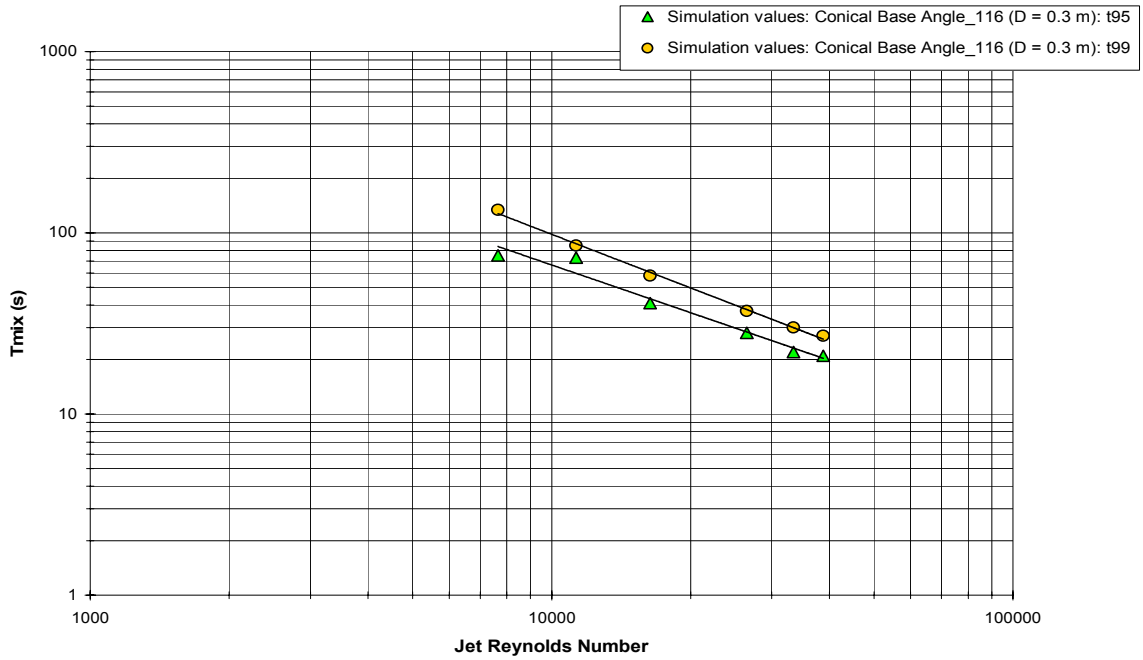

Figure 5.6: A plot of t_{95} and $t_{99,}$ for a tank with a cone angle of 116 degrees, versus a jet Reynolds number.

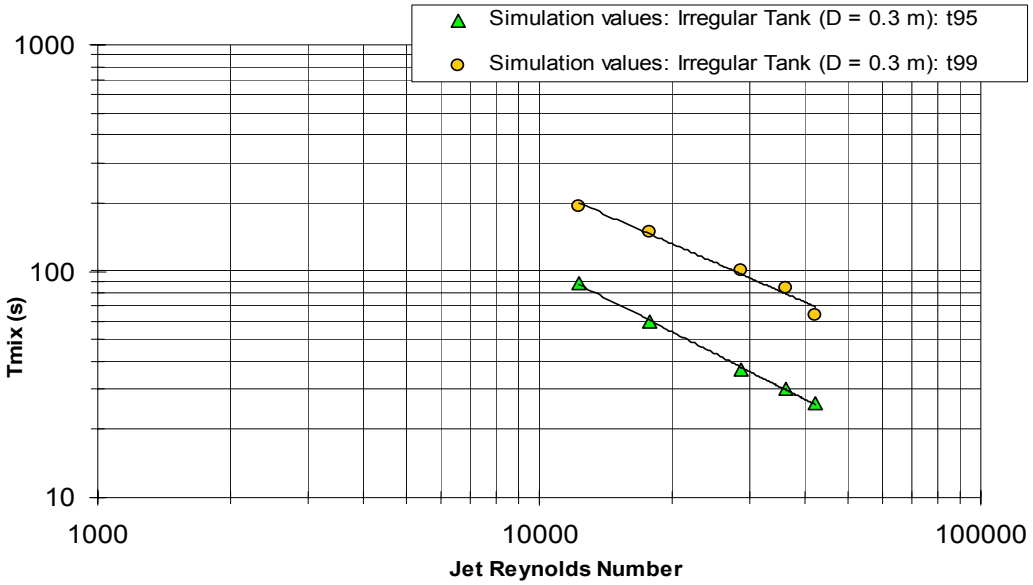

Figure 5.7: A plot of t_{95} and t_{99}, for a tank with a baffle, over a jet Reynolds number.

5.3 Scale-Up Studies

5.3.1 Literature Review

The effects of mixing are usually studied on pilot scale equipment. It is then necessary to establish a scale-up criterion to predict process results in larger equipment. The main objective of the scale-up is to design a large scale mixing system that will achieve the same mixing time quality as in a laboratory tank. Since the distributions of shear rate and energy dissipation widen as the volume is increased, the mixer design must be adjusted to obtain the same process result. Unfortunately it is not possible to maintain all the flow and shear relations after scale-up. For some applications, generalized correlations do exist but for applications like jet mixing, adequate correlations do not exist. In the latter case various methods of scale-up have been proposed based on geometric similarity. However, it is sometimes impossible to have a geometric similarity. Even if it is obtainable, dynamic and kinematic similarities may not be possible simultaneously so that the results of scale-up are not always predictable.

Model theory, similitude and dimensional analysis are techniques which help in scale-up. Practical applications of these techniques involve the use of dimensionless groups such as Reynolds number in correlations which describe the performance of a system in terms equally applicable to large or small systems.

Because of the complexity of mixing systems, knowledge is often lacking of the proper characteristic variables to use in a correlation. Another complication in the use of generalized dimensionless correlations for mixer scale-up lies in the difficulty of establishing an adequate performance parameter. In some cases there may be several

parameters which could be used. Consequently the correlations may vary greatly making scale-up more difficult and arbitrary. Further complications arise in applying principles of similitude to heterogeneous systems.

Several procedures for scale-up have been published. One general recommendation is that geometrical similarity should be maintained. This was proposed originally by Newton (1934) and Rushton (1945, 1951 and 1952) for the correlation of the performance of geometrically similar mixers. Sometimes it may be impossible or at least uneconomical to satisfy this criterion of similarity in every respect. Experience and/or experiment must be relied upon to establish what deviations are permissible. The other similarities which could be used as scale-up criteria are the kinematic and dynamic similarities. Kinematic similarity requires that all velocities in two different scales have a common constant ratio. Dynamic similarity requires that all pertinent force ratios must have a common constant ratio. The various forces encountered inside the stirred tanks are inertial, viscous, gravity and surface tension forces (Oldshue, 1983).

A popular scale-up parameter is the power input per unit volume of liquid to be mixed. Although it is not a universal criterion of scale-up, it is an important parameter to keep in mind when analyzing mixing processes. In general, to maintain an equal blend time on scale up, the power per unit volume almost has to increase with the square of the linear tank dimension. This is usually not practical. To maintain an equal superficial liquid velocity, calculated by dividing the cross-sectional area of the tank by the pumping capacity of the impeller, a constant peripheral speed is required. This is usually on the un-conservative side for scale-up, since the total pumping capacity and the power level to drop in proportion to the tank diameter.

The following possible form of the power input relationship for jet mixing was proposed

$P_j \alpha V^3.d^2$ and $Q_j \alpha V.d^2$

$\Rightarrow P_j \alpha Q_j.H_j$ (where, $H_j \alpha V^2$)

$\Rightarrow Q_jH_j \alpha V^3.d^2$

so, $(Q_j/H_j)*(1/d^2) \alpha (1/V)$

where, P_j is the jet power input, Q_j is the jet volumetric throughput, H_j is the liquid head, d is the jet diameter and V is the jet velocity. This indicates that increasing the jet velocity corresponds to increasing the proportion of power input dissipated as turbulence.

Another more general scale-up criterion is the Reynolds number, recommended by Rushton (1951), Levenspiel (1976) and Roy (1971). The problem with using Reynolds number criterion is not usually the scale-up itself, rather it occurs in obtaining a true relationship between the performance and the controlling variables or variable groups. In the case of jet mixing this refers to the relationship between mixing time and the jet Reynolds number.

The mixing time can be incorporated into a mixing time factor (F) which is a function of the jet Reynolds number. The inclusion of a jet Reynolds number in the equation reduces any problems the formula has in dealing with scale-up. This is because for successful use in scale-up, it is desirable to express the relationship between performance and operating variables in terms of dimensionless groups.

The conclusion that mixing time is a function of jet Reynolds number even when jet is turbulent can be explained by observing that the recirculation in the bulk of the tank is laminar.

The uncertainties inherent in scale-up of liquid-liquid systems require testing over a wide range of operating conditions in the laboratory and possibly the pilot plant to determine the sensitivity of each system to changes in dispersion characteristics.

5.3.2 Results

As evident from the above discussion, there occur various criteria for scale up studies. In the present study, the initial numerical model of Ahmad (2003) was geometrically scaled up. This is one of the common scale-up criteria applied industrially. For this purpose, the flat tank diameter was scaled to 5 times the original diameter, where as the jet diameter was scaled up 2.5 times.

Figure 5.8 shows a comparison between the experimental values of the 95% mixing time for flat base tank, and that from Fosset's and Grenville's correlation.

Fosset and Prosser's (1949) correlation: $t_{95} = 9.0 * D^2/(V_j * d_j)$

Grenville and Tilton's (1996) correlation: $t_{99} = 3.0 * (X/d_j)^2 * (d_j/V_j)$

It is worth noting that though Grenville's correlation gives 99% mixing time, it closely matches the 95% mixing time value from Fossett's correlation. The mixing time values from Fosset's and Grenville's correlation (using the same parameter as of the geometrical scaled up model) bear very close numerical resemblance to those calculated from same tank dimensions of Ahmad (2003). It is worth noting that the downward trend in the 95% mixing time with an increase in the jet Reynolds number is observed for all cases. Figure 5.9 shows a comparison of the simulation results for the scale-up geometry for Ahmad (2003). It is observed that there seems to be considerable degree of error in predicting t_{95} using Fossett & Processer and Grenville correlation. This error increases with the increase of jet Reynolds number.

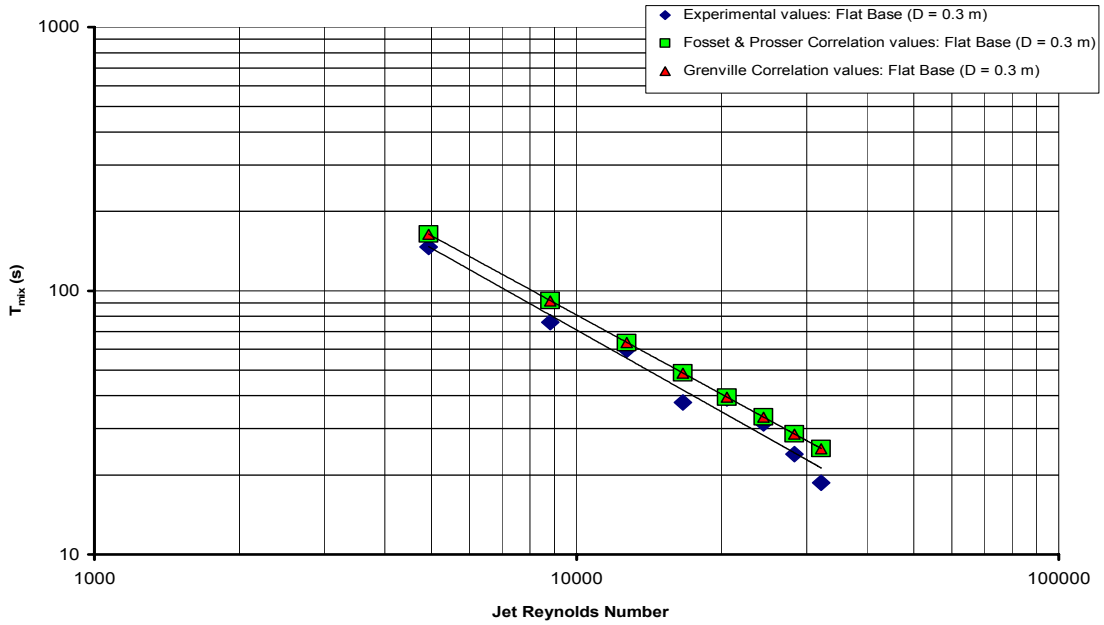

Figure 5.8: A plot of 95% mixing time for the experimental values and the corresponding values from the Fosset & Prosser and Grenville correlation for a flat base tank versus jet Reynolds number.

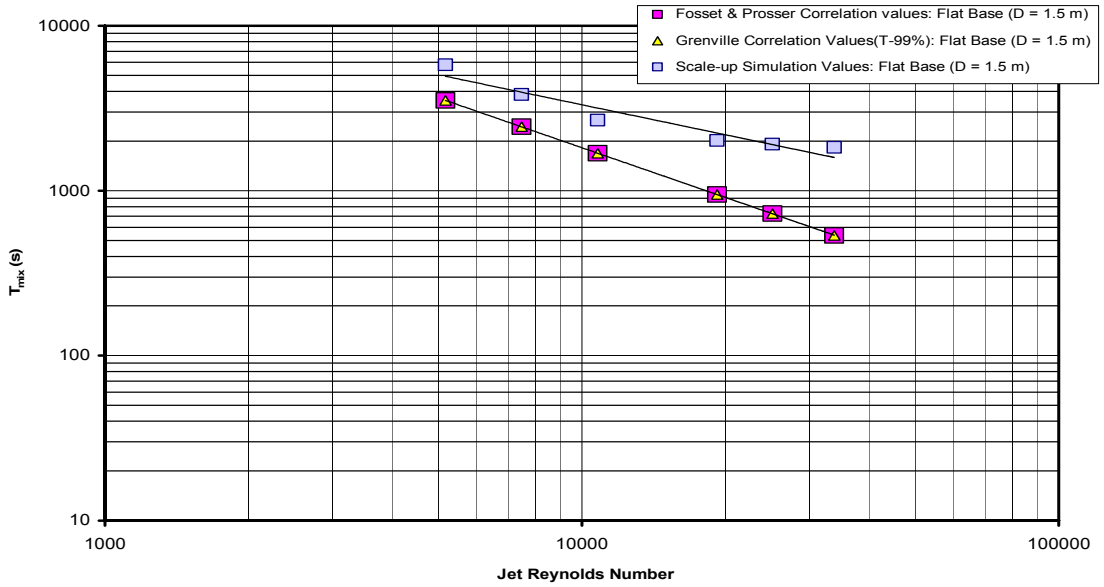

Figure 5.9: A plot of 95% mixing time for the simulation values and the corresponding values from the Fosset & Prosser and Grenville's correlation for a scale up geometry of a flat base tank versus jet Reynolds number.

Chapter 6

Experimental Study of Non Reactive Mixing in a Flat Base Cylindrical Tank

6.1 Introduction

Experiments were conducted to measure mixing time for two geometries of a liquid jet agitated tank. The first geometry was similar to that used in the simulation studies of the symmetric jet model of the liquid jet agitated tank (Ahmad, 2003). This set-up is more commonly used in the industry than the one used by Lane and Rice (1982) for their experiments and by Zughbi and Rakib (2000, 2002) for their simulations. This geometry can be described as an upright cylinderical tank with an outlet off center at the bottom face of the tank and an inlet, at the edge of the bottom face. The second geometry tested is similar to the first geometry with an asymmetric jet. This asymmetric jet is not directed towards the center of the tank but directed at an off-centre angle of 15^{o}. Conductivity was used as the measured variable.

In this work, two jet angles are frequently referred to and these are called, for ease of reference, an up-angle and a side-angle. An up-angle is the angle that the jet makes with the tank bottom as shown in Figure 6.1(a). A side-angle, shown in Figure 6.1(b), is the angle that the jet makes with a normal central plane passing through the outlet.

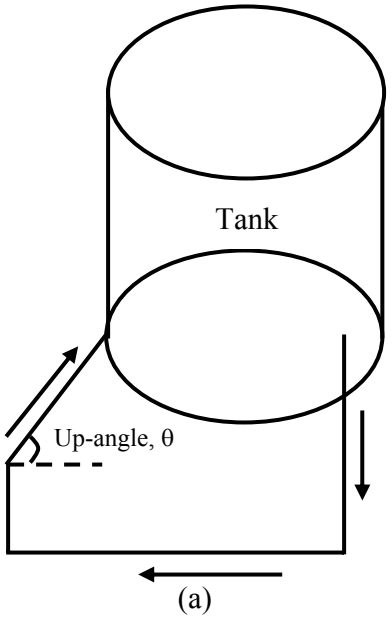

(a)

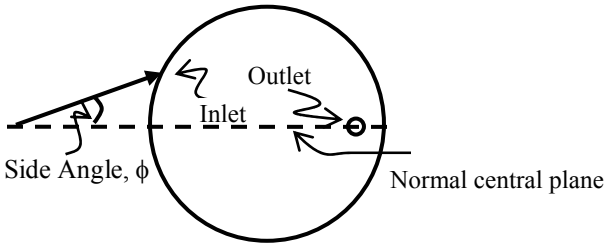

Tank bottom face, plan view

(b)

Figure 6.1: A schematic diagram of the angle that the jet makes with: (a) the tank bottom, referred as up-angle and, (b) the vertical central plane passing through the outlet, referred as side-angle.

6.2 Experimental Set Up

A schematic diagram of the experimental set-up is shown in Figure 6.2. A flat bottom cylindrical tank, 29.6 cm in diameter and 29.6 cm high, is used. The tank is made of Perspex glass. A pump-around, providing the liquid jet, takes suction from the tank base 2.5 cm form the tank wall and discharges symmetrically at the edge of the bottom face of the tank. The jet makes an angle of 45^{o} with the tank bottom and is directed towards the center of the tank. This angle is referred to as the *up-angle*.

A rotameter was used to measure the flow rate. This rotameter was calibrated prior to carrying out the experiments. The rotameter calibration was checked from time to time during this study to ensure continuing accuracy of its readings. The tank was sealed and has a hole in its top cover to add the tracer. Hydrochloric acid (7 M) is used as a tracer. A substantial increase in conductivity was achieved with the addition of 5ml of it. Desalinated water was used as process water. Figures 6.3 and 6.4 are photographs of various parts of the experimental set-up.

Another experimental set-up was, where the tank was identical to the previous-one but the jet was injected to create an asymmetric flow inside the tank. For the asymmetric case, the jet, as before, made an angle of 45^{o} with the tank base, referred to as up-angle. This jet also made 15^{o} angle with a plane passing through the jet axis and the center of the tank. This angle was referred to as the side-angle.

Experimental runs were carried out with a jet Reynolds number ranges from 4,662 to 40,250.

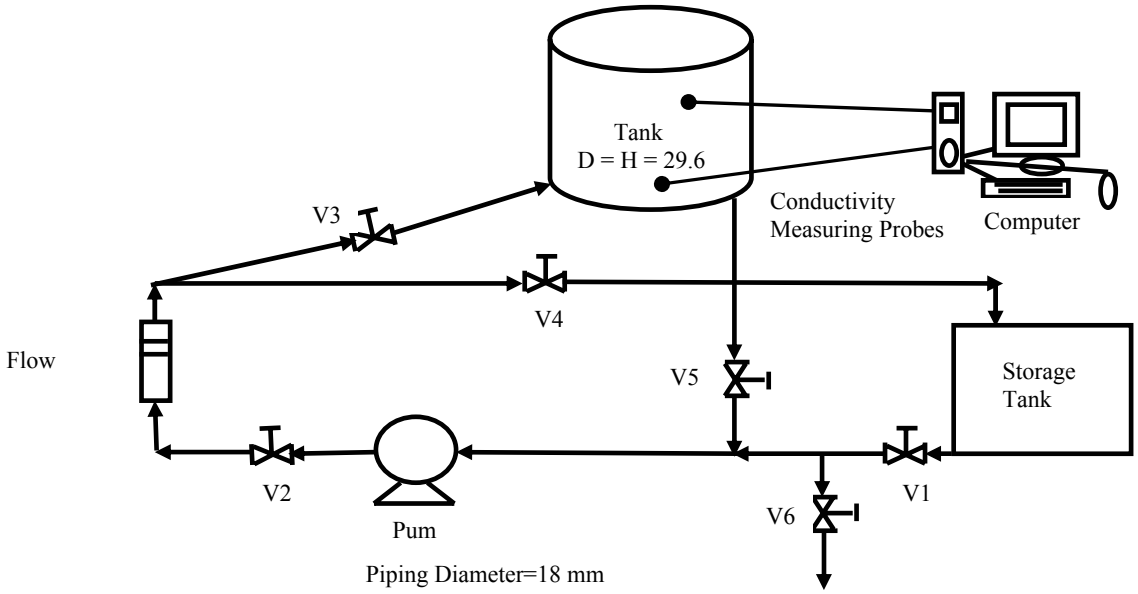

Figure 6.2: A schematic diagram of the experimental set-up.

(a)

(b)

Figure 6.3: (a) The conductivity measurement probe. (b) A photograph of the tank with two measuring probes and inclined jet entering the tank bottom edge at an angle of 45^{o} to the tank's base.

Figure 6.4: A view of the experimental set up showing the pump, piping, rotameter, storage tank, tank with an inclined jet entering through bottom edge, and conductivity measuring probes connected to a computer.

6.3 Measurement of Conductivity

A number of variables were used by previous workers as the measured variables in order to quantify the degree of mixing. Lane and Rice (1982), Perona *et al.* (1998), and Maruyama *et al.* (1982) used conductivity as a tool to quantify mixing. Others used fluorescence (Unger and Muzzio, 1999).

In this study conductivity is the measured variable. An Orion SensorLink Conductivity System is used to measure conductivity. It consists of an Conductivity probe, Orion SensorLink PCM 100 conductivity PCMCIA card, an Orion SensorLink cable to connect this card with an Orion Conductivity Cell-Model 11050 Epoxy 2-electrode, and Orion SensorLink software to record the measurements in a computer. The PCM 100 card is inserted in a a PCMCIA card dock. The conductivity of a solution with a specific electrolyte concentration changes with temperature. These probes have integral temperature sensor for a temperature range of 0 to 80^{o}C. Therefore the measured values are automatically temperature compensated. By definition, temperature compensated conductivity of a solution is the conductivity which that solution exhibits at the reference temperature. The reference temperature is chosen to be 25^{o}C for this study. The conductivity measurement range for these probes is form 1 μS/cm to 20 mS/cm, where S stands for Siemen, the unit of conductance. The accuracy for conductivity measurement is 0.5% of full scale, whereas that for temperature measurement is 1^{o}C (Orion instruction manual). Sensor Link software chooses the most accurate conductance range from one of the ranges given in Table 6.1. However if one knows the value of conductance for his sample, he can choose that on his own.

Table 6.1: Ranges for conductance available in an Orion Sensor-Link System.

Range 1	0.0 μS to 20 μS
Range 2	20 μS to 200μS
Range 3	200 μS to 2mS
Range 4	2 mS to 20 mS

Figure 6.5 shows this PCM 100 conductivity card. Two conductivity probes are used in this study. However, only one was used to log data at any time. Conductivity data was recorded every second during the experimental runs. The locations of the probes in the liquid jet agitated tank were carefully chosen with the help of results of computational fluid dynamics (CFD) simulations and experience. The probes were placed in positions where mixing time is expected to be the longest. These positions are associated with the lowest zones of velocity in the tank. Figure 6.6 shows the simulation results of the velocity fields in the agitated tank, and these low velocity zones can be easily identified. These zones are mixed last. So probe A was located near the tank bottom with the cell positioned at x = 0, y = -8.8 cm and z = 11 cm. It should be kept in mind that the origin of the coordinate system is located at the tank centre. Similarly probe B was located near the tank top at coordinates x = 2.8 cm, y = 9.5 cm and z = 0 cm.

Figure 6.5: A PCM 100 conductivity meter card.

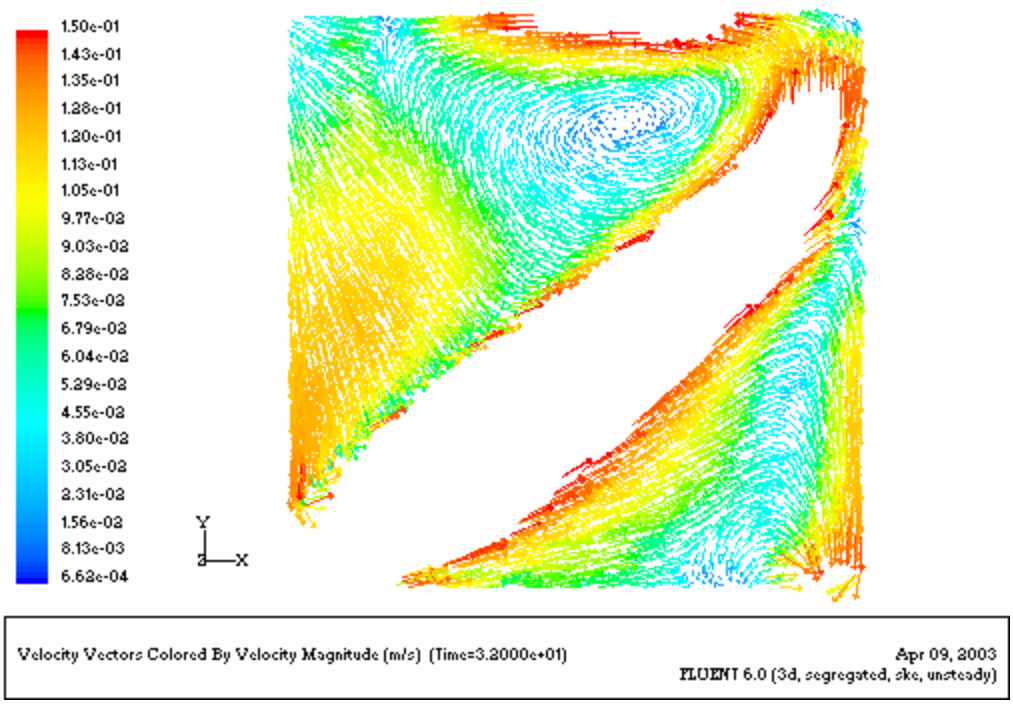

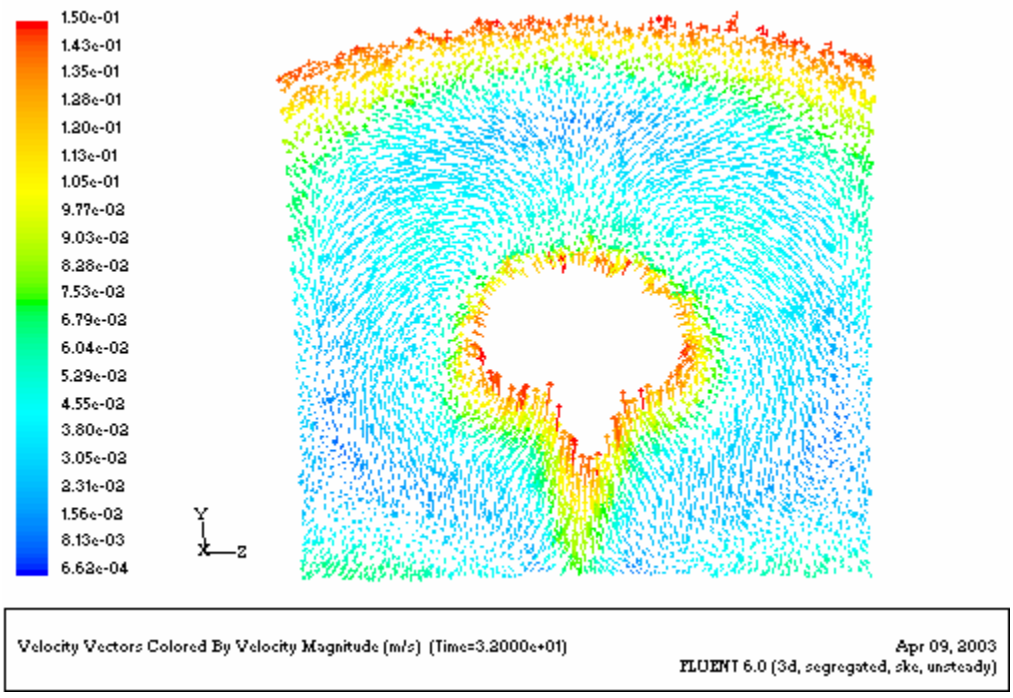

Figure 6.6: Velocity vectors for the low velocity range to identify the low velocity zones. The velocity vectors having values higher than 0.15 m/s are not shown in these figures.

6.4 Experimental Procedure

The steps followed for carrying out each experimental run are listed below. However, the rotameter was calibrated before the start of experiments.

1. Fill the storage tank with tap water up to an appropriate level.
2. Switch on the computer.
3. Insert the PCM 100 card in the PCMCIA card dock. A beep is heard when PCM 100 card is detected by the computer.
4. Connect the conductivity probe using the Orion Sensor Link cable with a PCM 100 card.
5. Start the Orion Sensor Link software.
6. As per procedure given in the manual of the PCM 100 conductivity meter (instruction manual), calibrate the conductivity probe to be used in the experiment by using freshly prepared 0.01M KCl standard solution.
7. Fix the probe at its location in tank.
8. Open valve V1, at the pump suction. This and other valves mentioned below are shown in Figure 6.2.
9. Partially open valve V2 at the pump discharge.
10. Open valve V3.
11. Remove the stopper placed at the tracer injection hole.
12. Make sure that valves V4, V5 and V6 are closed.
13. Start the pump.
14. When the tank is full, quickly close V1 and simultaneously open V5.

15. Fill the tank completely by taking water from the storage tank in a beaker through the tracer injection point at the tank's top surface.
16. Adjust the V2 opening to achieve the desired flow rate.
17. Measure 5 ml of 7M HCl by a pipette and transfer to a small beaker.
18. Open a new data file in the Orion Sensor Link software and choose 1 second interval to record the conductivity.
19. Click on the 

icon on the toolbar.
20. Wait until a constant conductivity value is displayed on the PC screen.
21. Switch off the pump.
22. Wait for some time so that water in tank becomes stagnant.
23. Add the measured quantity of HCl in the tank from the port in the tank top surface
24. Replace the stopper in the port.
25. Switch on the pump with the least possible time lag straight after the addition of HCl.
26. Wait until constant reading is shown by the software.
27. Click on the 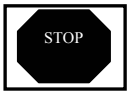

icon on the toolbar.
28. Stop the pump.
29. Save the data file in an appropriate folder with a suitable name.
30. Open drain valve V6 to drain tank.
31. Now refill the tank.
32. Keep on circulating this water for some time.
33. Stop pump.
34. Drain tank by opening drain valve V6.

35. Repeat steps 1 to 34 to carry out a new run.

36. Leave the probes dipped in desalinated water by filling the tank.

37. Place the stopper into the tracer injection hole to avoid water evaporation.

6.5 Experimental Results for Symmetric Jet Arrangement

Experimental runs were carried for different jet Reynolds numbers, Re_j. For each value of Re_j, three experimental runs were carried out. Figure 6.7 shows the values of the conductivity as a function of time, measured by probe A, for a jet Reynolds number of 32,166. These values are for 3 consecutive runs. All other runs show a similar trend. There are some differences in the value of conductivity from one run to another. These differences are mainly due to slight changes in the initial conductivity and also due to experimental error. The time required to achieve 95% mixing in this case is 18, 20 and 18 seconds for the first, second and third run respectively. The average mixing time is 18.67 seconds. So the maximum percentage error among these runs is 7% based on the average mixing time.

Figure 6.8 shows a plot of the experimentally measured 95% mixing time, by probe A as a function of Re_j. The mixing time decreases as the jet Reynolds number is increased. The data also shows a limited degree of scatter. Such a scatter was also obvious in the work of Lane and Rice (1982) who used a tank of about the same volume as the one used in this study. Perona et al. (1998) who used a much larger tank then the present one (about four times bigger) showed significantly more data scatter.

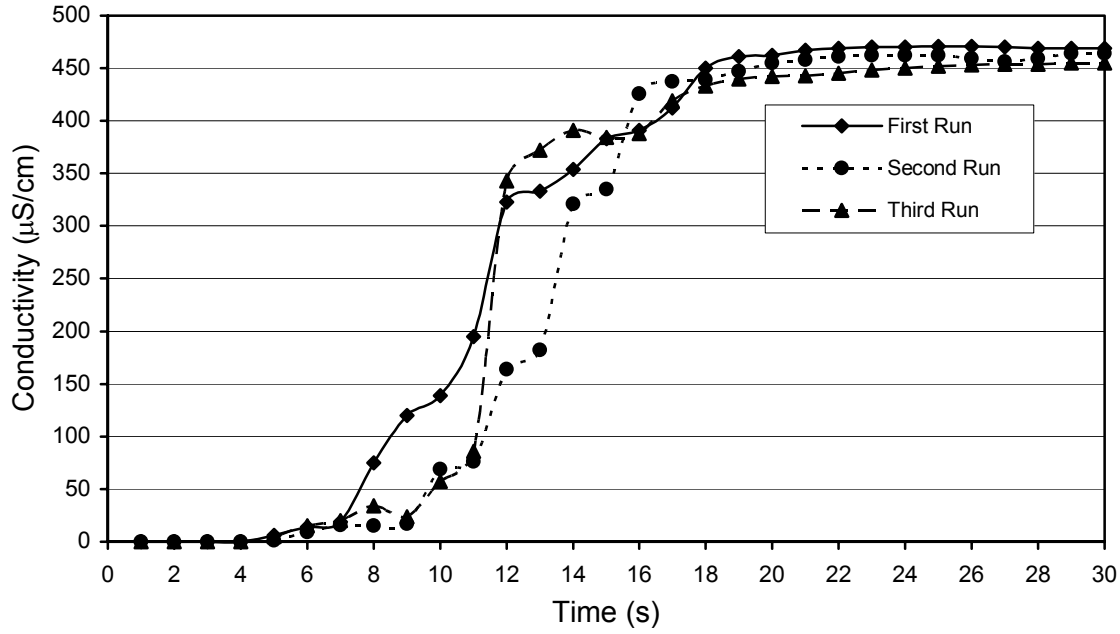

Figure 6.7: A plot of conductivity versus time measured by probe A for a jet Reynolds number, Re_j of 32,166 for symmetric jet arrangement.

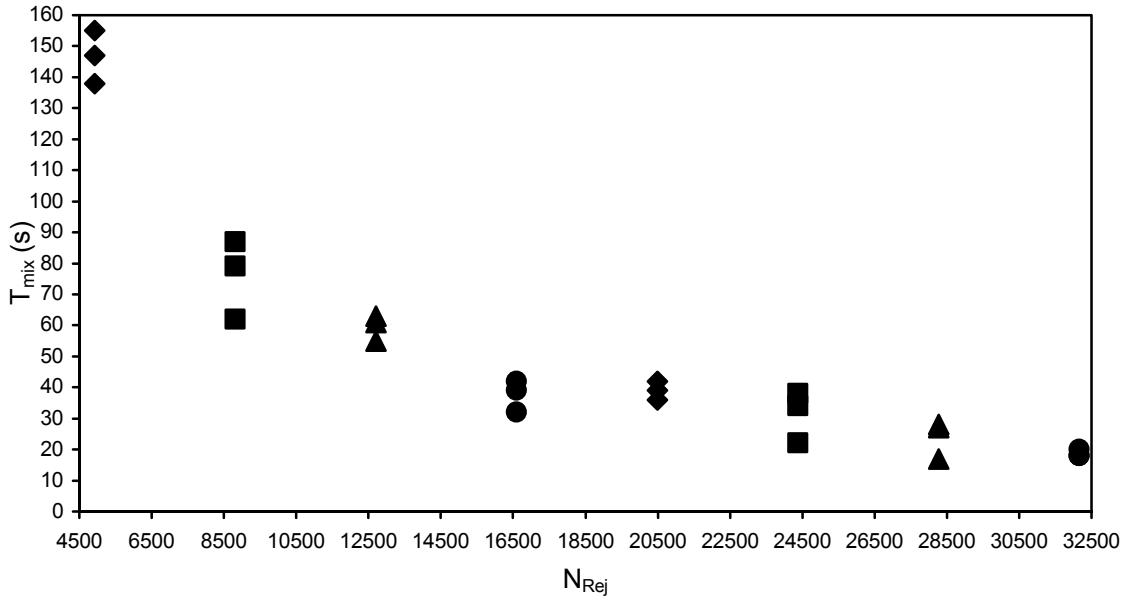

Figure 6.8: A plot of experimentally determined mixing time by probe A as a function of jet Reynolds number for the symmetric jet arrangement.

6.6 Experimental Results for an Asymmetric Jet Arrangement

In another experimental set-up the jet was not injected towards the tank center. The jet made an angle with vertical plane passing through the tank center and the pump-around off take. This angle was referred to as side-angle. The geometry used in this case had a side-angle of 15^{o}. This angle was chosen with the aid of CFD simulations. Preliminary CFD runs with a number of side-angles were performed and an angle which was expected to yield the largest reduction in mixing time was chosen.

The two conductivity probes were carefully chosen again with the aid of CFD. The positions were in the zones that were expected to experience the least velocity and consequently the slowest mixing. These positions were (0 cm, 28.8 cm, -13.8 cm) for probe A and (6.8 cm, 9.8 cm, 0 cm) for probe B, with the origin of coordinate axis at the centre of tank bottom face. However, only one probe was used to log data at any one time. Figure 6.9 shows a typical plot of conductivity measurements versus time measured by probe A for a jet Reynolds number of 28,273.

These curves depict a typical behavior of a mixing curve, i.e. start at an initial value, then increases to the equilibrium value. Mixing curves may show an overshooting or undershooting behavior before reaching the equilibrium value. The mixing time for these three runs is 32, 30 and 31 seconds. So the average mixing time for these runs is 31 seconds. The maximum percentage error is 3.2% based on the average mixing time.

Figure 6.10 shows a plot of experimentally measured 95% mixing time as a function of jet Reynolds number. The mixing time decreases as the jet Reynolds number increases. It is also observed that the rate of decrease of mixing time for $8{,}000 < Re_j < 16{,}000$ is higher than that for $16{,}000 < Re_j < 28{,}500$.

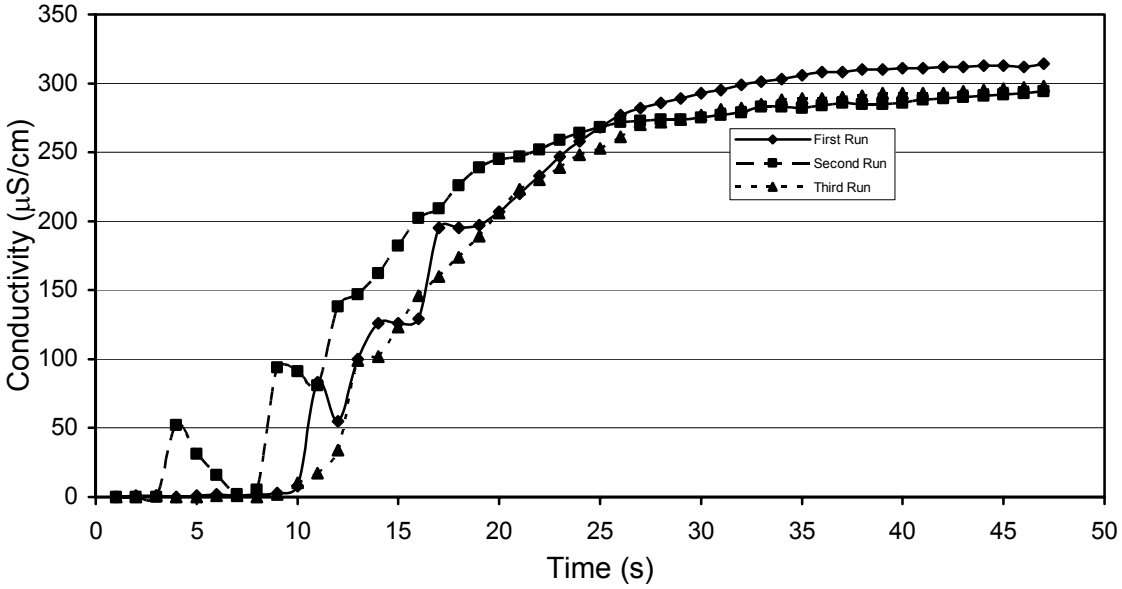

Figure 6.9: A plot of conductivity versus time measured by probe A for a jet Reynolds number of 28,273 for the asymmetric jet arrangement.

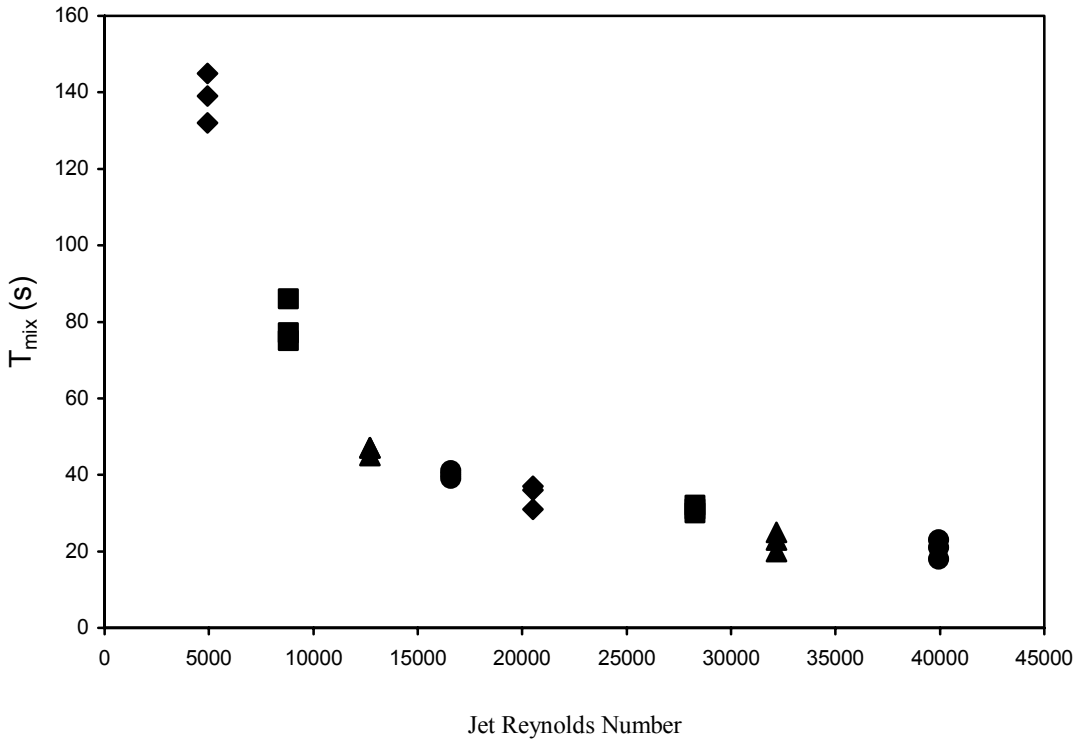

Figure 6.10: A plot of experimentally determined mixing time by probe A as a function of jet Reynolds number for the asymmetric jet arrangement.

6.7 Effect of Free Surface on Mixing Time

So far mixing has been studied in a tank full of liquid with a solid top. The effect of a free surface on mixing is important wherever the tank of interest is partially full. When the tank is full, the jet may hit the opposite wall and connect to it. Subsequently it will connect to the top cover as shown in Figure 6.11. However if there is a free surface, the jet may show a different behavior depending on the liquid height and the orientation and the momentum of the jet: (i) The jet could connect to the free surface, (ii) a fountain could form when the momentum of the jet increases, (iii) a blow-through may take place, ultimately as the jet punches through the liquid depth. Progression from (i) to (iii) above takes place as the jet momentum increases and/or as the liquid height is decreased. To investigate the effects of a free surface on mixing time, experimental runs were carried out using the 29.6 cm by 29.6 cm cylindrical tanks with the symmetric and the asymmetric arrangements. Runs were carried out for liquid heights of 15, 20 and 25 cm. Experiments were carried over a wide range of jet Reynolds number and the mixing time was measured by using conductivity as the measured variable. The 15, 20 and 25 cm cases had a free surface in them. The experimental results were compared with numerical results of a covered tank with the same dimensions using the validated models proposed by Ahmad (2003). Figure 6.12 shows a plot of the 95% mixing time obtained from simulation versus jet Reynolds number, for various H/D ratios. It should be noted that the volume of liquid was different in each of these cases. It is observed that the 95% mixing time for the liquid height of 20 and 25 cm is higher than that of the 30 cm case. The mixing time for the 15 cm liquid height is slightly lower than the 30 cm.

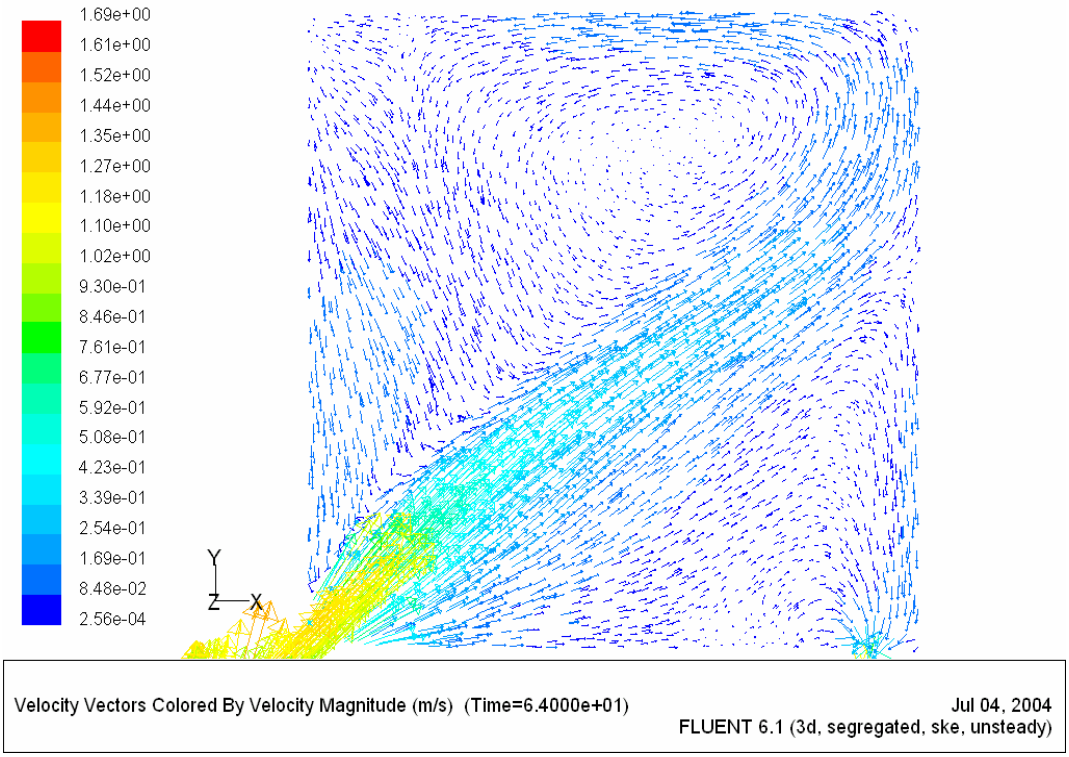

Figure 6.11: Velocity vectors in a flat bottom tank in a plane passing through the jet inlet and outlet

It can be concluded that the mixing time is a strong function of the aspect ratio and a weaker function of the volume of the tank.

Figures 6.12 to 6.14 show a comparison of the experimental values of the 95% mixing time with the simulation values for liquid heights of 15 cm, 20 cm and 25 cm respectively. Based on the previous discussion, this is a comparison of mixing with and without a free surface. Figure 6.13 shows that a free surface increases the 95% mixing time by as much as four times for a Re_j upto 20,000. For Reynolds numbers higher than 20,000, very little improvement in the 95% mixing time is observed. This is mainly due to the "fountain" phenomenon which was explained earlier. At these high Re_j, the jet punches through the liquid and no further jet momentum is transformed to the primary or slow moving fluid.

A similar trend is observed in Figure 6.14 when the increase in the 95% mixing time due to a free surface is about three times for a Re_j upto 20, 000. Figure 6.15 shows a two times increase in the 95% mixing time for a liquid height of 15 cm for Re_j upto 20,000. It is also observed that the onset of the fountain and wave motion is a strong function of the jet momentum and weaker function of the liquid height. Figure 6.16 shows clearly that for a liquid height of 15 cm, there is no surface movement for Re_j of 4,662 and 8,852. Surface waves and subsequently a fountain are observed for Re_j of 20,561 and higher which cause the increase in the 95% mixing time.

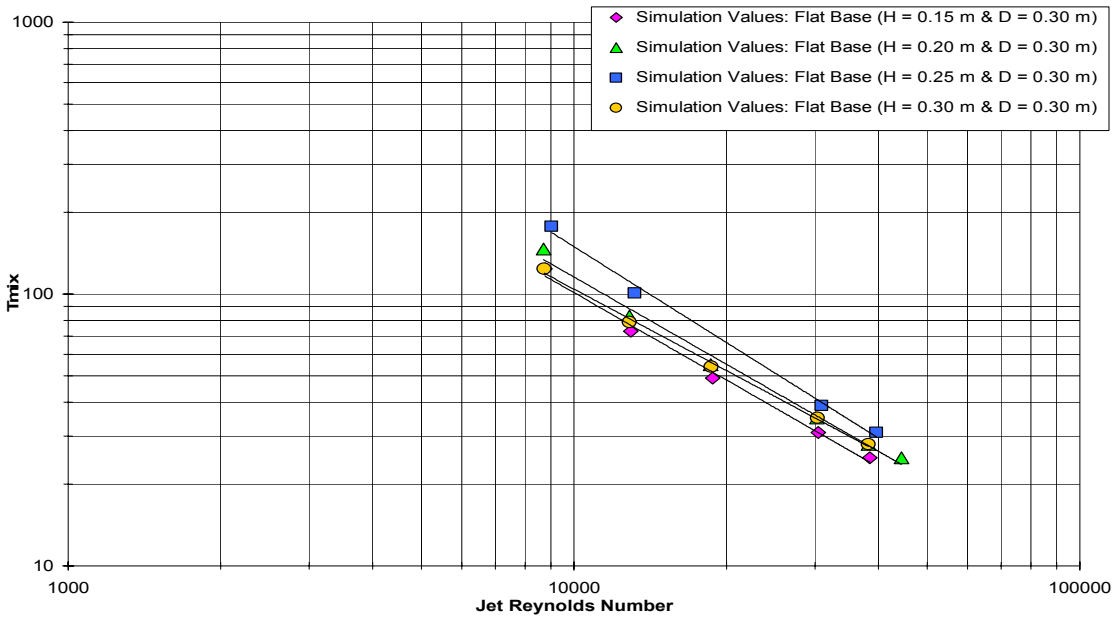

Figure 6.12: A plot of the 95% mixing time for various liquid height in tank.

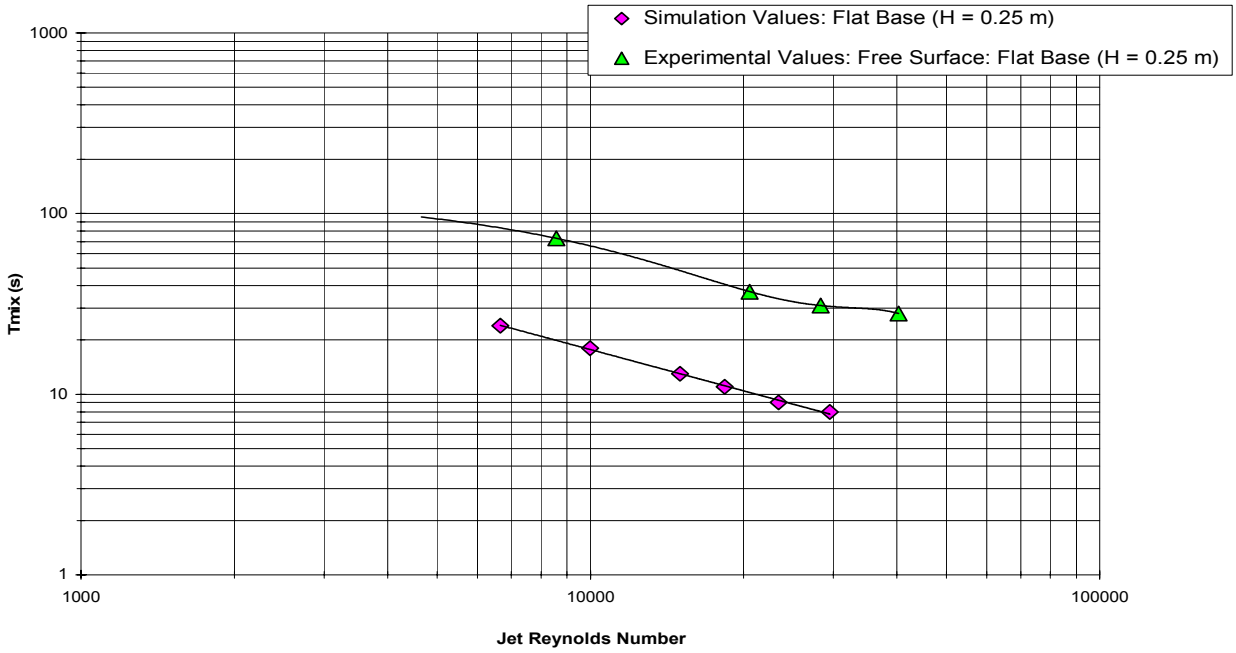

Figure 6.13: A plot of the 95% mixing time for a liquid height of 25 cm with and without a free surface.

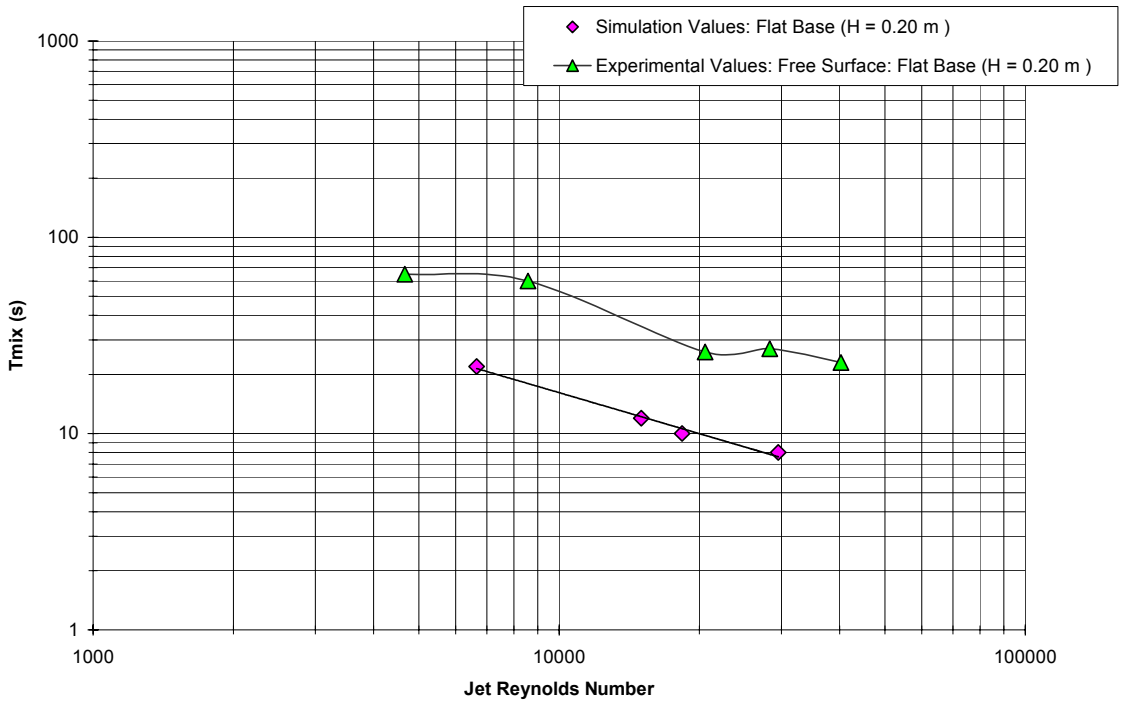

Figure 6.14: A plot of the 95% mixing time for a liquid height of 20 cm with and without a free surface.

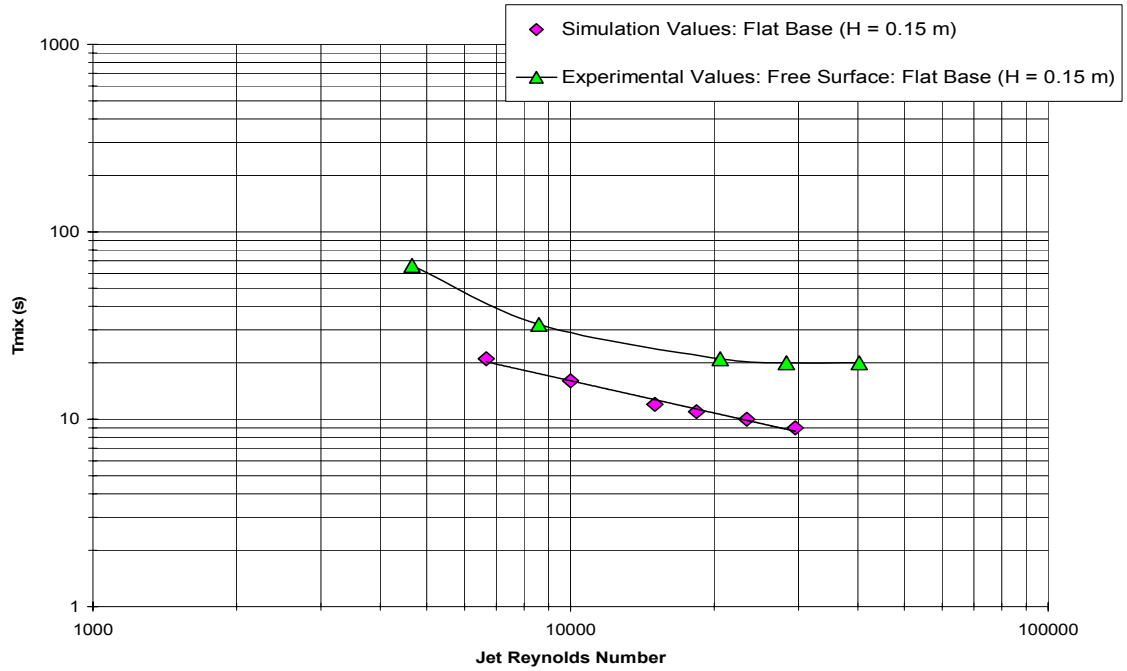

Figure 6.15: A plot of the 95% mixing time for a liquid height of 15 cm with and without a free surface

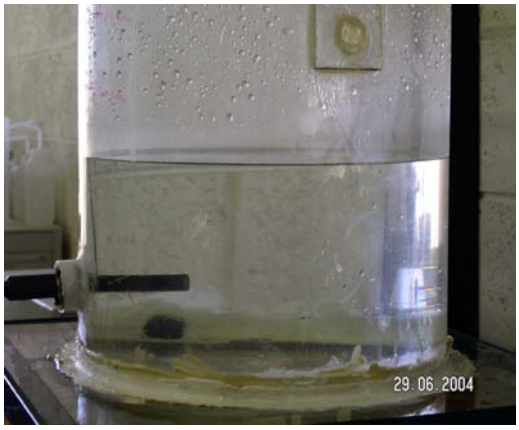

(a)

(b)

(c)

(d)

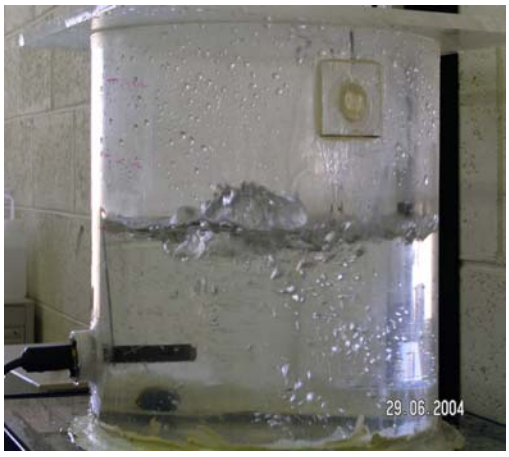

(e)

Figure 6.16: Free surface behavior at a jet Reynolds number (Re_j) of (a) 4,662, (b) 8,582, (c) 20, 561, (d) 28,294, and (e) 40,250, at a liquid height of 15 cm.

6.8 The Symmetric and Asymmetric Effects on Mixing Time with Free Surface for Variable Liquid Height in the Tank

Figure 6.17 shows that when a free surface exists, the 95% mixing time for a symmetric jet arrangement is 50% lower than that for an asymmetric jet arrangement for a jet Reynolds number of 8,582. This reduction in 95% mixing time reaches 25% for a jet Reynolds number of 40,250.

Figures 6.18 and 6.19 show that as the liquid height to tank diameter ratio changes from 25/30 to 20/30, the 95% mixing time when using the symmetric jet arrangement is about 48% lower than when using the asymmetric jet arrangement for a Re_j of 4,662. However for a Re_j of 40,250, 95% mixing time reduces to 18%. A similar trend is shown for H/D of 15/30.Whereas 95% mixing time for asymmetric jet at Re_j 4,662 is 51% lower and it overcomes its disadvantage and shows no improvement over symmetric jet at higher Re_j of 40,250.

These results show that a free surface in a mixing tank will increase the 95% mixing time by about 50% for a Re_j of 4,662 which decreases with Re_j. This is mainly due to the wave form motion and fountain development at the free surface at high Re_j. Both waves and fountains contribute to dampening the circulating jet. The results also show that the hydrodynamics of the flow inside the tank, with a free surface, become more difficult to predict when an asymmetric jet arrangement is used. For H/D ratios of 20/30 and 15/30 and Re_j higher than 28,294, asymmetric jet arrangement does not seem to offer any benefit over the symmetric jet arrangement. For all Re_j and H/D ratios, the symmetric jet arrangement gave shorter 95% mixing time over the asymmetric jet arrangement.

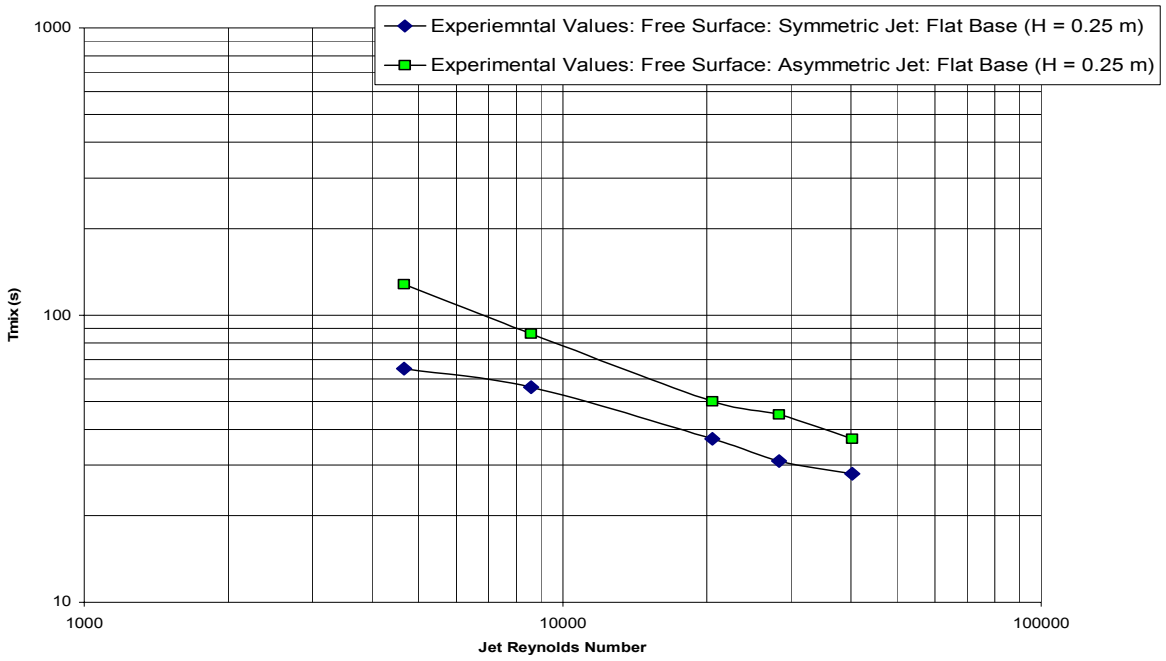

Figure 6.17 A plot of the 95% mixing time for the experimental values for a liquid height of 25 cm with a free surface, for symmetric and asymmetric jet arrangement.

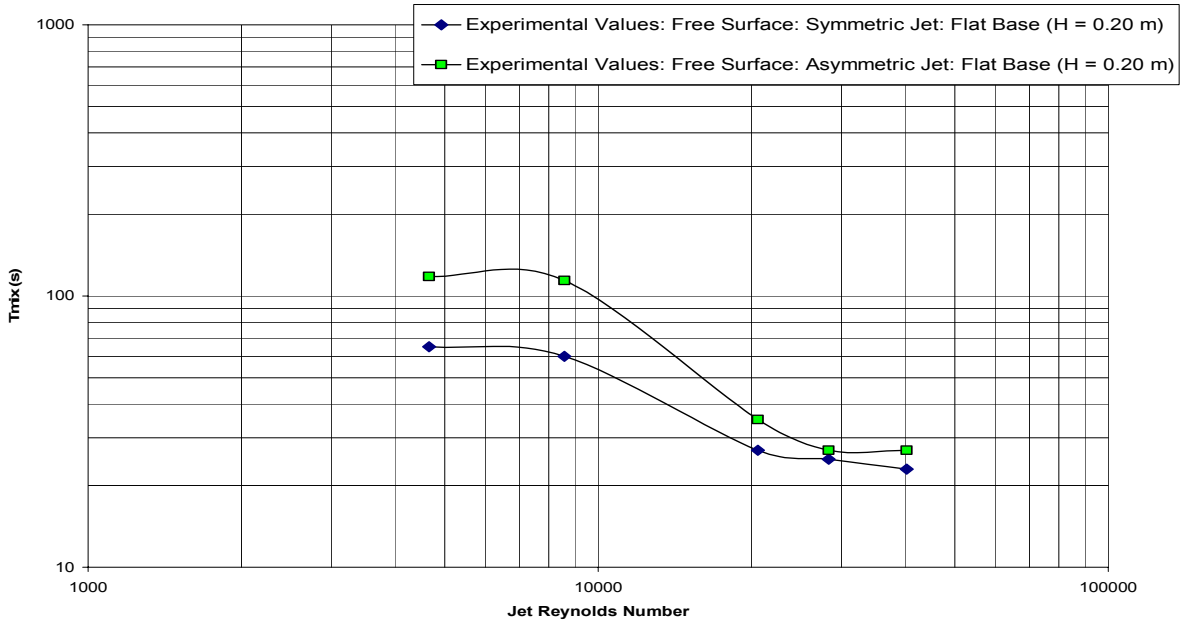

Figure 6.18: A plot of the 95% mixing time for the experimental values for a liquid height of 20 cm with a free surface, for symmetric and asymmetric jet arrangement.

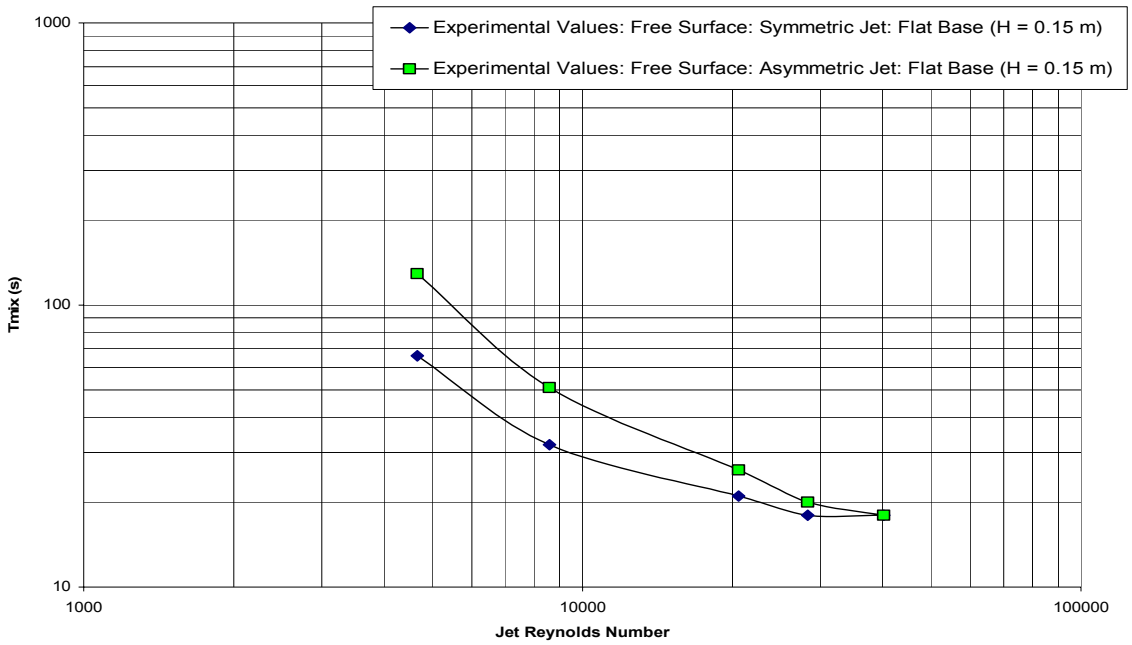

Figure 6.19: A plot of the 95% mixing time for the experimental values for a liquid height of 15 cm with a free surface, for symmetric and asymmetric jet arrangement.

Chapter 7

Experimental Study of Reactive Mixing in a Pipeline with a Side-Tee

7.1 Neutralization Reaction in a Pipeline

As discussed earlier, in order to study the effect the mixing on the extent of a chemical reaction, a neutralization reaction in a pipeline with a side tee is investigated. The pipe assembly consists of a main pipe with a side pipe making a 90^o with it. The assembly is a typical pipeline with a side tee. This side-tee works as a jet inlet to the main pipe. Depending on the side and main pipe velocity, the desired degree of mixing is achieved in a certain length of the pipe. This type of assembly is widely used in the mixing industry, because of the usage of a liquid jet minimizes contamination and maintenance needs.

The acid-base neutralization reaction studied was of Hydro-chloric (HCl) and Sodium Hydroxide (NaOH). The molarity of the base remained fixed as 1 whereas the molarity of the acid varied from 2 to 0.5. The flowrates to the main and the side pipes were varied so as to keep equimolar solution entering the main and the side pipe.

The reaction investigated i.s:

$$HCl + NaOH \rightarrow NaCl + H_2O \qquad (7.1)$$

In the experimental runs, U_j/U_m varied from as low as 7.92 to 33.15. Temperature profiles as function of the distance from the tee junction were obtained for various U_j/U_m

7.2 Experimental Set-Up

The experimental apparatus is shown in Figure 7.1. An assembly consisting of a main horizontal PVC pipe 3m long is employed as the main part of the rig. The rig has a replaceable facility (unions at both ends of a replaceable horizontal pipe) so that different diameters of main pipe may be used. Runs reported in this thesis were carried out using 1" diameter main pipe and side-tee of 1/4".

Experiments with different velocities were also carried out. Tests were done in Reynolds number range of 4,826-20,066. Suitable pumps are chosen to supply the main and the side fluids in adequate flow rates. Thermocouples and a PC having a data logging software OMEGA with suitable hardware to connect the thermocouples (at most sixteen) to a PC were used. The Output data from the thermocouples is fed to a PC for data logging and storage. Figure 7.2 shows the thermocouples along the arrangement on main and side pipes. Figure 7.3 shows photographic shots of the experimental apparatus.

7.3 Experimental Procedure

The experimental procedure is:

1. Check the data logging program OMEGA Quick Log if working and enabled.
2. Check and adjust the inlet and outlet valves of the both main and side pumps to required flow rates.
3. Start the heater.
4. Start the main pump, maintain a constant flow rate and take a note of the main fluid temperature.
5. Start the side pump. See that both flow rates become constant.

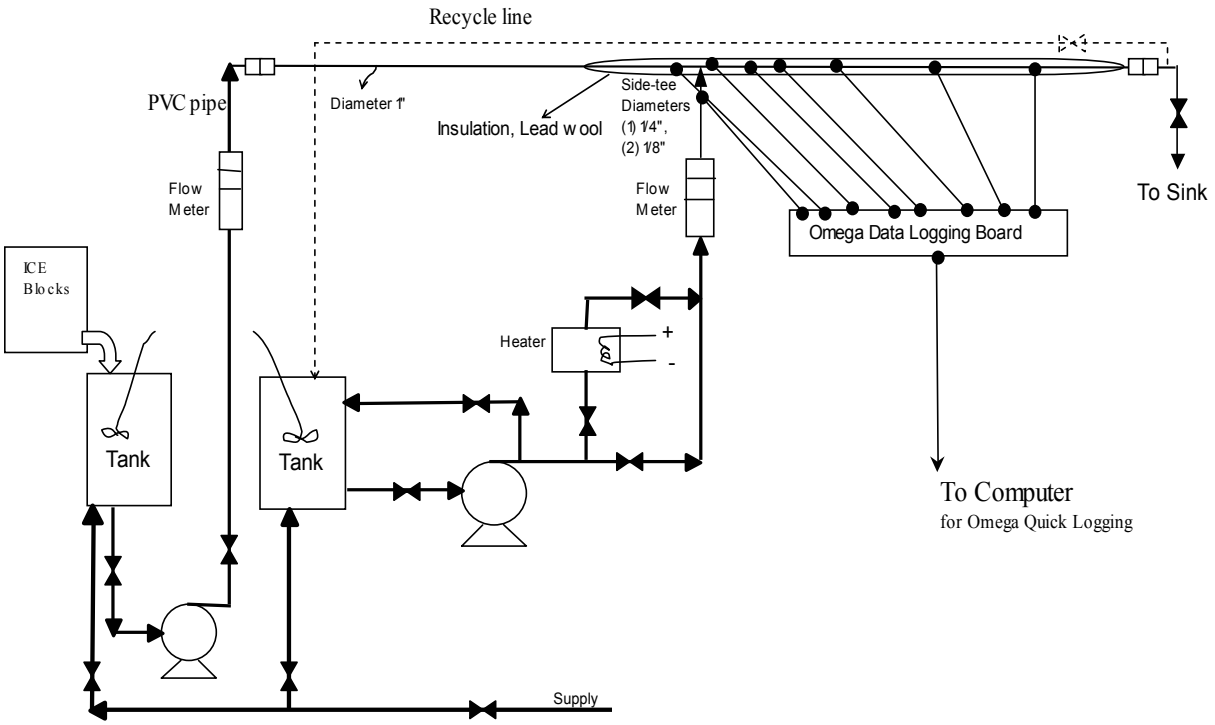

Figure 7.1: A schematic diagram of the experimental setup

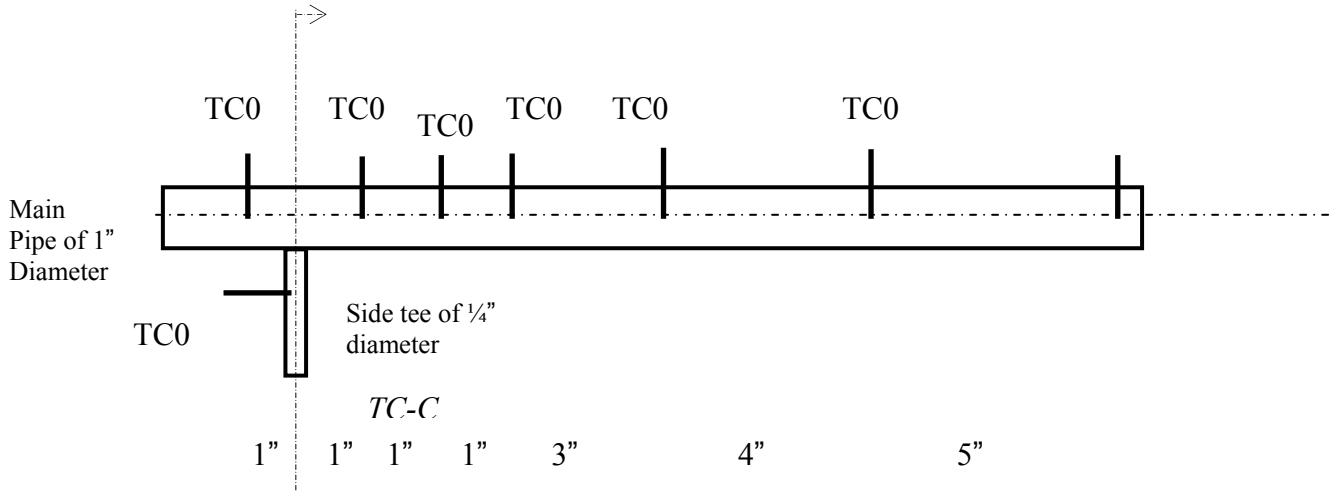

Figure 7.2: The Thermocouples (TC) arrangement of the experimental set-up, *TC-C* for center.

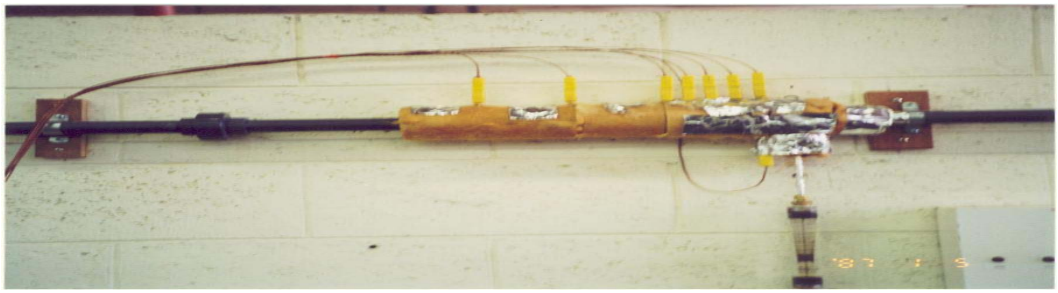

(a)

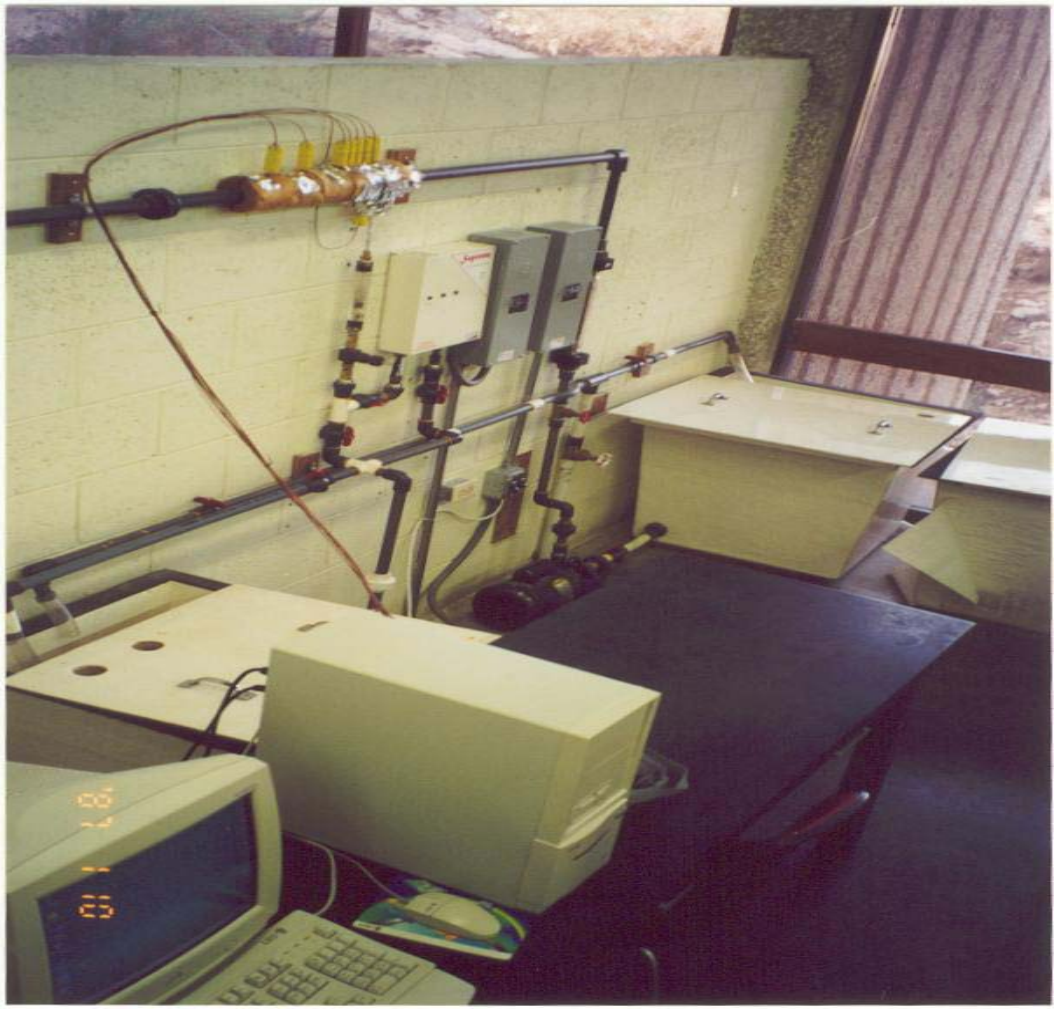

(b)

Figure 7.3: The Experimental setup (a) a view of the Tee-junction (insulated pipe parallel to ground with 90^{o} side-tee) (b) A full view, the main flow direction is from right to left.

6. Stop the main pump at the end of the run.
7. Check the side fluid temperature and stop the side pump.
8. Put off the heater.
9. Save the logged data.

7.4 Effect of U_j/U_m on the Chemical Reaction in a Pipe Line with a Side-Tee

The reaction of Sodium Hydroxide (NaOH) and Hydrochloric acid (HCl) was carried in a pipe and side-tee assembly. Hydrochloric acid was injected through the main pipe, while Sodium Hydroxide was pumped through a side tee. Both, U_m (main pipe velocity) and U_j (side jet velocity) were varied by controlling the volumetric flow rates for the two chemical species. Three values of Uj, namely 4.2, 5.3 and 6.3 m/s were used. Whereas, U_m varied between, 0.19 – 0.79 m/s. The combination of these U_j and U_m values gave different U_j/U_m ratios. This U_j/U_m varied from 7.97 to 33.16. Figures 7.4 to 7.10 show a plot of the temperature versus position along the main pipe. The temperature was measured using thermocouples. Figure 7.4 shows the temperature plot for a U_j/U_m of 16.15 and a U_j of 4.2 m/s. 1M HCl and 1M NaOH were used. Figures 7.5 to 7.10 show similar plots for various U_j/U_m.

In order to investigate the effects of convective mixing on the previous reaction, simulations for the non reactive system were carried out, assuming the system to consist of hot and cold stream.

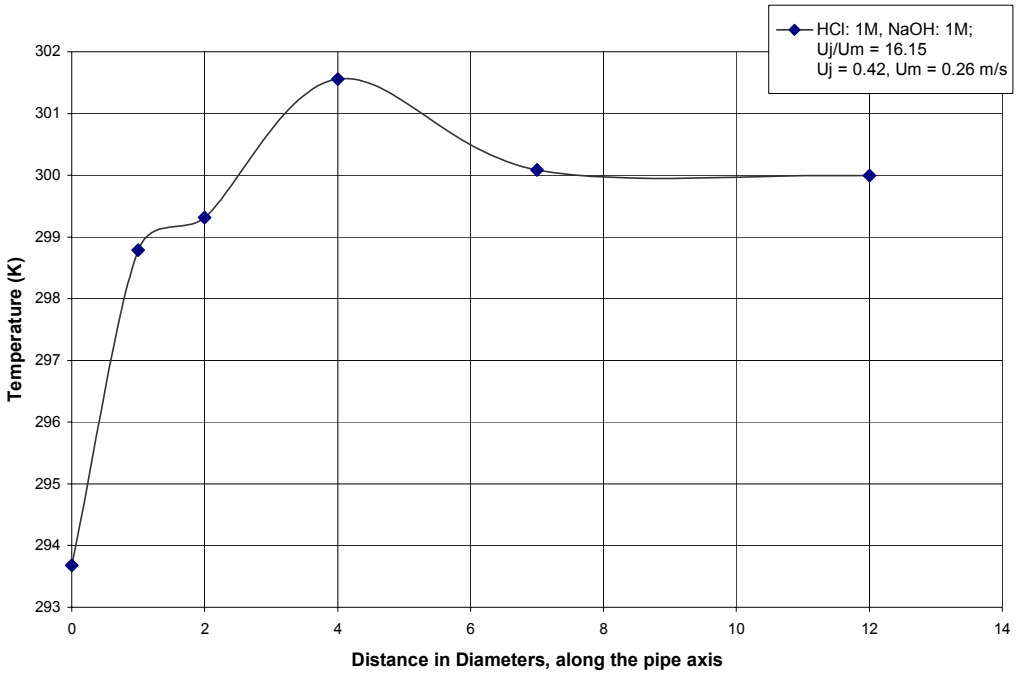

Figure 7.4: A plot of the temperature along the main pipe axis for a U_j/U_m of 16.15

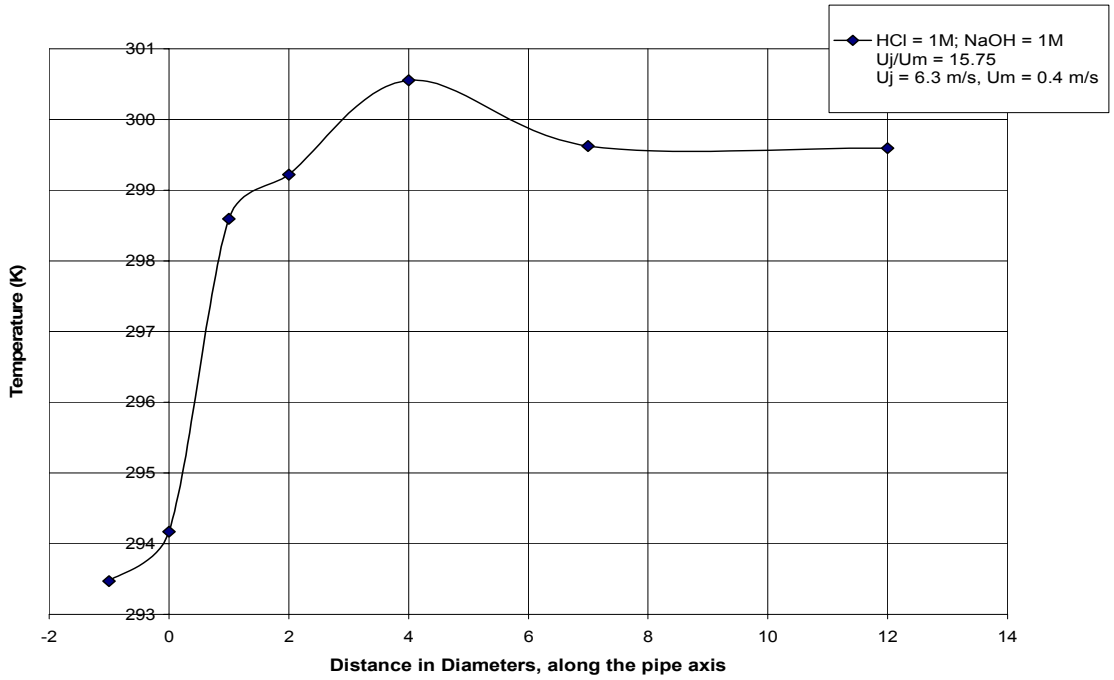

Figure 7.5: A plot of the temperature along the main pipe axis for a U_j/U_m of 15.75

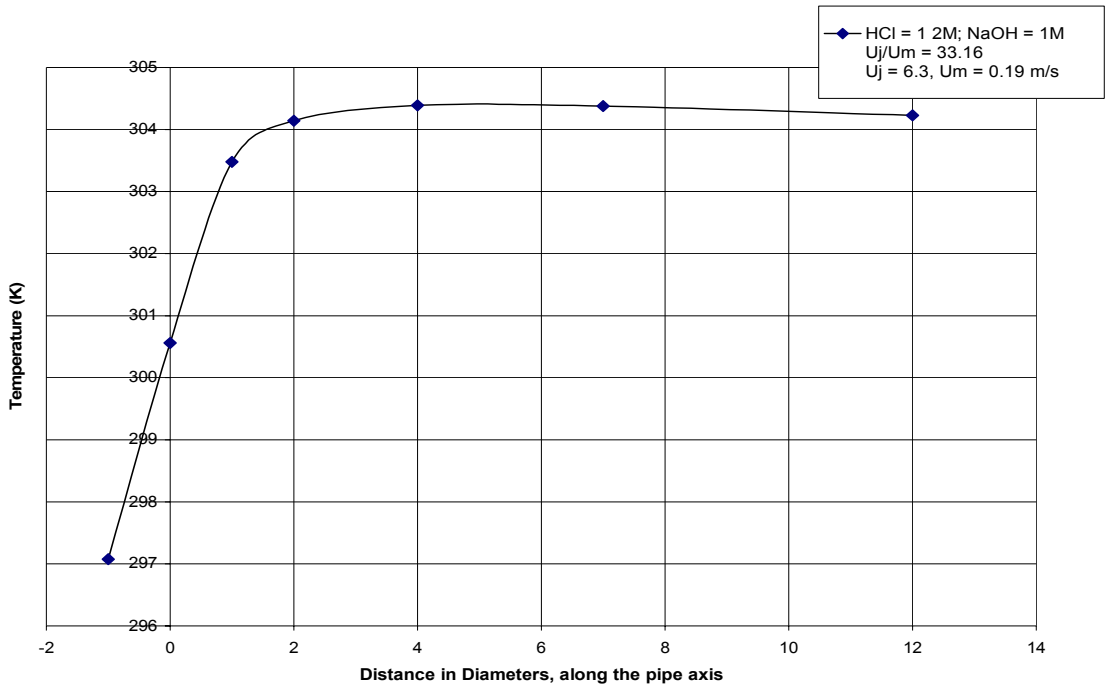

Figure 7.6: A plot of the temperature along the main pipe axis for a U_j/U_m of 33.16

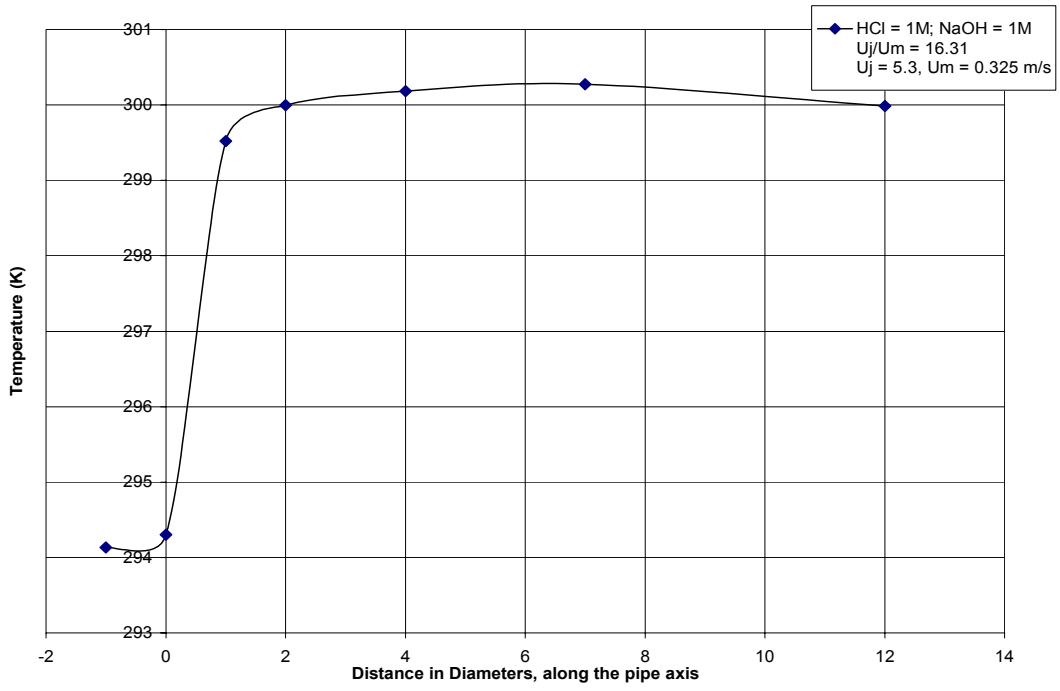

Figure 7.7: A plot of the temperature along the main pipe axis for a U_j/U_m of 16.31

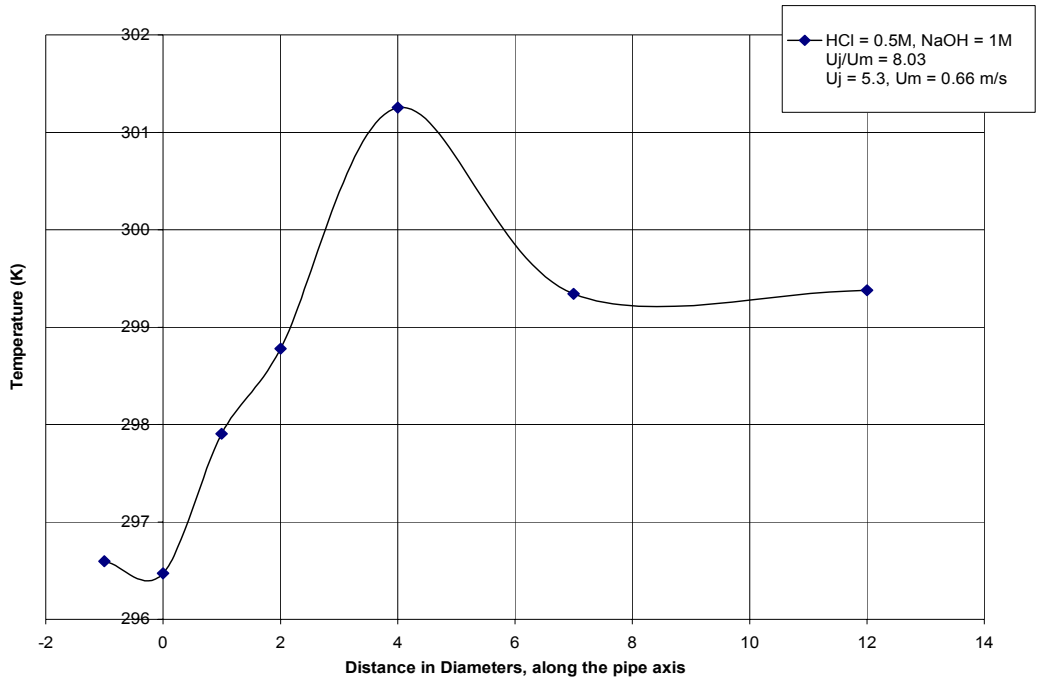

Figure 7.8: A plot of the temperature along the main pipe axis for a U_j/U_m of 8.03

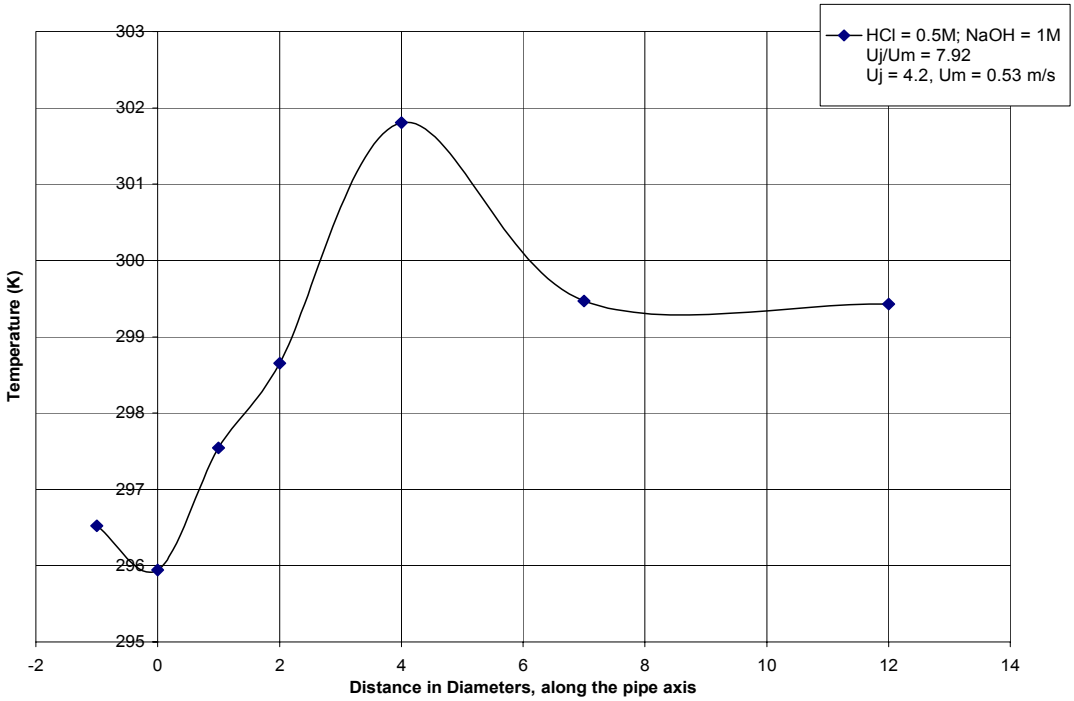

Figure 7.9: A plot of the temperature along the main pipe axis for a U_j/U_m of 7.9245

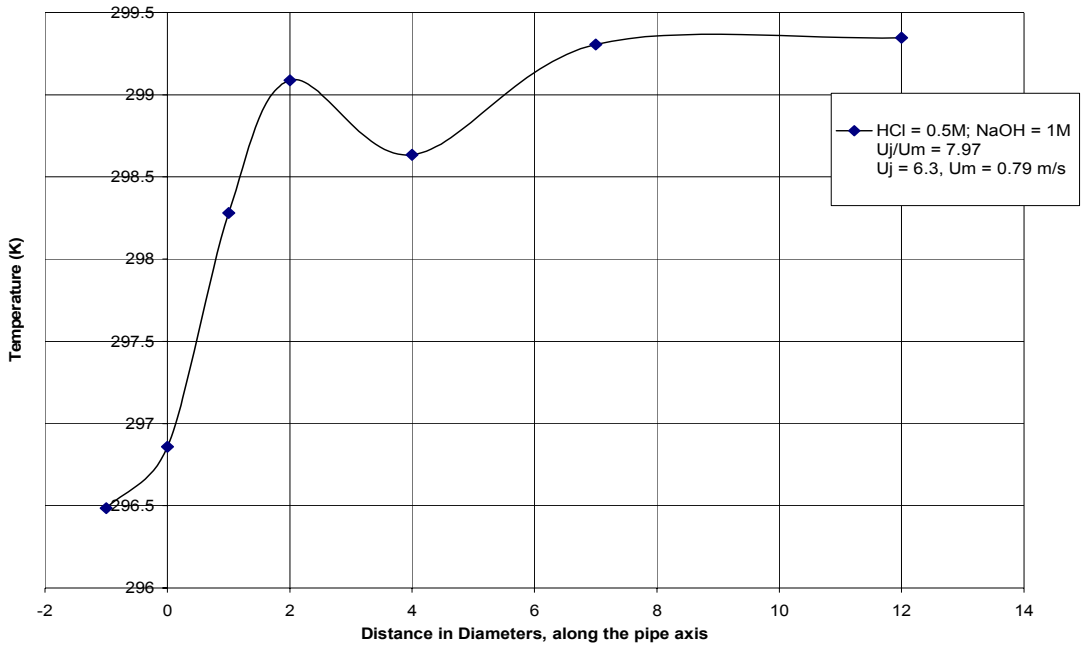

Figure 7.10: A plot of the temperature along the main pipe axis for a U_j/U_m of 7.9747

7.5 Effect of U_j/U_m on Reactive and Non Reactive Mixing

Figures 7.11 to 7.17 show a comparison of the temperature profile along the axis of the main pipe for a neutralization reaction and for physical mixing of hot and cold streams. The temperature rise of the reaction mixture is due to its exothermic nature. The non reactive system follows the regular mixing trend, observed on mixing hot and cold streams. The difference in the peak locations between the two systems is a result of the nature of each system. In the non-reactive system the jet stream carried all the extra energy and it had the highest temperature. In the reactive system, the temperature increased due to the heat of reaction which was generated as the acid and the base react.

The most important thing to notice in Figures 7.11-7.17 is that both reactive and non-reactive systems showed a similar trend. The pipe length required to reach equilibrium temperature for both systems was very close. This length means that 95% mixing for the non-reactive system has been achieved and it also means that the reaction of the acid and the base is complete.

The locations of the peaks in the reactive mixing curve are determined by the ratio of the side to main velocities (U_j/U_m). The individual values of U_j and U_m also have an impact on the location of the peak. Usually the peak occurs where the acid is well mixed with the base. The behavior of the jet will affect this location as shown in Figure 7.18.

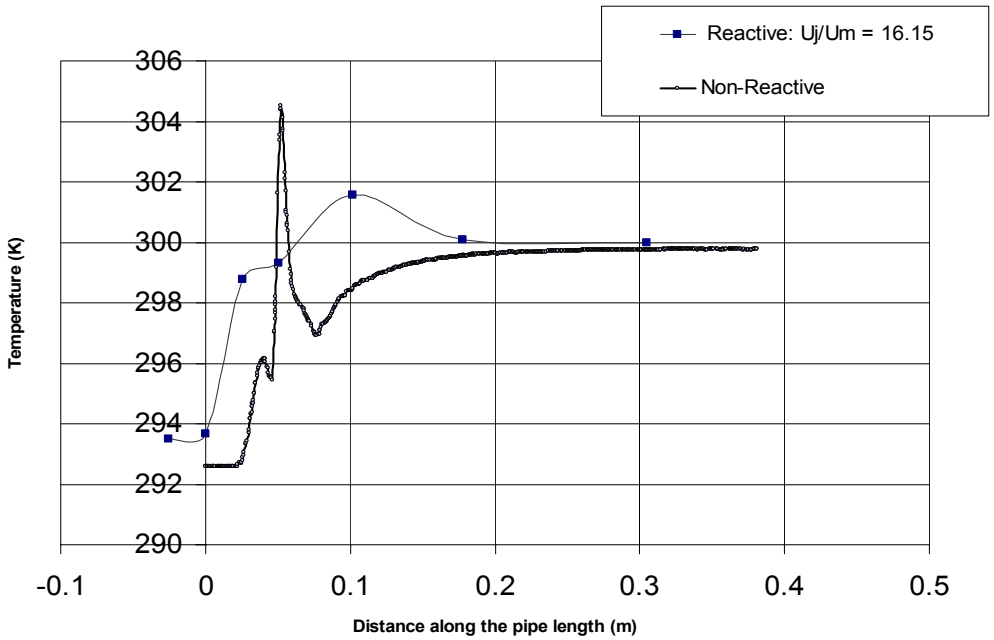

Figure 7.11: A plot of the temperature rise along the main pipe axis for a U_j/U_m of 16.15

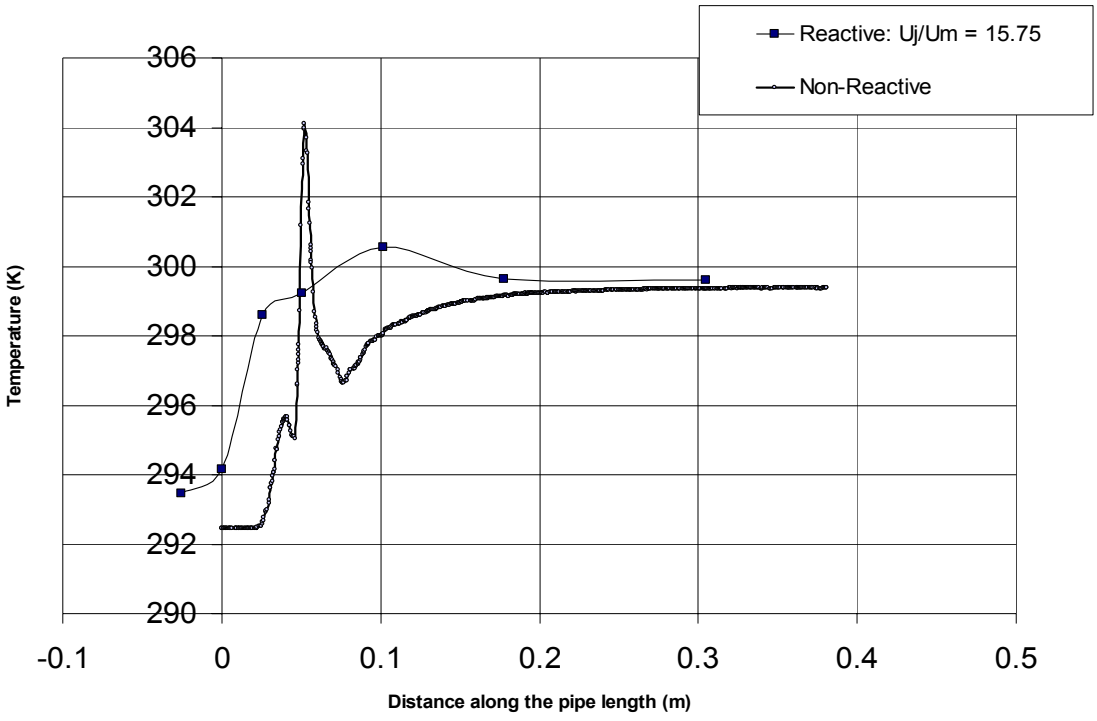

Figure 7.12: A plot of the temperature rise along the main pipe axis for a U_j/U_m of 15.75

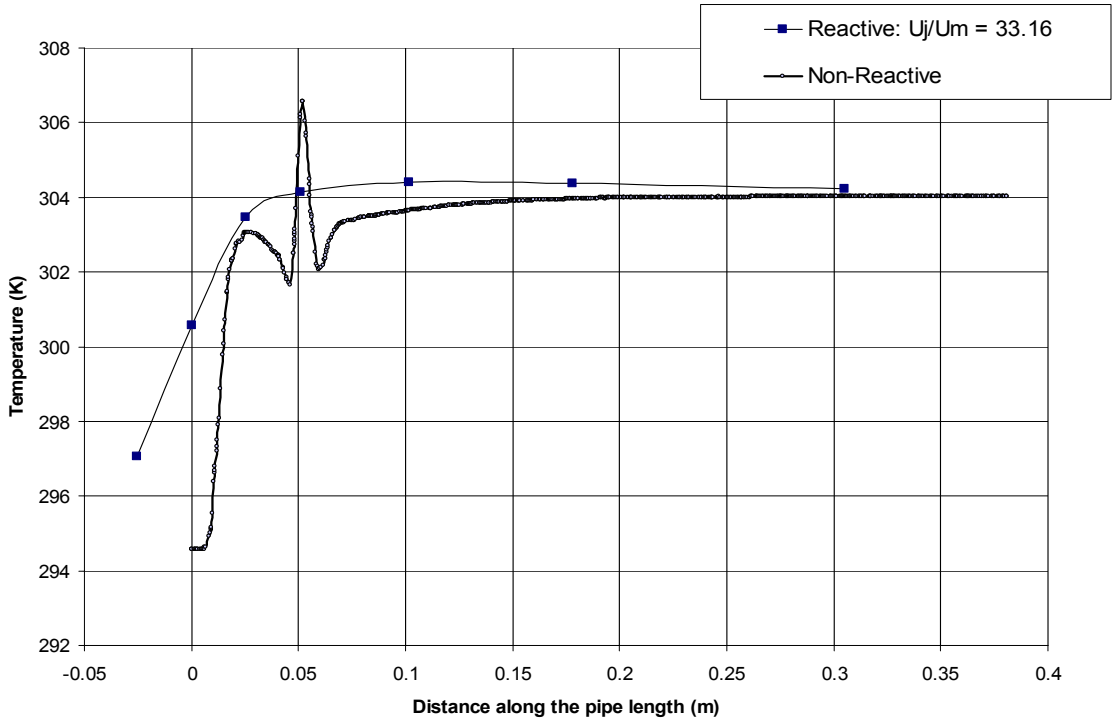

Figure 7.13: A plot of the temperature rise along the main pipe axis for a U_j/U_m of 33.16

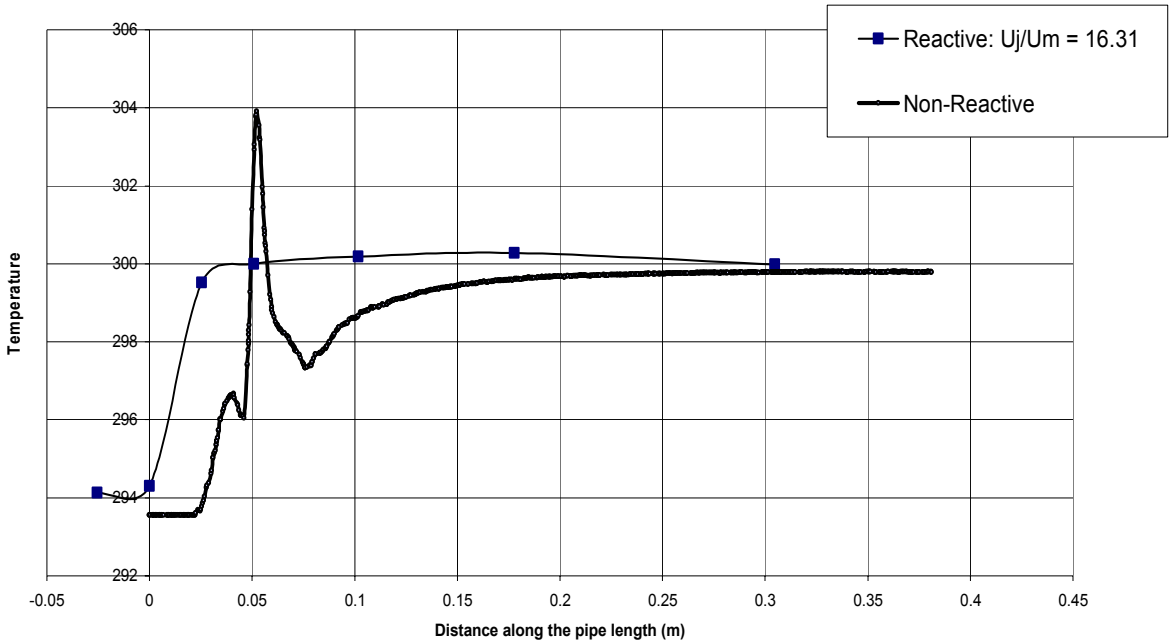

Figure 7.14: A plot of the temperature rise along the main pipe axis for a U_j/U_m of 16.31

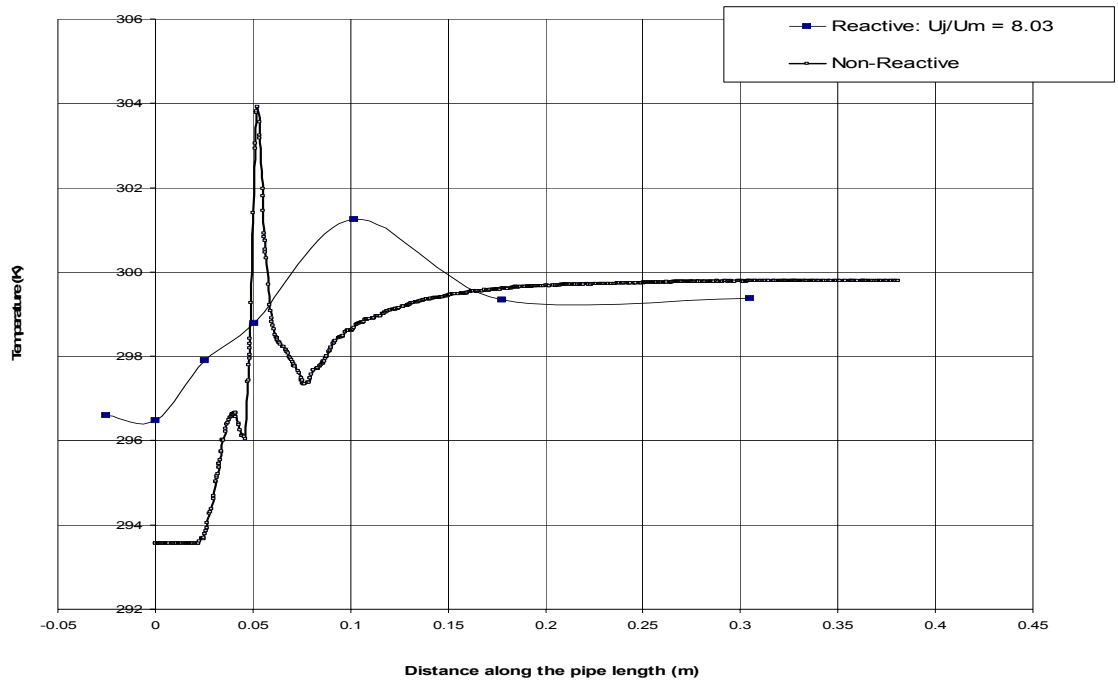

Figure 7.15: A plot of the temperature rise along the main pipe axis for a U_j/U_m of 8.03

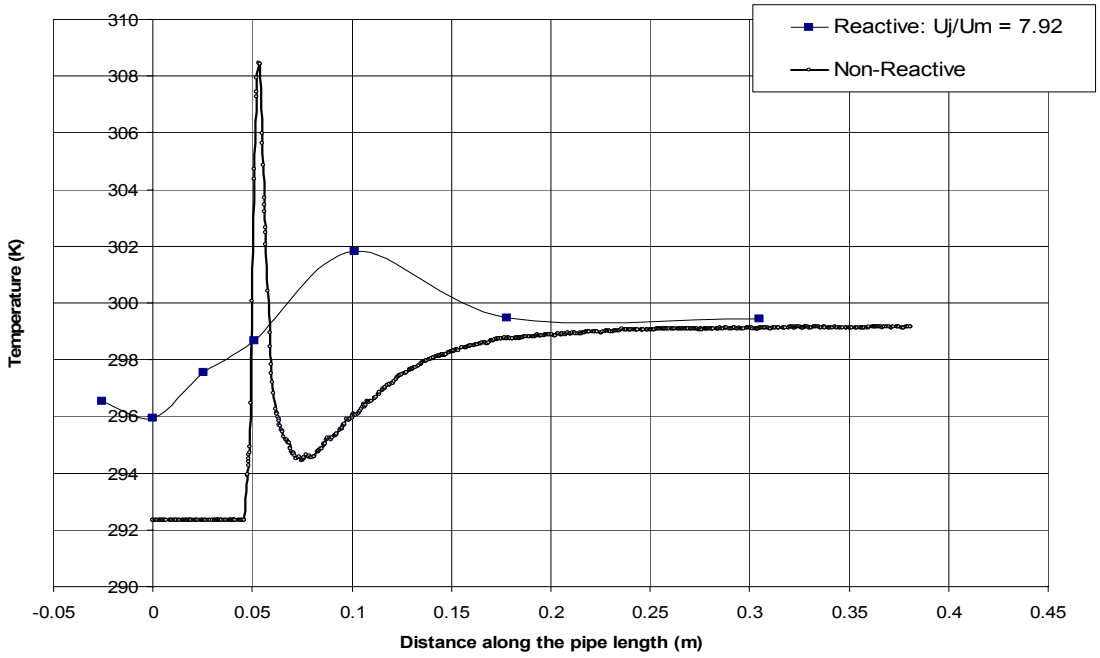

Figure 7.16: A plot of the temperature rise along the main pipe axis for a U_j/U_m of 7.92

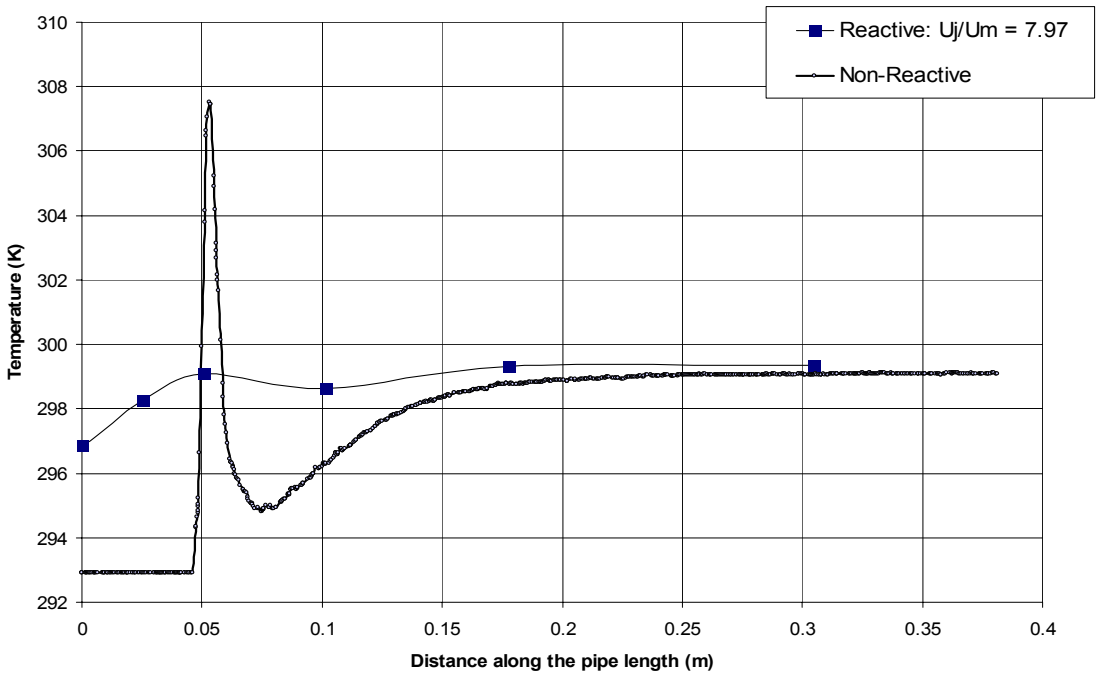

Figure 7.17: A plot of the temperature rise along the main pipe axis for a U_j/U_m of 7.97

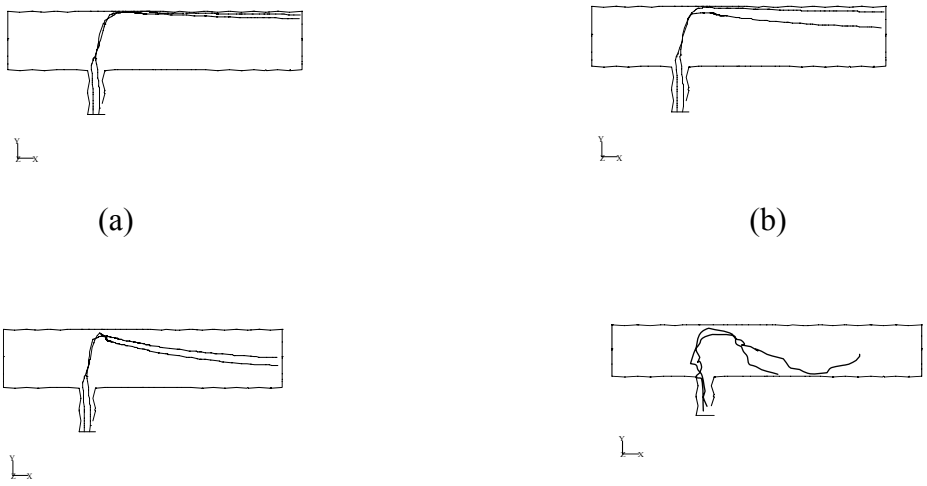

Figure 7.18: A path line diagram of side-jet bending into main fluid as U_j/U_m is increased (a) low (b) low to medium (c) high (d) Very high

Chapter 8

Conclusions

Non-reactive mixing in liquid jet agitated tanks and reactive mixing in pipelines with side tees were investigated in this study. Based on the results obtained the following conclusions are drawn:

1. CFD allowed thorough investigations of mixing studies. The mixing time was traditionally estimated experimentally by monitoring the values of the measured variable, temperature or conductivity, at one or two points. The 95% mixing time is then determined when the measured variable at these monitoring points are within ±5% of the equilibrium value. While analyzing CFD results, mixing time is calculated when the value of the measured variable at every point inside the domain, falls within the same 95% mixing criterion. Therefore, the experimental values are likely to be shorter than the real 95% mixing time if there was no monitoring point in the slowest mixing point. The location of such a point is not always easy to predict as it varies with the flow patterns inside the tank.
2. The shape of the bottom of the tank is found to have a limited effect on the mixing time in a jet agitated tank with a bottom pump around arrangement. For a tank with a hemispherical bottom having the same volume as a flat base tank with a 30 cm diameter and 30 cm in height, the 95% mixing time for a hemispherical bottom tank is found to be 18% to 25% lower than that of the flat base. However, the positions of

the low velocity zone change from near the bottom corner to somewhere near the tank wall in a plane normal to that passing through the jet inlet and outlet.

Tanks with conical bases seem to have shorter 95% mixing times. Keeping the volume of the tank constant, the mixing time was found to decrease as the cone angle was decreased. For a cone angle of 116^{o}, the mixing time reduced by 42% at Re_j of 9,000 to 28% at Re_j of 40,000, as compared to a flat based tank. However tanks with acute angles do not look favorable for construction, as the tanks aspect ratio tend to increase significantly.

3. Using a tank with an irregular shape in order to create asymmetry in the flow did not result in shortening the mixing time.
4. In the literature, a number of correlations suggested that t_{99}/t_{95} ranges from 1.44 to 1.59. Simulations in this study show that the t_{99}/t_{95} ratio ranges from 1.25 to 2.56. The predicted ratio for the same cases used in the literature show good agreement with the published data.
5. The existence of a free surface in a mixing tank with a symmetric jet arrangement (the tank is not covered or not completely full) increases the mixing time by almost 200% for H/D ratio of 25/30 and 20/30 and 100% for 15/30 and Re_j of 7,000. The effects of a free surface for the asymmetric jet arrangement seem to be more severe. The 95% mixing time when using an asymmetric jet arrangement is longer for $Re_j <$ 28,294 and 18% or lower for $Re_j >$ 28,294 for H/D of 20/30, 11% and lower for 15/30 and 50% or lower for H/D ratio of 25/30.

6. A fast neutralization reaction in a pipeline with a side-tee is controlled by convective mixing only. The pipe distance downstream of the side-tee required for the reaction to be completed is the same as that required for a hot and cold stream to mix.

References

Ahmad, I., Effects of Geometry and Flow Asymmetry on Mixing in Liquid Jet Agitated Tanks, *M. S. Thesis*, King Fahd University of Petroleum & Minerals, May 2003.

Ahmad, I., and Zughbi H. D., Mixing in Liquid Jet Agitated Tanks: Effects of the Jet Asymmetry, *ICCBPE*, Malaysia, August 2003.

Angst, W., Bourne, J. R., and Sharma, R. N., Mixing and Fast Chemical Reactions-V, Influence of Diffusion within the Reaction Zone on Selectivity, *Chemical Engineering Science*, 37 (8), 1259-1264, 1982.

Baldyga, J., J. R. Bourne, and B. Zimmermann, Investigation of Mixing in Jet Reactors using Fast, Competitive Consecutive Reactions, *Chemical Engineering Science*, 49 (12), 1937, 1994.

Baldyga, J., J. R. Bourne, B. Dubuis, A.W. Etchells, R. V. Gholap, and B. Zimmermann, Jet Reactor Scale-Up for Mixing-Controlled Reactions, *Trans. Institution of Chemical Engineers*, 73, Part A, 497-502, 1995.

Baldyga, J. and W. Orciuch, Closure problem for precipitation, *Transactions of the Institution of Chemical Engineers*, 75(A), 160-170, 1997.

Baldyga, J. and W. Orciuch, Barium Sulphate Precipitation in a pipe- an Experimental Study and CFD Modelling, *Chemical Engineering Science.,* 56, 2435-2444, 2001.

Belevi, H., Bourne, J. R., and Rys, P., Mixing and Fast Chemical Reactions-II, Diffusion-Reaction Model for the CSTR, *Chemical Engineering Science*, 36 (10), 1649-1654, 1981.

Bourne, J. R., An Experimental Study of Micromixing Using Two Parallel Reactions, *Fluid Mechanics of Mixing: Modelling operations and experimental Technology*, Kluwer Academic Publishers, 207-215, 1992.

Bourne, J. R, Mixing on the molecular scale (Micromixing), *Chemical Engineering Science*, 38(1), 5-8, 1983.

Bourne, J. R, and Toor H. L., Simple Criteria for Mixing in Complex Reactions, *AIChe Journal*, 23 (4), 602-604, July 1977.

Bourne, J. R, Kozicki, F., Moergeli, U., and Rys, P., Mixing and Fast Chemical Reaction-III: Model-Experiment Comparisons, *Chemical Engineering Science*, 36 (10), 1655-1663, 1981.

Coldrey, P. W., *paper to IChemE Course*, University of Bradford, 1978.

Cozewith, C., Computer Simulation of Tee Mixer for Non reactive and Reactive Flows, *Ind. Eng. Chem. Res.,* 30 , 270-275, 1991.

Cozewith, C. and Busko, M., Design Correlations for Mixing Tees, *Ind. Eng. Chem. Res.*, 28, 1521-1530, 1989.

FLUENT Manuals, Fluent Inc., Lebanon, NH, USA, 1998.

Forney, L. J., and Gray, G. E., Optimum Design of a Tee Mixer for Fast Reactions, *AIChe Journal*, 36 (11), 1773-1776, 1990.

Forney, L. J., and Lee, H. C., Optimum Design for pipeline Mixing at a T-Junction, *AIChe Journal*, 28 (6), 980-987, November 1982.

Forney, L. J., Nafia, N., and Vo, H. N., Optimum Jet Mixing in a Tubular Reactor, *AIChE Journal*, 42 (11), 3113-3122, November 1996.

Forney, L. J., and Kwon, T. C., Efficient Single-Jet Mixing in Turbulent Tube Flow, *AIChE Journal*, 25 (4), 623-630, July 1979.

Fossett, H., and Prosser, L. E., The Application of Free Jets to the Mixing of Fluids in Bulk, *J. Inst. Mech. Eng.*, 160, 224, 1949.

Fox, E. A., and Gex, V. E., Single-Phase Blending of Liquids, *AIChE Journal*, 2, 539, 1956.

Gosman, A. D., and Simitovic, R., An Experimental Study of Confined Jet Mixing, *Chemical Engineering Science*, 41 (7), 1853, 1986.

Grenville, R. K., and Tilton, J. N., A New Theory Improves the Correlation of Blend Time Data from Turbulent Jet Mixed Vessels, *Trans IChemE*, 74 A, 390, April 1996.

Gray, J. B., Mixing: Theory and Practice, Turbulent Radial Mixing in Pipes Vol. III, Academic Press, 1986.

Hansen, L., Guilky, P. A., MacMurtry and J. C. Klewicki, The Use of Photoactivable Fluorophores in the Study of Turbulent Pipe Mixing: Effect of Inlet Geometry, *Meas. Sci. Technol*., II, 1235-1250, 2000.

Nienow, A. W., Harnby, N., and Edwards, M. F., Introduction to Mixing Problems, *Mixing in the Process Industries*, Butterworth Heinemann, Oxford, 1997.

Hayes, R. E., Afacan, A., Boulanger, B., and Tanguy, P. A., Experimental Study of Reactive Mixing in a Laminar Flow Batch Reactor, *Trans IChenE*, 76, Part A, 73-81, January 1998.

Hilby, J. W., and Modigell, M., Experiments on Jet Agitation, *6th CHISA Congress, Prague* 1978.

Jayanti, S., Hydrodynamics of Jet Mixing in Vessels, *Chemical Engineering Science,* 56, 193-210, 2001.

Keeler, R. N. Petersen, E. E., and Prausnitz, J. M., Mixing and Chemical Reaction in Turbulent Flow Reactors, *AIChe Journal.*, 11 (2), 221-227, March 1965.

Khang, S. J., and Levenspiel, O., New Scale-up and Design Method for Stirrer Agitated Batch Mixing Vessels, *Chemical Engineering Science*, 31, 569, 1976.

Khokhar, Z. H., Investigations of Mixing in Pipelines with Side-, Opposed-, Multiple Tees, *M. S. Thesis*, King Fahd University of Petroleum & Minerals, November 2002.

Khokhar, Z. H., H. D. Zughbi, and R. N. Sharma, Mixing in Pipeline with Side-Tees, *6th Saudi Engineering Conference,* December 2002.

Khokhar, Z. H., Zughbi, H. D. and Siddiqui Shad, Effects of Jet Arrangement on Mixing in Pipeline with Side-tees, *ICCBPE Conference*, Sabah, Malaysia., August 2003.

Lane, A. G. C., Liquid Jet Mixing in Tanks, *Ph.D. Thesis*, Loughborough University of Technology, December 1981.

Lane, A. G. C., and Rice, P., An Experimental Investigation of Liquid Jet Mixing Employing a Vertical Submerged Jet, *IChemE Symposium Series No. 64,* K1- K14, 1981.

Lane, A. G. C., and Rice, P., An Investigation of Liquid Jet Mixing Employing an Inclined Side Entry Jet, *Trans IChemE*, 60, 171, 1982.

Lane, A. G. C., and Rice, P., The Flow Characteristics of a Submerged Bounded Jet in a Closed System, *Trans IChemE*, 60, 246, 1982.

Li, K. T., and Toor, H. L., Turbulent Reactive Mixing with a Series-Parallel Reaction: Effect of Mixing on Yield, *AIChE Journal*, 32 (8), 1312-1320, August 1981.

Mao, K. W. and Toor, H. L., Second–Order Chemical Reactions with Turbulent Mixing, *Ind. Eng. Chem. Fundam.,* 10 (2), 192, 1971.

Manthawar A., Non-Ideal Reactor Modeling for Complex Reactions, *ChE 525 Project*, Illinois Institute of Technology, Chicago, US, 2001.

Maruyama, T., Ban, Y., and Mizushina, T., Jet Mixing of Fluids in Tanks, *J. Chem. Eng. Japan.,* 15, 342, 1982.

Maruyama, T., Jet Mixing of Fluids in Vessels, *Encyclopedia of Fluid Mechanics*, Gulf Publishing Company, Houston, 2, 544, 1986.

Maruyama, T., Mizzzzushina, T., and Hayashiguchi, S., Optimum conditions for jet mixing in turbulent pipe flow, *International Chemical Engineering*, 23 (4), 707- 716, October 1983.

McKelvey, K. N, Yieh, H., Zakanycz S., and Brodkey R. S., Turbulent Motion, Mixing and Kinetics in a Chemical Reactor Configuration, *AIChe Journal*, November 1975.

Monclova, L. A, and Forney, L. J., Numerical Simulation of a Pipeline Tee Mixer, *Ind. Eng. Chem. Res.*, 34, 1488-1493, 1994.

Newton, I., Motte's translation revised by Cajori, *Principa.*, book II, proposition XXXII, Cambridge University Press, 1, 1934.

Okita, N., and Oyama, Y., Mixing Characteristics in Jet Mixing, *Jap. Chem. Eng.*, 1 (1), 92, 1963.

O'Leary, C. D., and Forney, L. J., Optimization of in-line Mixing at a 90^{o} Tee, *I & EC Prioc. Des. and Dev.*, 24, 332, 1985.

Oldshue, J. Y., Scale-up, *Fluid Mixing Technology*, (McGraw Hill Publication Co.), New York, 192, 1983.

Ou, J. J., and Ranz, W. E., Mixing and Chemical Reactions, Chemical Selectivites, *Chemical Engineering Science*, 38 (7), 1015-1019, 1983.

Patankar, S. V., *Numerical Heat Transfer and Fluid Flow,* McGraw Hill, New York, 1980.

Patwardhan, A. W., CFD modeling of jet mixed tanks, *Chemical Engineering Science*, 57, 1307, 2002.

Perona, J. H., Hylton, T. D., Youngblood, E. L., and Cummins, R. L., Jet Mixing of Liquids in Long Horizontal Cylindrical Tanks, *Ind. Eng. Chem. Res.*, 38, 1478, 1998.

Rakib, M. A., Numerical Investigations of Mixing in a Fluid Jet Agitated Tank, *M.S. Thesis,* King Fahd University of Petroleum & Minerals, K.S.A., 2000.

Revill, B. K., Jet Mixing, *Mixing in the Process Industries*, (Eds: Harnby, N., M. F. Edwards, and A. W. Nienow; Butterworth), London, 1997.

Roy, P. W., Recent Trends in Mixing Equipment, *Chem. Eng*, 78, 86, 1971.

Ruston, J. H., Mixer Performance Data from Pilot Plants, *Ind. Chem. Eng.*, 37 (5), 422, 1945.

Ruston, J. H., The Use of Pilot Plant Mixing Data, *Chem. Eng. Prog.*, 47 (9), 485, 1951.

Ruston, J. H., Mixing of Liquids in Chemical Processing, *Ind. Chem. Eng.*, 44 (12), 2931, 1952.

Singh, M. and Toor, H. L., Thermal Method of Measuring Concentration During Turbulent Reactive Mixing, *AIChE Journal*, 39 (5), 757-760, May 1993.

Sroka, L. M. and Forney, L. J., Fluid Mixing in a 90^{o} Pipeline Elbow, *Ind. Eng. Chem. Res*., 28, 850-856, 1989.

Tosun, G., A Study of Micromixing in Tee Mixers, *Ind. Eng. Chem. Res.,* 26 , 1184-1193 1987.

Unger, D. R. and Muzzio F. J., Laser-Induced Fluorescence Technique for the Quantification of Mixing in Impinging Jets*,* 45 (12), 2477, 1999.

Van de Vusse, J. G., Vergleichende Ruhrversuche Zum Mischen Losllicher Flussigkeiten en Einem 12000 m^3 Behalter, *Chemie-In-Genieur-Technik.,* 31, 583, 1959.

Vassilatos, G., and Toor, H. L., Second-Order Chemical Reactions in a Nonhomogenous Turbulent Fluid , *AIChe Journal*, 47 (8), 666-672, July 1965.

Verchuren, I. L. M., Wijers, J. G., and Keurentjes, J. T. F., Effect of Mixing on Product Quality in Semibatch Stirred Tank Reactors, *AIChe Journal*, 47 (8), 1731-1739, August 2001.

Verchuren, I., Feed Stream Mixing in Stirred Tank Reactors, *Ph.D. Thesis*, Eindhoven University of Technology, The Netherlands, September 2001.

Yao, W., Takahashi K., and Koyama, K., Theoretical Tool for Optimum Design of Mixer, and Visualization and Quantification of Mixing Performance, *Journal of Chemical Engineering of Japan,*, 31 (2), 220-227, 1998.

Yuan L. L. and R. L. Street, Large-eddy simulations of a round jet in cross flow, *J. Fluid Mech.,* 379, 71-104, 1999.

Zughbi, H. D., and M. A., Rakib, Mixing in a Fluid Jet Agitated Tank, *AICHE Annual Meeting*, Los Angeles, November 2000.

Zughbi, H. D. and M. A. Rakib, Investigations of Mixing in a Fluid Jet Agitated Tank, *Chem. Eng. Comm.*, 189 (9), 1038, 2002.

Zughbi, H. D., and M. A. Rakib, Numerical Simulations of mixing in a jet agitated large horizontal cylindrical tank, *Sixth Saudi Engineering Conference*, Vol. II, 183-195, December 2002.

Zughbi, H. D., and M. A. Rakib, Mixing in a Fluid Jet Agitated Tank: Effects of Jet Angle and Elevation and Number of Jets, *Chemical Engineering Science*, 59, 829-842, 2004.

Zughbi, H. D., Z. H. Khokhar, and R. N. Sharma, Numerical and Experimental Investigations of Mixing in Pipelines with Side and Opposed Tees, *AICHE Annual Conf.*, Indianapolis, November 2002.

Zughbi, H. D., Khokhar, Z., Ahmad, I. and Rakib, M. A., Optimum Design of Mixers Using Computational Fluid Mechanics, *Petrotech 2003*, Bahrain, September 2003.

Zughbi, H. D. and Ahmad, I. Effects of Tank Geometry and Jet Asymmetry on Mixing in a Jet Agitated Tank, *AICHE Annual Conf.,* San Francisco, November 2003.

Zughbi, H.D., Khokhar, Z. H., and Sharma, R. N., Mixing in Pipeline with Side and Opposed Tees, *Ind. Eng. Chem. Res.*, 42, 5333-5344, 2003.

Vita

Name: Shad Waheed Siddiqui

Date & Place of Birth: March 20, 1978 in Unnao, India

Permanent Address: 362-A, Civil Lines
Unnao - Hardoi Road
Unnao-209801 (U.P.)
India

Email: swsiddiqui@hotmail.com
swsiddiqui@rediffmail.com

Nationality: Indian

Educational Qualification:

Master of Science in Chemical Engineering, June 2004
King Fahd University of Petroleum & Minerals
Dhahran-31261
Saudi Arabia

Bachelor of Technology in Chemical Engineering, June 2001
Aligarh Muslim University
Aligarh-202002
India